APPENDIX A[1]

ACOUSTIC MODELING APPROACH AND METHODOLOGY

[1]This document was prepared by Marine Acoustics, Inc. under contract to the National Marine Fisheries Service (Contract: GS-10F-0164N; Order: DG133F06NC2020) for use in the preparation of the *Draft Programmatic Environmental Impact Statement for the Geological and Geophysical Exploration of Mineral and Energy Resources in the Gulf of Mexico*.

Table of Contents

1.0 INTRODUCTION
- **1.1 Overview**
- **1.2 Acoustic Modeling Approach**
- **1.3 Acoustic Thresholds**

2.0 DETAILS OF THE ACOUSTIC IMPACT MODELING
- **2.1 Source Description and Modeling**
- **2.2 Survey Operations**
- **2.3 M-weighting**
- **2.4 Environmental Modeling**
- **2.5 Marine Mammal Densities**
- **2.6 Acoustic Integration Model© (AIM) Modeling**
  - **2.6.1 Introduction to AIM**
  - **2.6.2 AIM Simulation of the Various Seismic Survey Types**
    - ***2.6.2.1 Ocean Bottom Seismic Survey***
    - ***2.6.2.2 Two-Dimensional Survey***
    - ***2.6.2.3 Three-Dimensional Survey***
    - ***2.6.2.4 Wide Azimuth Survey***
    - ***2.6.2.5 3D High-Resolution Survey***
  - **2.6.3 Data Convolution to Create Animat Exposure Histories**
  - **2.6.4 Application of Exposure Criteria**
  - **2.6.5 AIM Animat Movement and Diving Pattern Details**
  - **2.6.6 Animal Behavior Parameters**
  - **2.6.7 AIM Results and Adjustments**

3.0 SUMMARY

4.0 LITERATURE CITED

1.0 INTRODUCTION

1.1 OVERVIEW

The purpose of this appendix is to document the overall approach and to identify the specific model, acoustic source, environmental and biological data and modeling techniques used to calculate the potential acoustic impacts of the proposed actions, which are presented in Chapter 4 of this PEIS. The general philosophy used in determining these estimates was that "reasonably" representative values be employed when the calculations were made. This approach is based on the knowledge that an exact predictive modeling of: a) exactly which source would be employed at each site, b) the exact environmental acoustics conditions at each site, c) the timing of each survey, and d) the marine animals present at each site of source operations, could not be known at any given time (without extensive surveys immediately prior to or during the survey) and particularly not for the period of this document (i.e., the next five years). The "reasonable" approach described in this appendix, in general, examined the potential range of each variable and identified what were typically used or expected to be used during execution of the proposed action. In some situations, even the extreme range of variable values had minimal affect on the results, or the low occurrence of some of the values in the range allowed an obvious selection for modeling. For example, nearly all of the deep-water sites had very fine silts, clayey silt and clay as the predominant bottom types and clay's characteristics were used when modeling the acoustic propagation in those sites, since the bottom properties of the other sediments were very similar. However, in the case of the airgun source used for modeling, there are numerous possible source arrays that could be used based on the company performing the survey, the location, the ships available, etc. Here, the source identified by industry and the Bureau of Offshore Energy Management, Regulation, and Enforcement (BOEM; previously Minerals Management Service (MMS) of the U.S. Department of the Interior) as a typical source for these surveys, was used in the modeling. And even though it is not the strongest source identified, it better represents a typical source array and its potential impacts. Also, it is estimated that the percentage of time that strong and weaker sources are used over the duration of the proposed action will only slightly change the overall estimated impacts and in fact over time tend to average out to an impact similar to that predicted for the modeled array.

The basic acoustic terminology used in this appendix is presented in numerous published sources (e.g., ANSI, 1986, 1984; Richardson et al., 1995; NRC, 2003; Southall et al., 2007). The main definitions used in this assessment are provided below (Southall et al., 2007):

- *Pulses:* Pulses are brief, broadband, atonal, transient sounds; e.g., explosions, gun shots, airgun pulses, and pile driving strikes. Pulses are characterized by a rapid rise from ambient pressure to maximal pressure, and (at least near the source) by short duration.
- *Nonpulse (intermittent or continuous) sounds*: Nonpulse sounds can be tonal, broadband, or both. Nonpulse sounds can be of short duration but they lack the rapid rise times of true pulses. Nonpulse sounds include those from shipping, aircraft, drilling, and active sonar systems. Due to certain propagation effects, it is possible that a sound that is pulsed near the source may be perceived by a distant receiver as a nonpulse sound.
- *Peak sound pressure*: This is the maximum instantaneous sound pressure measurable in the water at a specified distance from the source airgun. The units of pressure are

typically bars (English) or, in metric units, either Pascals (Pa) or micropascals (μPa). The metric values are commonly expressed in logarithmic form as decibels relative to 1 μPa (dB re 1 μPa).

- *Peak-to-peak sound pressure*: This is the algebraic difference between the peak positive and peak negative sound pressures. Units are the same as for peak pressure. When expressed in dB, peak-to-peak pressure is typically ~ 6 dB higher than peak pressure.
- *Root mean square (RMS) sound pressure*: In simple terms, this is an average sound pressure over some specified time interval. For airgun pulses, the averaging time is commonly taken to be the approximate duration of one pulse, which in turn is commonly assumed to be the time interval within which 90% of the pulse energy arrives. The RMS sound pressure level (in dB) is typically ~10 dB less than the peak level, and ~16 dB less than the peak-to-peak level.
- *Sound pressure levels (SPLs)*: SPLs are givens as the dB measures of the pressure metrics defined above. The RMS SPL is dB re: 1 μPa for underwater sound and dB re: 20 μPa for aerial sound.
- *Source Level (SL):* SL is the received level measured or estimated at a nominal distance of 1 m from the source. It is often expressed as dB re: 1 μPa at 1 m or in bar-m. For a distributed source, such as an array of airguns, the nominal overall source level, as used in predicting received levels at long distances, exceeds the level measurable at any one point in the water near the sources.
- *Sound exposure level (SEL or energy flux density)*: This measure represents the total energy contained within a pulse, and is in the units dB re 1 μPa^2-s. For a single airgun pulse, the numerical value of the SEL measurement, in these units, is usually 5–15 dB lower than the RMS sound pressure in dB re 1 μPa, with the "RMS – SEL" difference often tending to decrease with increasing range (Greene, 1997; McCauley et al., 1998).
- *Duration:* Duration is the length of the sound, usually measured in seconds. For an impulsive sound such as an airgun pulse, the duration may be calculated in a number of different ways. Greene (1997) described duration of an airgun pulse as the interval over which 90% of the sound energy arrives at the receiver.

Over the past decade, NMFS guidelines regarding levels of impulsive sound that might cause disturbance or injury have often been based on the "RMS sound pressure" metric. However, the RMS value depends on the extent to which the sound pulse has been "stretched" in duration during propagation, which varies with environmental conditions, so the RMS measure is often criticized (e.g., Madsen, 2005). There is now reason to believe that auditory effects (especially physiological effects like PTS and TTS) of transient sounds on marine mammals are better correlated with the amount of received energy than with the level of the strongest pulse and therefore SEL is increasingly the unit of choice in evaluations.

1.2 Acoustic Modeling Approach

There are two steps to the modeling effort: 1) the determination of the 3-D acoustic field emanating from the sound sources and how it propagates through the water; and 2) the determination of the net exposure of marine animals that reside in the exposed volume.

Historically, the seismic community and NMFS have used a simplified approach to estimate the potential impacts to marine mammals for airgun sources. In this document, this methodology is called the line-transect calculation methodology. Essentially, this methodology consisted of: 1) determination of the estimated threshold isopleth range from the source (nominally these thresholds were the 160 dB received level for Level B and 180 dB received level for Level A (cetaceans) harassment under the Marine Mammal Protection Act (MMPA)) (see Table A-1) for the airgun sources; 2) assumption that a cylinder whose radius matched the range to these isopleths and encompassed the entire water column, was ensonified to that threshold; 3) calculating the surface area ensonified by this water column as the source moved along its track; and 4) multiplying that resultant ensonified surface area by the density of each marine mammal species present to estimate that species numbers of MMPA Level A and B potential harassment takes. This methodology will be included in this document for comparison and continuity.

Additionally, a more sophisticated approach will be included in this document. This approach will use a more detailed modeling of the source and its properties, the acoustic propagation field in three dimensions, and three dimensional animal placement and movement to better calculate the potential impacts to marine mammals. For this methodology, the first step is largely controlled by properties of the source, such as its movement in time and space, and the sound field it generates at any point in time. This is a function of the geometric organization (array configuration) of its sound generators, and the spatial, spectral and temporal properties of the sound field that they produce. Propagation modeling further analyzes the effects of the physical properties of the ocean, the bottom and the surface on the sound field as it propagates out from the source.

The second step requires knowledge of the diving and movement characteristics of the animals residing in the exposed region. Time-based integration models, such as the Acoustic Integration Model© (AIM)[1], as used in this modeling effort, are necessary to fully evaluate the exposure. The advantage of these tools is that they not only provide a more accurate and detailed model of the exposures of a population of marine animals in the three dimensions and time, but they also provide: 1) statistical data on each individually modeled animal and the population as a whole; 2) rate of exposure (sounds per unit time) over the duration of a survey; and 3) the data necessary to determine effects based on more sophisticated thresholds, such as sound exposure level, SEL.

1.2.1 Propagation Modeling

1.2.1.1 Overall Modeling Assumptions

For the more complex modeling effort detailed in this appendix the following general assumptions were made:

[1] MAI's Acoustic Integration Model©, or AIM, is a software package developed to predict the acoustic exposure of marine animals from an underwater sound source. The unique and principal component of AIM is a 3-D movement engine, which programs the geographic and vertical movements of sound sources and simulated marine animals. In 2006, the Center for Independent Experts (CIE) conducted a review and assessment of AIM. The CIE panel concluded that AIM is a credible tool for developing application models (Independent System for Peer Review 2006).

- The far-field broadband signal from the typical airgun array nominally includes significant components up to 1,000 Hz, with the peak amplitude in the far-field near-horizontal spectrum typically occurring between 50 and 100 Hz;

- The modeling needed to address all of the acoustic survey types are identified in Chapters 1 and 2;

- A nominal or representative source, as identified by BOEMRE and industry, will be used for source modeling and source specification identification;

- Conditions to be modeled need to include all potential survey areas in the northern Gulf of Mexico, including three water depths: shallow, slope, and deep water, and all four seasons;

- Animal density estimates would use the best available data, which would need to be specified by location and season for the modeling effort; and

- Animal movement modeling would use the best available input data.

1.2.1.2 Acoustic Propagation Model Selection

Three acoustic propagation models were readily available and generally considered capable of meeting the modeling objectives, allowing for the limitations of the models as derived from Dozier and Cavanagh (1993) and OAML (2002). These models are: a) a U.S. Navy-approved version of the Parabolic Equation (PE) Model; b) the Comprehensive Acoustic Simulation System/Gaussian Ray Bundle (CASS/GRAB) Model; and c) the Bellhop Model. Although all three acoustic models potentially can be used for this modeling effort, each has water depth and frequency limitations. After a review of the capabilities and limitations of each model, the CASS/GRAB model was selected for this analysis because: a) it is capable of modeling propagation between 50 Hz and 1,000 Hz; b) its built-in array beamformer code has been found to be adequate for modeling the array patterns throughout the analysis frequency range; c) it is readily compatible with the supporting databases that would be used; d) it allows a selection of the range and depth steps (i.e., the resolution of the modeled propagation field) that is necessary; and e) it allows an examination of the spreading of the seismic signal as caused by the acoustic multi-path throughout the propagation field.

CASS/GRAB is a U.S. Navy standard acoustic propagation model that is applicable for frequencies between 150 Hz and 100 kHz (OAML, 2002). The U.S. Navy sponsor for the CASS/GRAB model states that, although it had been tested and provided good predictions at frequencies down to 50 Hz, the lower limit has not been approved nor implemented in the U.S. Navy's Oceanographic and Atmospheric Master Library (OAML) (2002) database. CASS/GRAB does have a nominal [depth > 2×π×wavelength] limitation, so for depths less than approximately 100 m for a 100 Hz signal, care must be exercised when using this model.

1.2.1.3 Overview of Essential Supporting Databases

- **Surface Loss Model—**Surface Loss Models are available and function well down to a frequency of 1 Hz. The specific model used for this modeling effort was the U.S. Navy standard OAML (2002) surface reflection coefficient model. This model is directly available internal to the CASS/GRAB model.

- **Bathymetry—**This modeling effort will use Digital Bathymetry Data Base–Variable resolution (DBDB-V) (0.1-2.0 nautical miles resolution) (OAML 2002).

- **Bottom Loss—**Bottom loss characterization for specific sites must be determined individually, with the task becoming more complex with lower frequencies. The specific model used for this modeling effort was the Rayleigh bottom reflection coefficient model. This model is directly available internal to the CASS/GRAB model.

- **Sound Velocity Profile (SVP)—**The SVPs used in this modeling effort were derived from the monthly-averaged Generalized Digital Environmental Model (GDEM) database.

1.2.1.4 AIM Modeling and Comparative Assessment of Exposure

The Acoustic Integration Model© (AIM) is a four-dimensional, individual-based, Monte Carlo statistical model designed to predict the exposure of receivers to any stimulus propagating through space and time. The central component of AIM is the animat movement engine, which moves the stimulus source and animal receivers through four dimensions (time and space) according to user inputs. AIM uses external range-dependent stimulus propagation models (e.g., CASS/GRAB for this modeling effort) and additional propagation models can be integrated to accommodate any class of propagation stimuli, including acoustic and explosive.

1.2.2 Overall Modeling Approach

The following step-wise modeling approach is included to illustrate the overall approach to predict the acoustic impacts of seismic (airgun) sources in the Gulf of Mexico for the proposed action:

- The GDEM database of SVPs was used to extract SVP for the GOMEX and to characterize the water body into four SVP regions;

- SVP for winter, spring, summer and fall were then examined for these regions (note after examination of the SVPs it was determined that the summer and winter propagation patterns captured the extremes of the possible propagation fields and that the spring and fall were transitions between these extremes. In shallow water, both seasons were effectively iso-velocity, which resulted in minimal differences in transmission loss, thus only winter profiles and modeling were used there. But for the deep and intermediate (slope) cases, both the summer and winter profiles were subsequently modeled.);

- DBDB-V was used to determine where the four SVP regions overlap with the three depth sub-regions, characterized as shallow, slope, and deep;

- Consider the SVP regions with the three depth sub-regions, and determine if any of the resulting acoustic propagation situations are duplicative and can be eliminated to reduce the number of acoustic model runs required;

- The spectrum of the airguns below 1,000 Hz was divided into the American National Standards Institute (ANSI) standard 1/3rd octave bands;

- CASS/GRAB was utilized to construct the 3-D beam patterns for the source for each of these 1/3rd octave bands. Embedded in this modeling for each of 1/3rd octave bands are the specific source levels and beam patterns for that 1/3rd octave. It should be noted that these beam patterns were compared to a 3-D beam pattern produced by an industry model (GUNDALF) and the difference was minimal.

- CASS/GRAB was run for each of the 1/3rd octave bands, for a total of 5 separate propagation situations and 2 seasons, as identified above. Each of these propagation runs included a 15° resolution in azimuth to fully characterize propagation for that site. As expected, the 50 to 100 Hz bin typically showed less TL on a per-Hz basis than was evident for higher frequencies, but occasionally some slight near-surface ducting was observed at the higher frequencies (i.e., 600-1,000 Hz);

- In order to capture the broadband nature of the transmission loss for the seismic signal a technique was developed which integrates the 1/3rd octave transmission loss fields for the specific seismic signal and spectrum identified as the nominal case. The resulting TL estimate provides a reasonable but conservative estimate of the received level footprint for the airgun source, which reflects contributions to the result from the entire source spectrum, for each 15° azimuth for each site; and

- AIM is used to estimate the impacts per survey block, based on the transect line geometry for each type of survey in each modeled site, for each of the thresholds used in the modeling.

1.3 ACOUSTIC THRESHOLDS

1.3.1 Historical Criteria.

Since the mid-1990s, the National Marine Fisheries Service (NMFS) has specified that marine mammals exposed to pulsed sounds with received levels exceeding 180 or 190 dB re 1 μPa (RMS) for cetaceans and pinnipeds, respectively, were considered to exceed Level A (Injury) levels (NMFS, 2000). Similarly, NMFS also considers that cetaceans and pinnipeds exposed to levels ≥160 dB re 1 μPa (RMS) were considered to exceed Level B (Behavioral) levels (Table A-1). For all of these criteria, the exposure level was the maximum acoustic RMS pressure level received by an animal.

Table A-1. Historical Injury and Behavior Criteria for Cetaceans and Pinnipeds, as Recognized and Used by the U.S. National Marine Fisheries Service

Group	Level A (Injury) Pressure (dB re 1 μPa RMS)	Level B (Behavior) Pressure (dB re 1 μPa RMS)
Cetaceans	180	160
Pinnipeds	190	160

1.3.1.1 Injury Criteria.

The 180- and 190-dB re 1 μPa (RMS) criteria were determined before there was specific information about the received levels of underwater sound that would cause temporary or permanent hearing damage in marine mammals. Subsequently, data on received levels that cause the onset of temporary threshold shift (TTS) have been obtained for certain toothed whales and pinnipeds (Kastak et al., 1999, 2005; Finneran et al., 2002, 2005). A group of specialists in marine mammal acoustics, the "noise criteria group", has recommended new criteria, based on current scientific knowledge, to replace the somewhat arbitrary 180 and 190 dB (RMS) criteria (Southall et al., 2007).

Recently acquired data indicate that TTS-onset in marine mammals is more closely correlated with the received energy levels than with RMS levels. In odontocetes and the more sensitive pinnipeds exposed to nonpulse sound, TTS onset occurs near 195 and 183 dB re 1 μPa^2-s, respectively (Southall et al. 2007). In odontocetes exposed to impulse sounds, the TTS threshold can be as low as approximately 183 dB re 1 μPa^2-s. The corresponding value for pinnipeds is less well defined. There are published data on levels of nonpulse sound (Kastak et al., 1999, 2005) but not of impulse sound eliciting TTS in pinnipeds. Based on the results for nonpulse sound, plus the known tendency in other mammals for lower TTS thresholds with impulse than with nonpulse sound, the TTS thresholds for pinnipeds exposed to impulse sound may be as low as 171 dB re 1 μPa^2-s in the more sensitive species, such as the harbor seal.

There are no specific data concerning the levels of underwater sound necessary to cause permanent hearing damage (permanent threshold shift or PTS) in any species of marine mammal. However, data from terrestrial mammals provide a basis for estimating the difference between the (unmeasured) PTS thresholds and the measured TTS thresholds. A conservative (precautionary) estimate of this offset between TTS and PTS thresholds, when sound exposure is measured on a sound exposure level (SEL) basis (received energy levels), is to add 15 dB to the TTS value for impulsive sounds and 20 dB for nonpulse sounds (Southall et al. 2007). Thus, now-available data indicate that the lowest received levels of impulsive sounds (e.g., airgun pulses) that might elicit slight auditory injury (PTS) are 198 dB re 1 μPa^2-s in cetaceans (i.e., 183 + 15 dB), and 186 dB re 1 μPa^2-s in the more sensitive pinnipeds (i.e., 171 + 15 dB). Corresponding values for nonpulse sounds (e.g., marine vibrator sweeps) are 215 re 1 μPa^2-s in cetaceans (i.e., 195 + 20 dB) and 203 dB re 1 μPa^2-s in the more sensitive pinnipeds (e.g., 183 + 20 dB) (Southall et al., 2007). These SEL measures are all assumed to be taken using M-weighting; i.e., somewhat down-weighting the energy for frequencies near and especially beyond the lower and upper frequency limits of hearing in the relevant marine mammal group (Southall et al. 2007).

The noise criteria group also concluded that receipt of an instantaneous flat-weighted peak pressure exceeding 230 dB re 1 µPa (peak) for cetaceans or 218 dB re 1 µPa (peak) for pinnipeds might also lead to auditory injury even if the aforementioned cumulative energy-based criterion was not exceeded (Table A-2).

The primary measure of sound used in the proposed new criteria is the received sound energy, not just in the single strongest pulse, but accumulated over time. The most appropriate interval over which the received airgun signal should be accumulated is not well defined. However, pending the availability of additional relevant information, the noise criteria group has suggested considering noise exposure over 24-hr periods.

Table A-2. Injury and Behavior Exposure Criteria for Cetaceans and Pinnipeds, as proposed by Southall et al., (2007)

	Level A (Injury)		**Level B (Behavior)**
	Pressure	Energy	Pressure
Group	(dB re 1 µPa RMS)	(dB re 1 μPa^2-s)	(dB re 1 µPa RMS)
Low Freq. Cetaceans	230	198	*
Mid. Freq. Cetaceans	230	198	*
High Freq. Cetaceans	230	198	*
Pinnipeds (in water)	218	186	*

Sources: NMFS, 2005; Southall et al., 2007. Note: * means not specified in Southall et al., 2007

1.3.1.2 Behaviour Criteria

As noted above, the existing U.S. NMFS criterion for potential disturbance to marine mammals from airgun-based seismic surveys is 160 dB re 1 μPa (RMS). The noise criteria group concluded that available data are insufficient as a basis for recommending any specific alternative disturbance criteria applicable to multiple-pulse sounds like airgun array sounds (Southall et al., 2007). Other methodologies, including the possible use of a risk continuum function as was used in the SURTASS LFA Sonar FEIS and FSEIS (DoN, 2001a and DoN, 2007a) are being examined for Level B impact assessment for various sources at this time, but none has been applied to the impact analysis for this PEIS.

Acoustic impact criteria applicable to other types of biota are less well developed than are the criteria for cetaceans and pinnipeds. There is an ongoing effort to develop science-based criteria for fish and sea turtles.

2.0 DETAILS OF THE ACOUSTIC IMPACT MODELING

2.1 SOURCE DESCRIPTION AND MODELING

2.1.1 Acoustic Source Levels

As stated previously in Section 1.2 of this appendix, the source levels (peak-to-peak, zero-to-peak, and RMS) and the far-field broadband signal spectrum used for this modeling effort were provided by industry and consist of measured values for the identified "nominal" airgun array modeled throughout this analysis. Since the majority of the threshold criteria use an RMS received pressure level to estimate potential impact to marine mammals, the source will be modeled as a point source with the appropriate beam pattern (for each one-third octave band) and RMS pressure source level.

The exception to this approach is necessitated by the SEL threshold criteria identified in Section 1.3 of this appendix, which uses an integrated energy received level, or sound exposure level (SEL). Typically, the SEL of a signal can be conservatively estimated by the equation:

$$\text{SEL in dB re 1 } \mu\text{Pa}^2\text{-s} \approx \text{SL(RMS)} + 10\text{LOG}_{10}(T_{DUR}])$$

Where:

SL(RMS) = the RMS SL of the pulse in dB re 1μPa @ 1 m.

T_{DUR} = the duration of the dominant pulse.

The difficulty here is in selecting an appropriate value for the duration of the signal, because the spreading of the signal is a function of: a) the source depth; b) the range and depth from the source; and c) the propagation conditions for the modeled site. There is not a simple or easily identified rule or equation which can readily provide the value of the effective spreading of the signal as it propagates out from the source, especially for the various water depth and

propagation modes necessary to represent the entire Gulf of Mexico. However, detailed and accurate calculations of the signal spread is a natural by-product of the acoustic propagation modeling, because the CASS/GRAB model used in this analysis calculates the arrival structure of the numerous acoustic multi-paths that the signal uses for each range and depth step of the overall solution. As part of the acoustic propagation modeling effort described later in this appendix, the signal spread or signal duration was examined for the three depth regions of the Gulf of Mexico, for six different frequencies modeled at each site, for four depth slices in the propagation field out to at least 30 km. The result of this examination was for any multi-path arrival whose received level was within 20 dB of the maximum arrival value for that depth and range from the source, no signal duration exceeded 0.1 s. And most of the signal durations were one or more orders of magnitude below 0.1 s (i.e., they were 0.01 s or less in duration). Therefore, a conservative value of 0.1 s is used for the signal duration for this analysis, with a resulting SEL value of 220 dB re 1 μPa^2-s at one meter from the modeled point source (SEL = 230 + 10 LOG_{10} [0.1] = 220 – 10 = 220 dB re 1 μPa^2-s at 1 m).

2.1.2 Beamforming

Modeling the physical acoustics of airgun operations can be complicated. There are specifically designed and dedicated programs that predict the output characteristics of single airguns and airgun arrays. GUNDALF is one such program. GUNDALF takes into account airgun interactions including non-linearities and interactions between sub-arrays: “No assumptions of linear superposition are made and the engine is capable of modeling airgun clusters down to the 'super-foam' region where the bubbles themselves collide and distort. GUNDALF has been calibrated against both single and clustered guns for a number of different gun types under laboratory conditions and accurately predicts peak to peak and primary to bubble parameters across a very wide range of operating conditions” (Hatton, 2008).

CASS/GRAB is a U.S. Navy standard model that can be run internally and whose performance has been well documented (Weinberg, 2001). While CASS/GRAB does not model bubble interactions, it can (unlike GUNDALF), model the propagation of acoustic energy out to long distances through a complex marine and sub-bottom environment, a necessary part of this study. However, we must first determine how well the CASS/GRAB array beam generator model captures the important features of airgun array operation. To do so we compared GUNDALF results for an airgun array used in this PEIS (Figure A-1) with CASS/GRAB beamforming and propagation runs for the same array parameters. It is important to recognize that although

GUNDALF and CASS/GRAB may perform similar functions/calculations, but they may follow a different order of computation. Most relevant here is that the beam pattern generator of GUNDALF takes into account air/water surface interactions. The CASS/GRAB beam pattern generator model does not; it assumes a free field when calculating the beam pattern. Surface interactions and other environmental factors are taken into account by CASS/GRAB during the propagation modeling step.

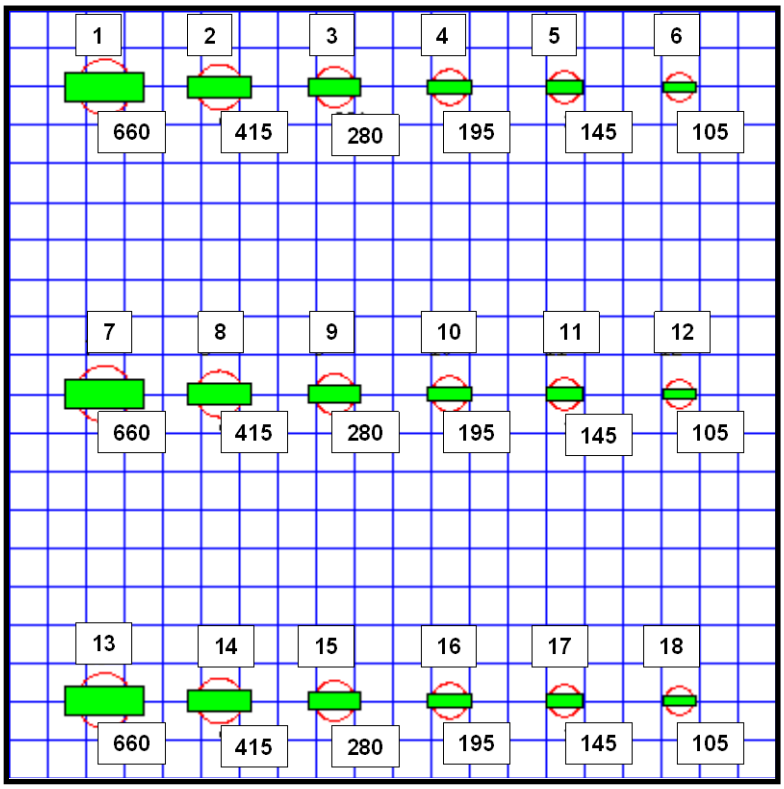

Figure A-1. Airgun Array Used for GUNDALF Modeling and CASS/GRAB Comparison. Values Listed are Airgun Number (above) and Volume in Cubic Inches (below).

The first comparison is between the inline directivity (along the tow axis of the array) and the crossline directivity (perpendicular to the tow axis), as modeled by GUNDALF and by the CASS volumetric array beam pattern model. Figures A-2 and A-4 show the inline and crossline beam patterns, respectively, produced by GUNDALF. In Figure A-2 and A-4, horizontal lines (black and gray) are the frequencies used for comparison with CASS/GRAB model results. The gray arrowhead points out a null, or ghost, at 125 Hz and the white arrowheads point out the peak side beams for the source at 125 Hz. Figures A-3 and A-5 show the inline and crossline beam patterns from the CASS/GRAB array beam pattern model. The beam patterns in these two figures are shown as attenuation in dB, as it is produced and used in CASS/GRAB. The overall beam pattern is well accounted for by the beam pattern-generator model of CASS. Note, however, that the 'ghosting' effects due to interaction with the air/water surface are not accounted for here. They are included later in the modeling process of the CASS/GRAB model. The important issue is the agreement of the overall beam pattern.

There is very good agreement between beam patterns generated by GUNDALF and by the CASS array beam pattern generator. However, an obvious feature that is missing from the CASS beam pattern is destructive interference, or 'ghost' lines, that result from acoustic interaction with the air/water surface. As pointed out above, the CASS beam pattern model does not take into account surface interactions at this stage, whereas they are included in GUNDALF.

In order to verify that the CASS/GRAB model does eventually and accurately include the effects of the surface "ghosting," it is necessary to examine the propagation "field plot" (i.e., modelled transmission loss field, as a function of range and depth) in the immediate vicinity of the array as modelled by CASS/GRAB. Note that with CASS/GRAB the three dimensional volumetric airgun array has been modelled as a point source with a beam pattern, and it is this beam pattern, which includes ocean surface reflections, which will be seen in these field plots. For simplicity here, examples will be given at the lower frequencies where the beam patterns are the simplest (i.e., the fewest side-lobes and generally the widest beams), but comparisons were made for all frequencies up to 1,000 Hz and all bearings (i.e., -90 to +90 degrees) and the CASS/GRAB model demonstrated very good agreement with that produced by the GUNDALF model.

At 75 Hz, the CASS/GRAB field plots for inline and crossline directions are show in Figures a-6 and A-7. As expected when compared to the gray lines at 75 Hz in Figures A-2 and A-4, the main beam points directly downward and it is about 100 degrees wide (50 degrees to each side of vertical) and there is no ghost null. Also, there are no real side lobes or side beams at this frequency. Note also that all of the field plots presented here do not have equal range and depth scales, so care must be taken when measuring angles in these figures. As the frequency increases in Figures A-2 and A-4, the main beam width continues to decrease, until at about 125 Hz the ghosting null nearly completely eliminates the main beam at a directly downward direction. Figures A-8 and A-9 show the inline and crossline field plots for the CASS/GRAB model at 125 Hz. Note the that the downward beam is greatly reduced and actually less than the side beams, which occur at about 60 and 50 degrees, respectively for the inline and crossline cases. As the frequency continues to increase to 175 Hz, Figures A-10 and A-11, the CASS/GRAB main beam has grown again to a width of about 70 or 50 degrees for the inline and crossline cases, respectively, and a strong ghost null is present at about 45 degrees and a small side lobe at about 70 to 80 degrees.

For completeness, examples of CASS/GRAB field plots are also provided for 300 Hz (Figures A-12 and A-13) and 1,000 Hz (Figures A-14 and A-15).

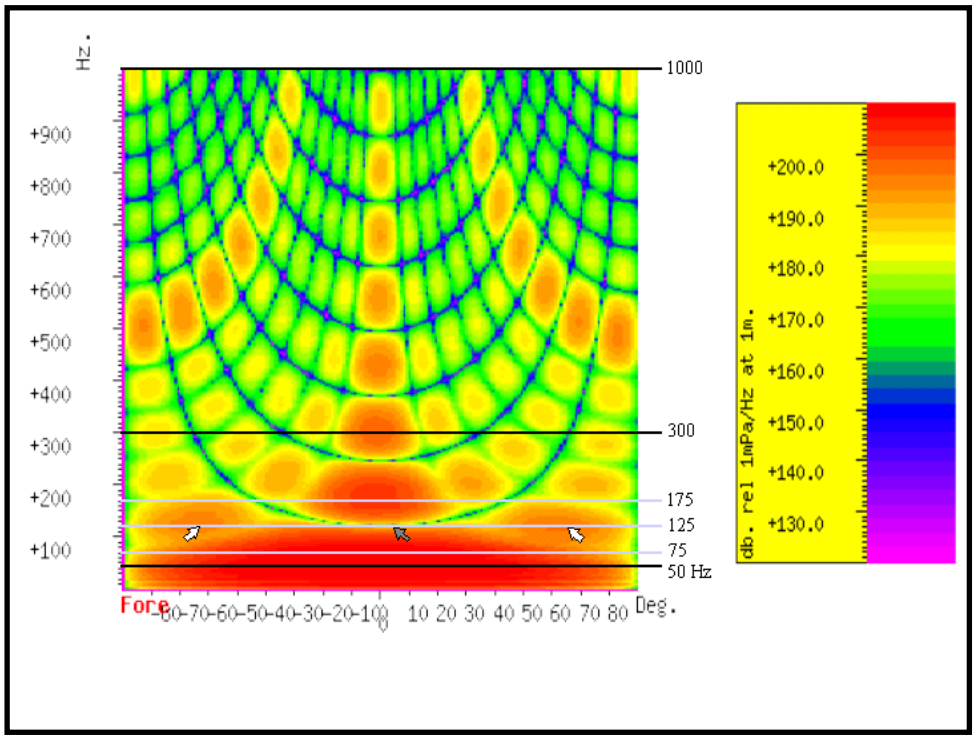

Figure A-2. GUNDALF Array Beam Pattern - Inline Direction (i.e., along the tow axis of the array).

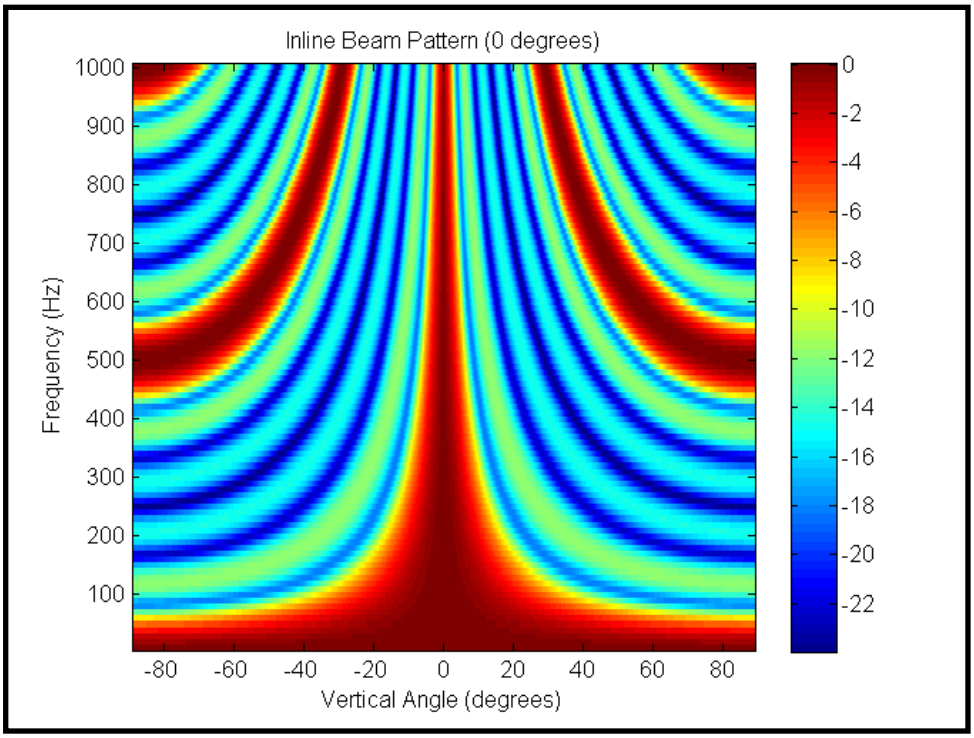

Figure A-3. CASS/GRAB Array Beam Pattern – Inline Direction.

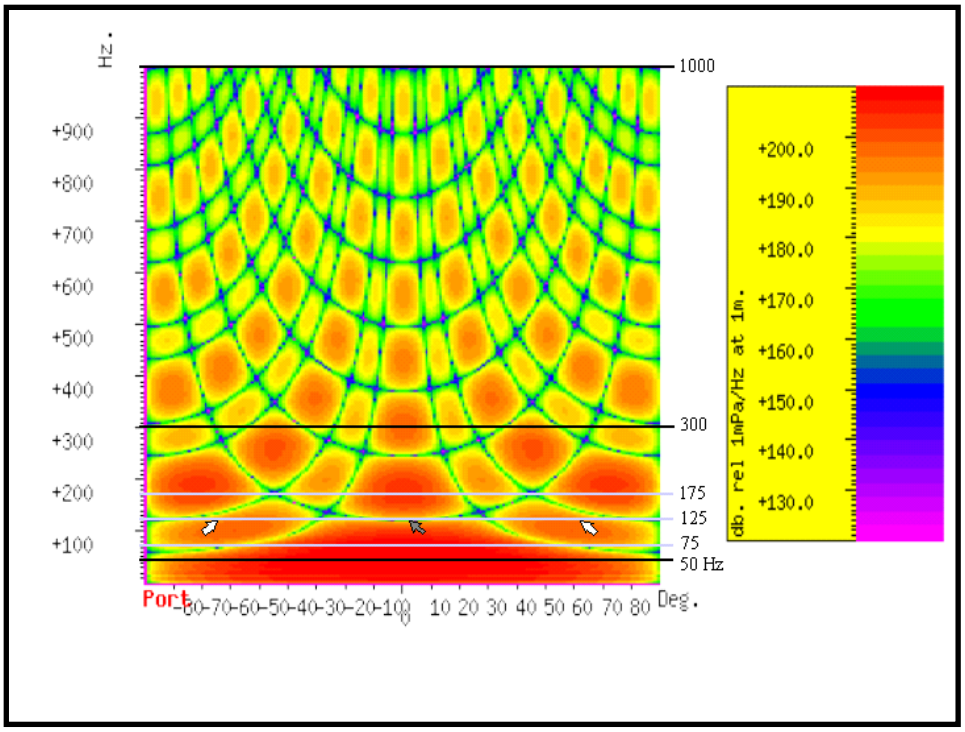

Figure A-4. GUNDALF Array Beam Pattern - Crossline Direction (i.e., perpendicular to the tow direction).

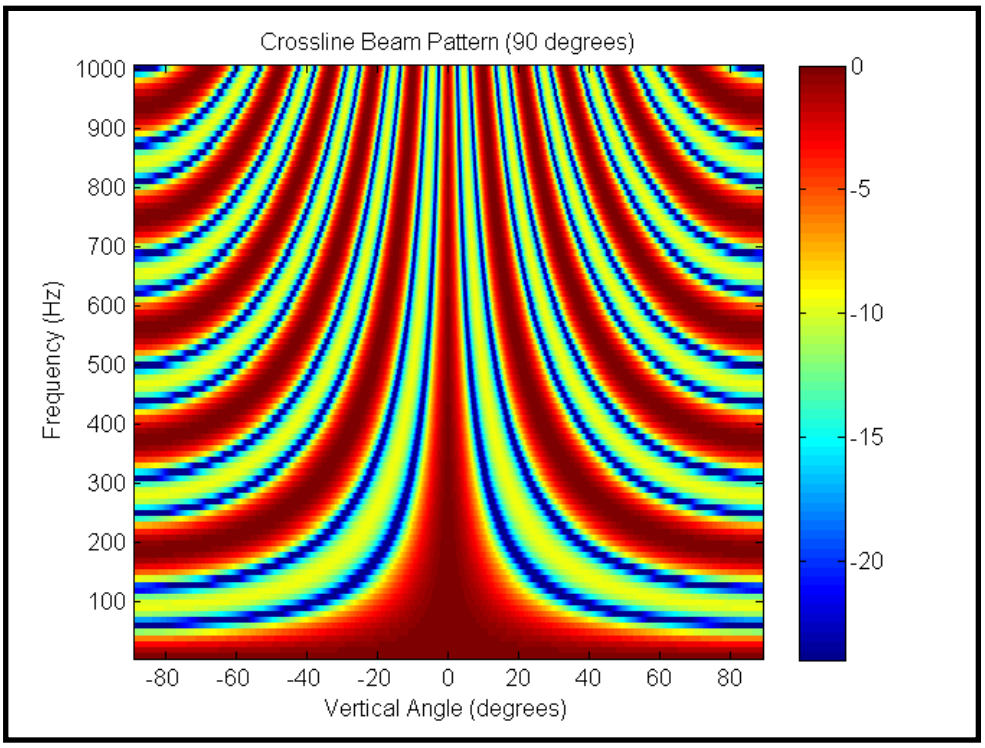

Figure A-5. CASS/GRAB Array Beam Pattern – Crossline direction.

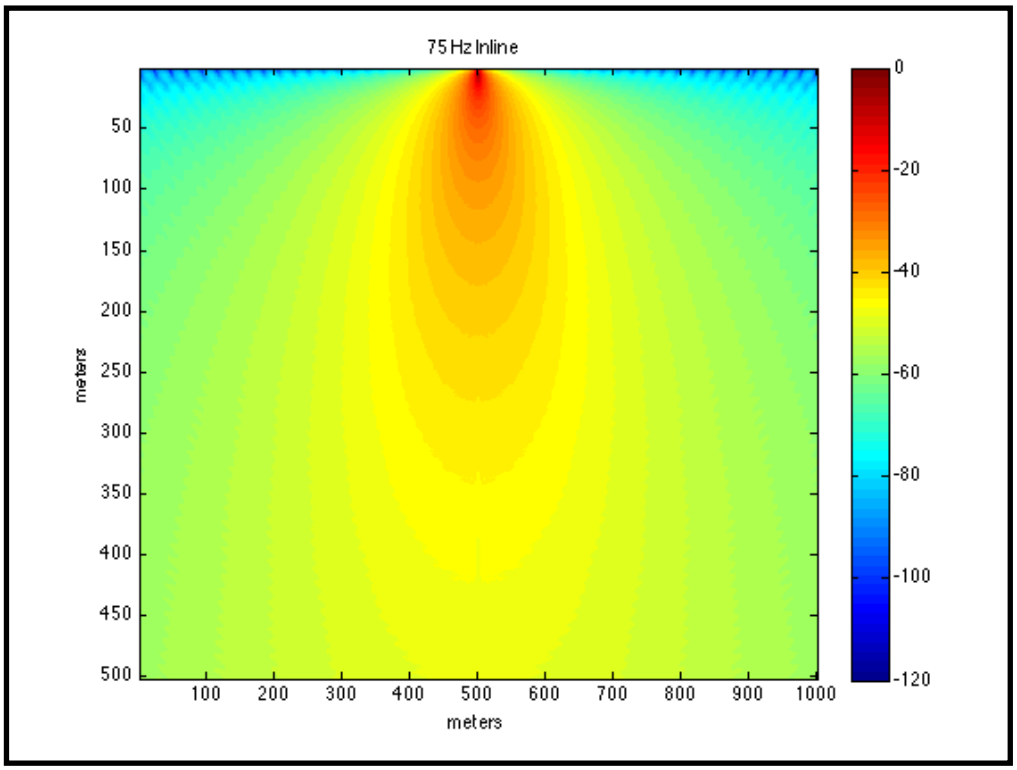

Figure A-6. CASS/GRAB Inline Field Plot for 75 Hz.

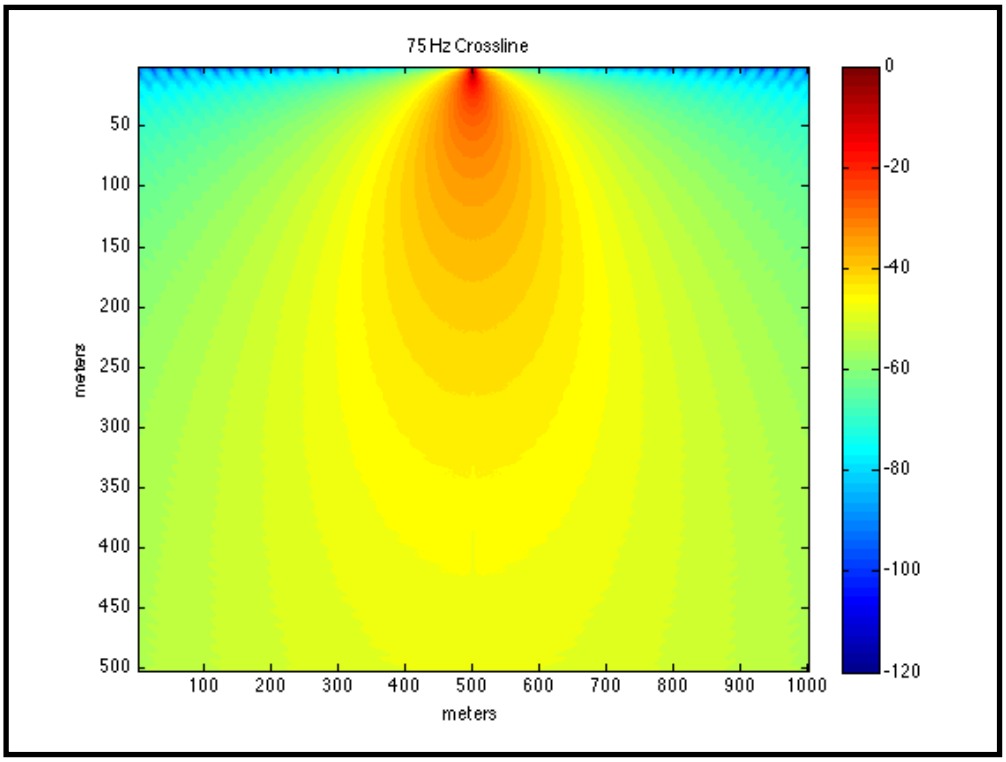

Figure A-7. CASS/GRAB Crossline Field Plot for 75 Hz.

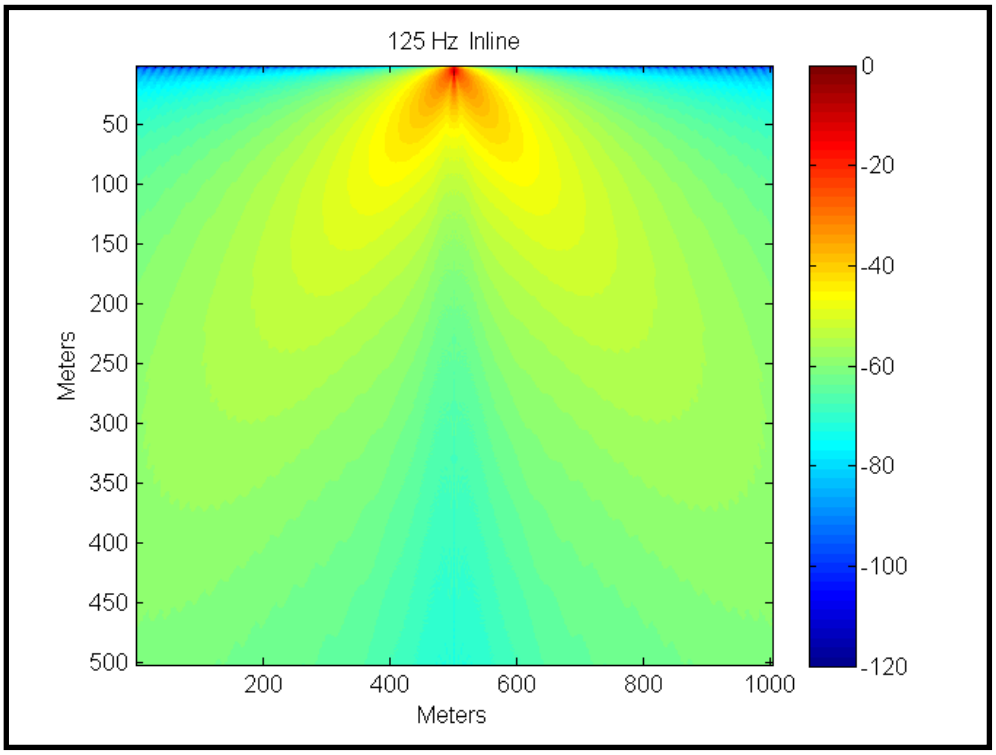

Figure A-8. CASS/GRAB Inline Field Plot for 125 Hz.

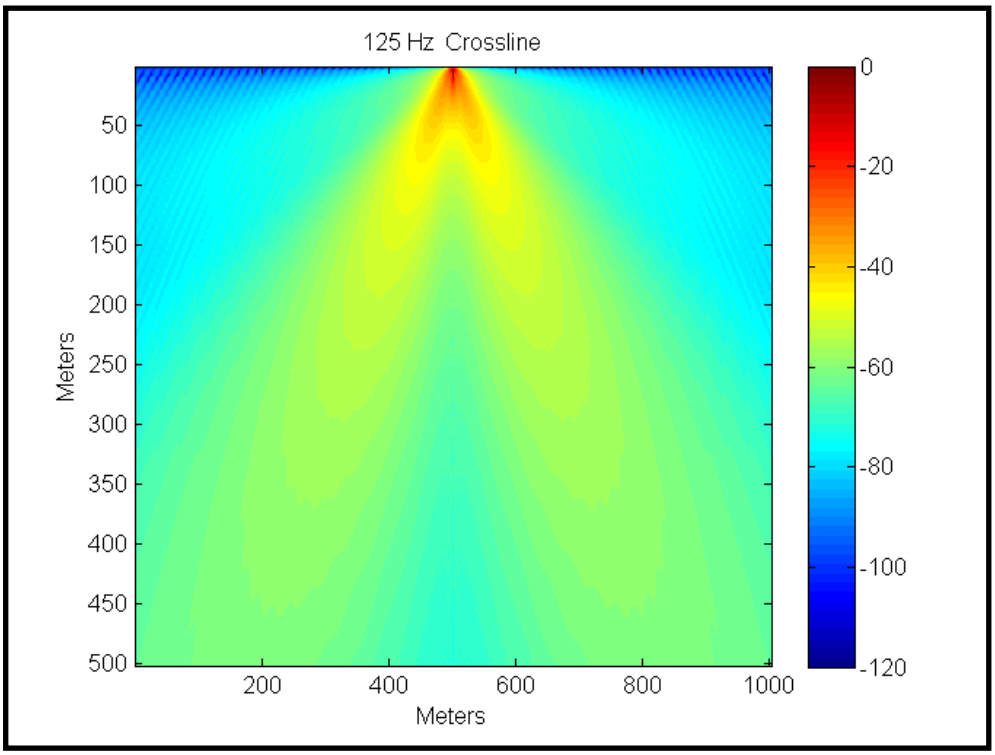

Figure A-9. CASS/GRAB Crossline Field Plot for 125 Hz.

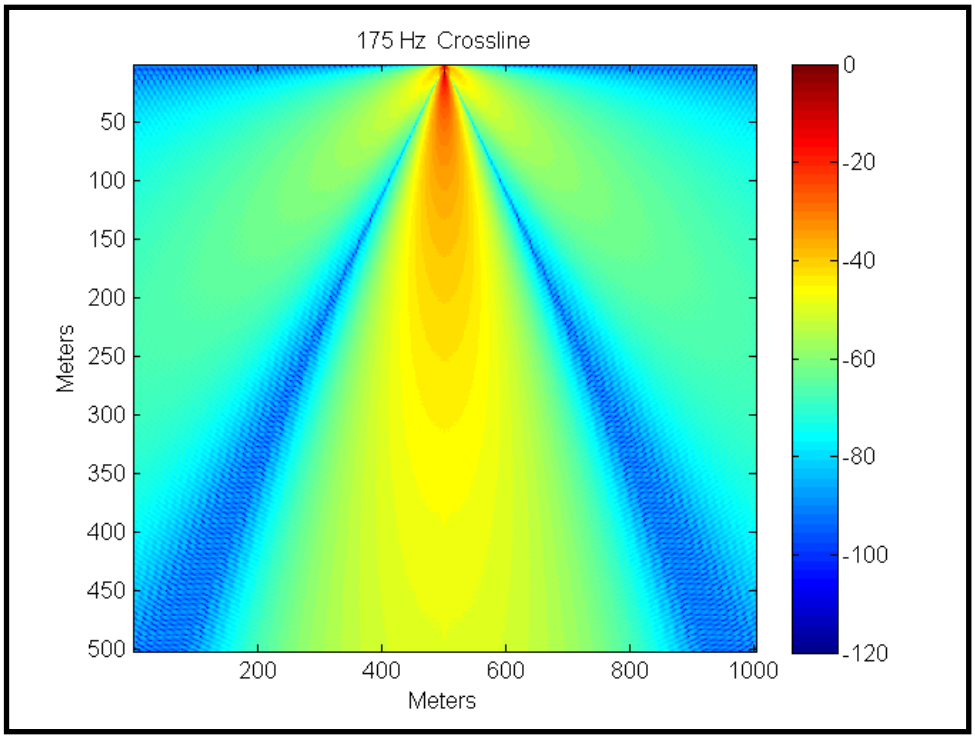

Figure A-10. CASS/GRAB Inline Field Plot for 175 Hz.

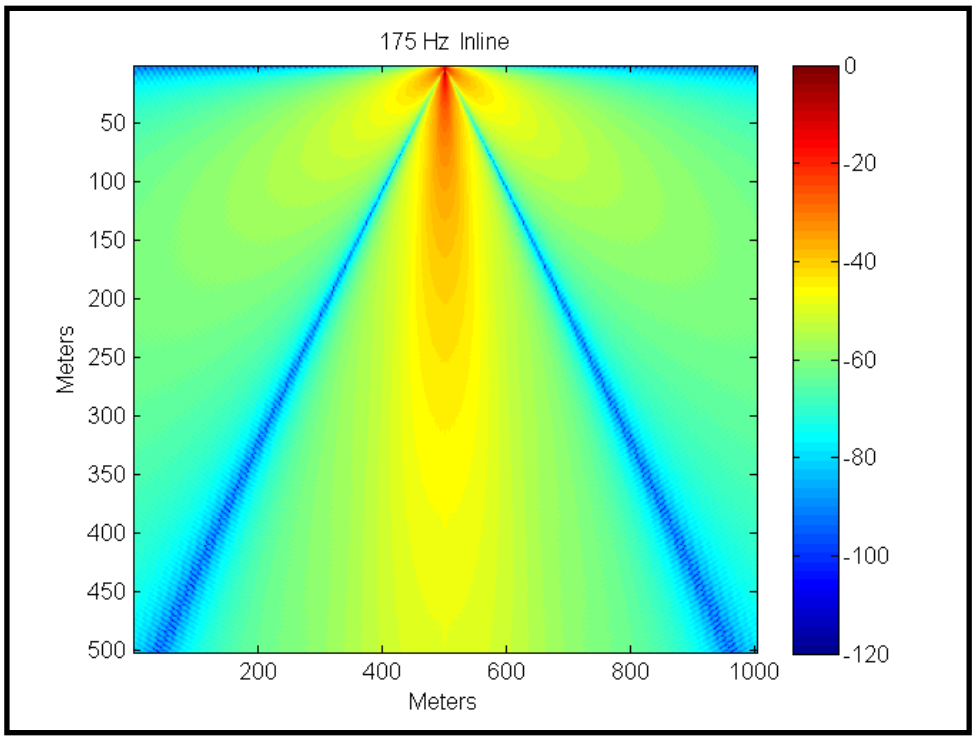

Figure A-11. CASS/GRAB Crossline Field Plot for 175 Hz.

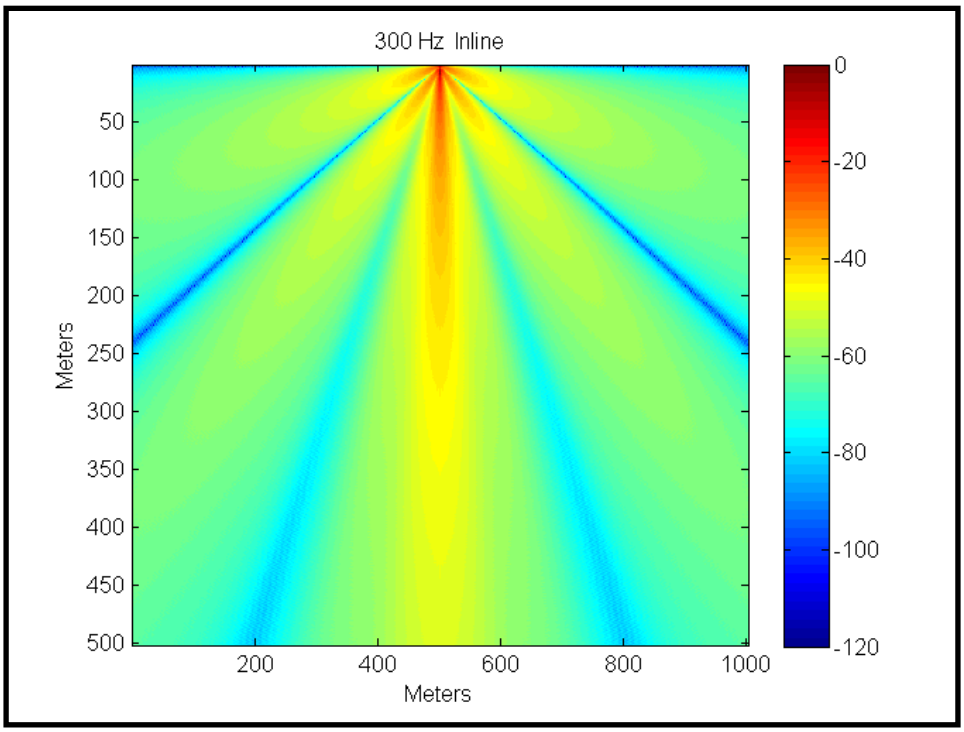

Figure A-12. CASS/GRAB Inline Field Plot for 300 Hz.

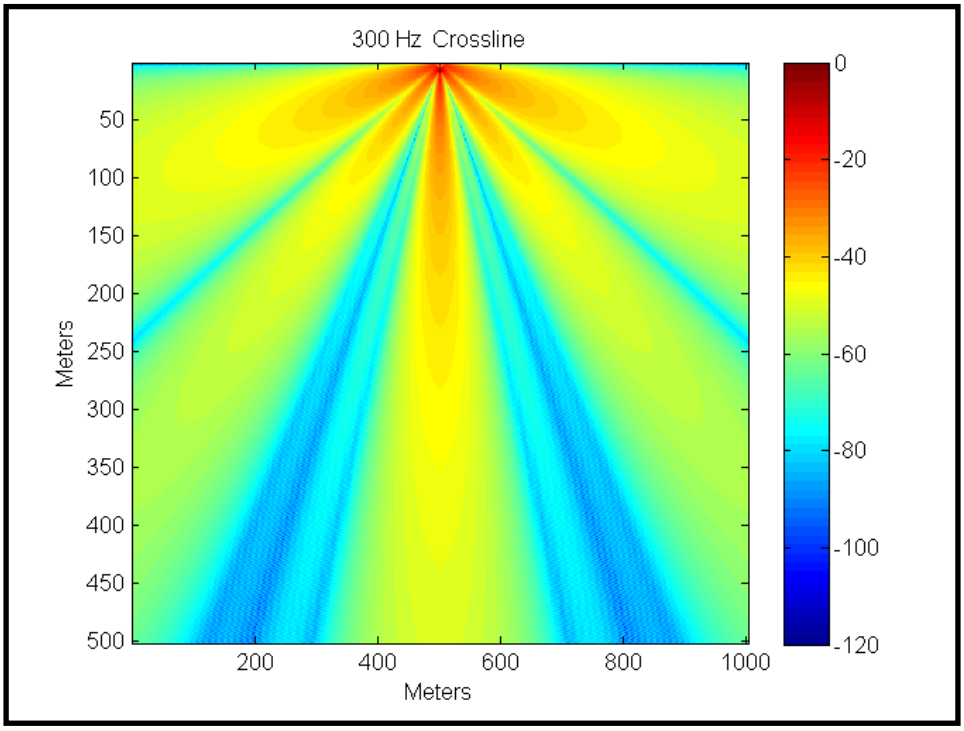

Figure A-13. CASS/GRAB Crossline Field Plot for 300 Hz.

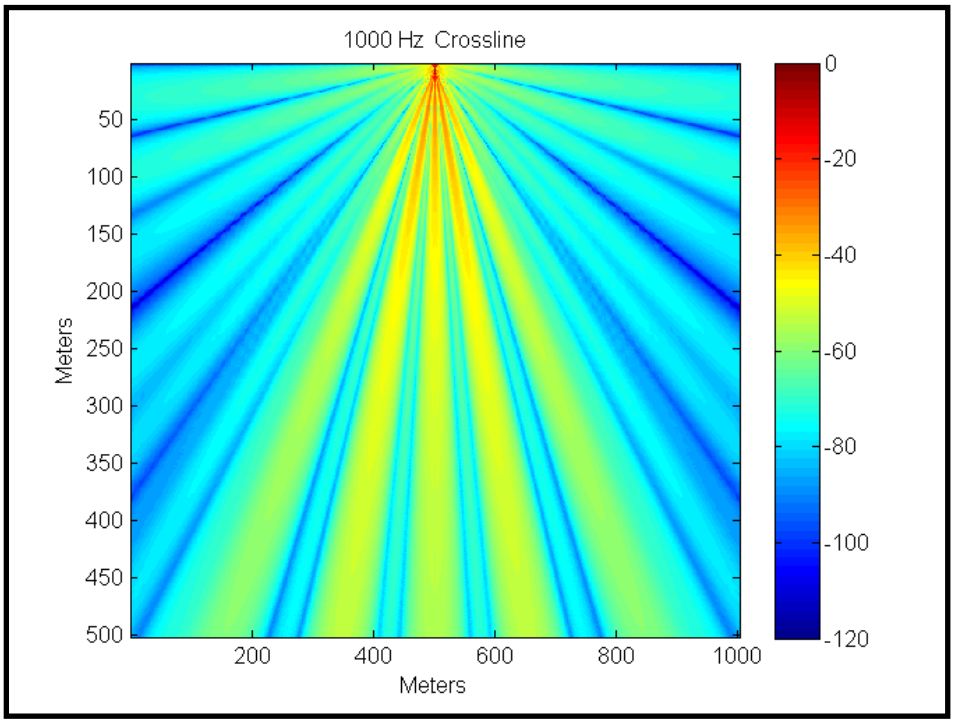

Figure A-14. CASS/GRAB Inline Field Plot for 1,000 Hz.

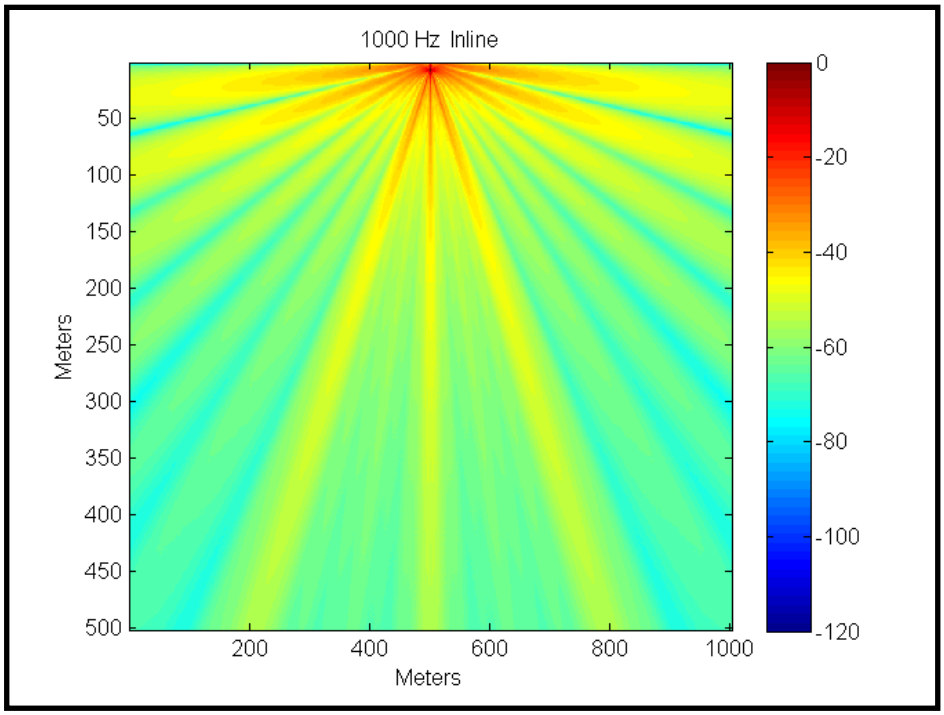

Figure A-15. CASS/GRAB Crossline Field Plot for 1,000 Hz.

2.2 SURVEY OPERATIONS

Details of the various survey types and how they were modelled are provided in Section 2.6 of this appendix.

2.3 M-WEIGHTING

Southall et al. (2007) formally introduced the concept of M-weighting, which is designed to account for the different hearing sensitivities of different groups of marine mammals. The basic M-weighting functions are shown in Figure A-16. For all analyses in this document, M-weighting will only be applied to MMPA Level A impact calculations, and then only when specifically identified.

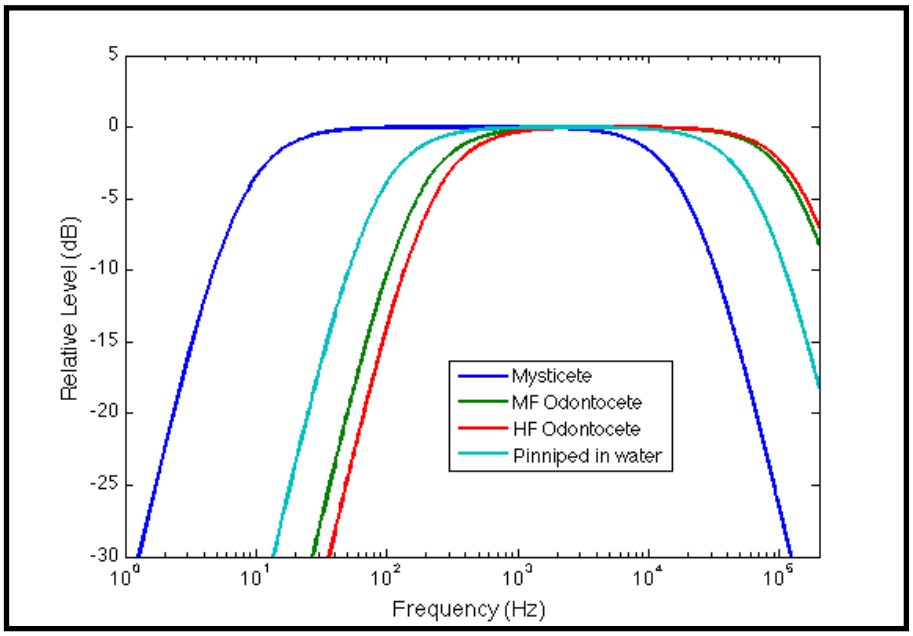

Figure A-16. M-weighting Functions for In-water Marine Mammal Species.

The goal of this section is to explain the conversion of these spectral presentations into a scalar that represents the effect of M-weighting upon a broadband source. Figure A-17 shows the spectrum of an airgun signal as simulated by the GUNDALF model (Hatton, 2008) as a black line. The spectrum was then weighted by summing the spectrum of the airgun with the M-weighting functions for the mysticete and mid-frequency (MF) odontocetes categories. The difference between the M-weighted and flat curves was then determined and shown as the red and blue curves, respectively.

Subsequently, the amplitudes were converted from decibels to pressure values for each curve, and the pressures for frequencies between 10 and 1,000 Hz were then summed. Frequencies below 10 Hz were excluded as a conservative application of the M-weighting functions. The

ratio of the sums of the M-weighted and un-weighted pressures were then converted back to decibels. These scalar values represent the net difference in the received level at the animal due to the effects of M-weighting and are presented in Table A-3.

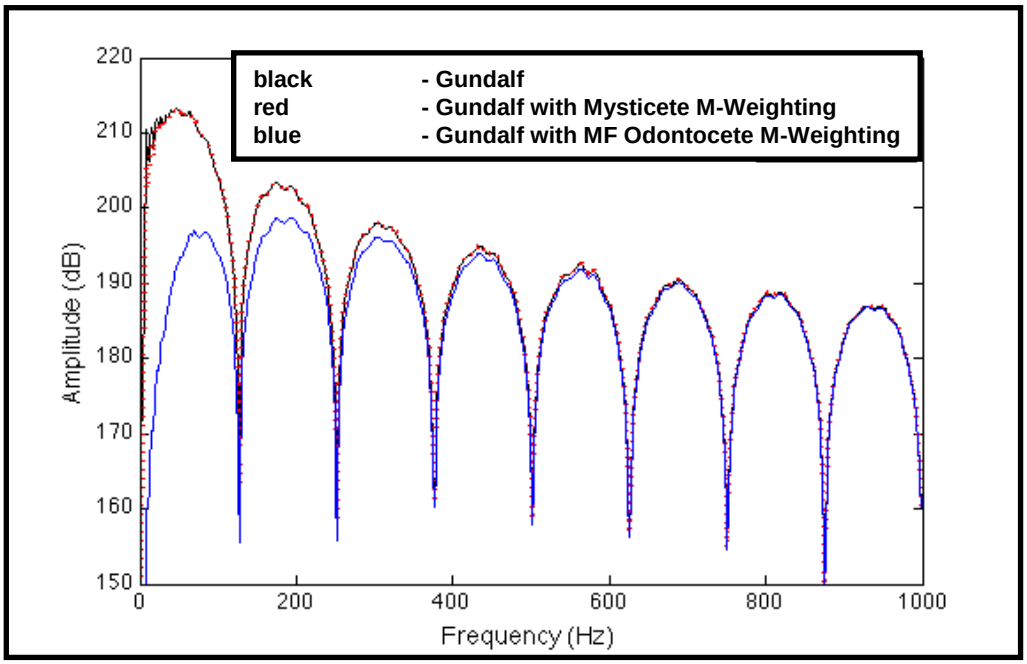

Figure A-17. Effect of M-weighting on Airgun Frequency Spectrum.

This procedure accounts not only for the effect of the M-weighting, but the spectral characteristics of the original signal itself. The scalar values in Table A-3 should be applicable to most, if not all, airgun signals, but not other broadband signals. This procedure can be repeated for other broadband signals with other spectral characteristics.

Table A-3. Scalar Offset values for M-weighting.

M-weighting Class	dB offset
low-frequency cetaceans	-0.3
mid-frequency cetaceans	-10.4
high-frequency cetaceans	-12.2
pinnipeds in water	-6.5

2.4 ENVIRONMENTAL MODELING

2.4.1 INTRODUCTION

As previously mentioned in Section 1.2, the acoustic modeling effort involved two main steps: (1) physical acoustic modeling to predict the three dimensional (3-D) underwater sound field around airgun sources; and (2) use of a second model to determine and correctly interpret the exposure of marine animals exposed to that sound field. The Acoustic Integration Model (AIM) will be used to complete the second step and that will be discussed further in Section 2.6 below. This section will describe the environmental modeling methodology used to characterize the sound field around the airgun sources.

The overall approach to the environmental modelling effort is to use the best available propagation models and databases to characterize the underwater sound propagation for the Gulf of Mexico (i.e., those portions of the northern Gulf of Mexico regulated and leased by BOEM and potentially those regulated by the various states too) for potentially, year-round source operations. Due to the nature of the airgun sources, the frequency range of interest was identified to be between 50 and 1,000 Hz. Although airguns can and do produce acoustic energy above 1,000 Hz, the reduced source levels at these frequencies (i.e., typically 20 to 30 dB less than the maximums at frequencies between 50 and 200 Hz (see Figure A-2) or measured at more than 70 dB less than the maximum values (note that the difference between these two spectrums is that for the former the values are modelled at the source, and for the latter they are measured at 9,000 meters after propagation loss, where higher attenuation selectively reduces the higher frequency portion of the spectrum), along with the increased attenuation of acoustic signals as frequency increases, ensure that using 1,000 Hz modelling adequately and conservatively represents this higher frequency portion of the spectrum. Because of the requirement to ensure that the frequency-dependent beamforming and source spectrum levels of the sources is appropriately accounted for in the modelling, an eigenray propagation model was selected for ease of examining numerous intermediate stages of the results in the modelling effort.

2.4.2 POTENTIAL ISSUES WITH MODELING METHODOLOGIES

Three potential issues arise due to the identified need to model shallow water in the Gulf of Mexico. The first issue is that the combination of the shallow water depth and the lowest frequencies to be modeled (i.e., 25 to 50 Hz) ensure that the acoustic propagation model (CASS/GRAB) is operating at the edge (or even slightly beyond the edge) of the "2 Pi lambda" limitation of the physics upon which the model is based (i.e., two times Pi times the wavelength of the frequency being modeled). Beyond this limitation, the accuracy and reliability of the model's results degrades in unpredictable ways (i.e., minor changes in a seemingly innocuous parameter may cause a rapid change in the results). During the modeling effort, extra care was taken to examine the shallow water modeling results for these frequencies to determine if any unpredicted behavior occurred in these results. The combined facts that: a) no unusual results were observed, and b) these low frequencies were not the dominant contributors to the spectrum of the received acoustic energy, indicates that any error arising for this reason should not be considered significant.

The second issue also results as a combination of the water depth and frequency of the transmitted signal. The eigenray model, as it was used here, assumes that the source is a sufficient distance from any boundaries (i.e., the surface and the ocean bottom) so that a far-field beam pattern can be superimposed on the calculated eigenrays as corrections to the source level. These corrections are a function of azimuthal bearing and angular difference from the main lobe or the vertical reference. In actuality, for the lowest frequencies examined, the beam pattern probably does not completely form in the shallow water case before the acoustic energy interacts with the bottom. This complication is reduced somewhat by the fact that the main source of acoustic energy propagating out from the source comes from the angles nearer to the horizontal plane and not the more vertical rays, which do interact with the bottom frequently and rapidly attenuate. The near-horizontal rays generally have a greater distance to travel before bottom interactions. As will be shown later in this section, the generally iso-velocity character of the sound velocity profiles for the modeled shallow water area, will allow these near-horizontal rays to propagate with limited surface and bottom interaction, or at very low grazing angles (i.e., low levels of reflection loss) and thus be the driving factor for received acoustic energy at ranges beyond approximately the first kilometer.

The third and final issue is the degree of accuracy with which the bottom parameters are known and modeled, especially for the lower frequencies, which are much more capable of penetrating the sediment. As will be discussed below, this modeling effort generally used a "representative" value for the range of parameters available or possible in the modeled areas, but also tended to err on the conservative side by using those parameters which resulted in a lesser value of transmission loss (i.e., a higher received level at the modeled animals). Therefore, the possible detrimental effects of this issue are minimized in the modeling parameters selected. Finally, it should be noted that for a "representative" study like this one, the results should not be compared to measured data of any type, especially for a specific situation, without exercising extreme care.

2.4.3 MODELING PARAMETER AND DATABASE SELECTIONS

The following discussion specifies the acoustic propagation model, input databases and other support data used to model and characterize the year-round propagation expected to be present in the Gulf of Mexico. All models and databases needed to be capable of handling the entire spectrum of conditions potentially present in the Gulf of Mexico (i.e., those portions of the northern Gulf of Mexico regulated and leased by BOEM), from the very shallow near-coastal waters out to the deep waters of the Gulf. Additionally, this section will identify the methodology used to select a limited number of representative sites, which are then used to adequately characterize the acoustic propagation of airgun sources throughout the specific area.

2.4.3.1 Acoustic Propagation Model

The acoustic propagation model is the U.S. Navy standard Comprehensive Acoustic Simulation System (CASS) Model version 4.0 and the Gaussian Ray Bundle (GRAB) version 2.0. CASS provides the interface to the various environmental, system and propagation models available and already embedded in it, while GRAB (the default eigenray calculation model) was the actual eigenray calculation engine used for these calculations. CASS/GRAB is a range-dependant

model that is capable of incorporating the specific beam patterns produced by the airgun array (for the full range of specific frequencies selected) and the historic environmental parameters for the ocean sound velocity profile, bathymetry, ocean surface conditions and the characteristics of the ocean bottom. Officially, GRAB can accurately model active-source range-dependent propagation and reverberation for frequencies from 150 Hz to 100 kHz (OAML, 2002). However, additional testing of the model down to 50 Hz has been conducted satisfactorily and it is believed that eventually the official frequency range for this model will be expanded to recognize this fact.

2.4.3.2 Sound Velocity Profiles

The ocean database used to supply the sound velocity profiles (SVPs) used in this study is the U.S. Navy standard Generalized Digital Environmental Model Variable Resolution (GDEM-V) database, version 3.0. GEDM-V provides a global-gridded monthly mean (and standard deviation) of ocean salinity and temperature. For the region being studied here, this database provides resolution of 15-arc minutes in both latitude and longitude. A plot of the GDEM-V province numbers for the Gulf of Mexico (Figure A-18) shows a total of 5 provinces, identified as 159, 166, 176, 183 and 181, in the portion of the Gulf of Mexico covered by this document (i.e., the area north of the thick black line in Figure A-18). Two of these provinces only occur for a very small area (i.e., <1% of the area of the Gulf of Mexico being studied) and only adjacent to the area's boundaries in the extreme southeastern portion of the study area (i.e., roughly in the vicinity of the Florida Keys and the Dry Tortugas Islands). For simplicity, these two GDEM-V profiles, 181 and 183, will not be analyzed further. The remaining three profiles, 159, 166, and 176 will be used for all subsequent acoustic propagation modeling. A plot of the average monthly values for each of these three provinces (Figures A-19, A-20 and A-21) shows the monthly changes to the profiles throughout the year.

For each of the three provinces, representative SVPs were selected for each of the four seasons and the resulting modeled propagation predictions were examined. It was determined that, as expected, the summer and winter propagation conditions were the extremes of the environment, and in all cases sound propagated better during the winter. In shallow water, both seasons were effectively iso-velocity, which resulted in minimal differences in transmission loss, thus only winter profiles and modeling were used there. But for the deep and intermediate (slope) cases, both the summer and winter profiles were subsequently modeled.).

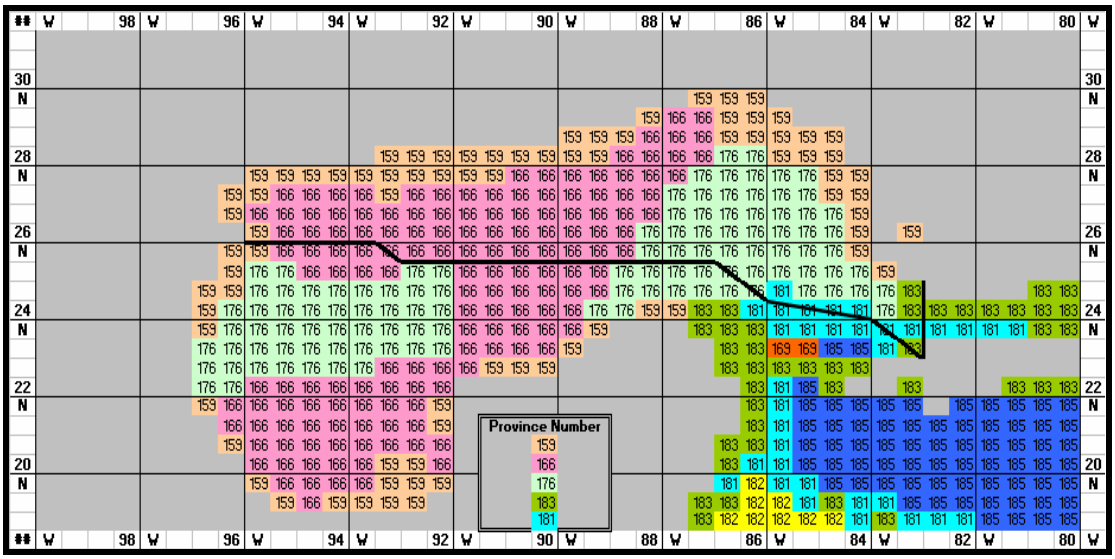

Figure A-18. GDEM Province Numbers Plotted for the Gulf of Mexico.

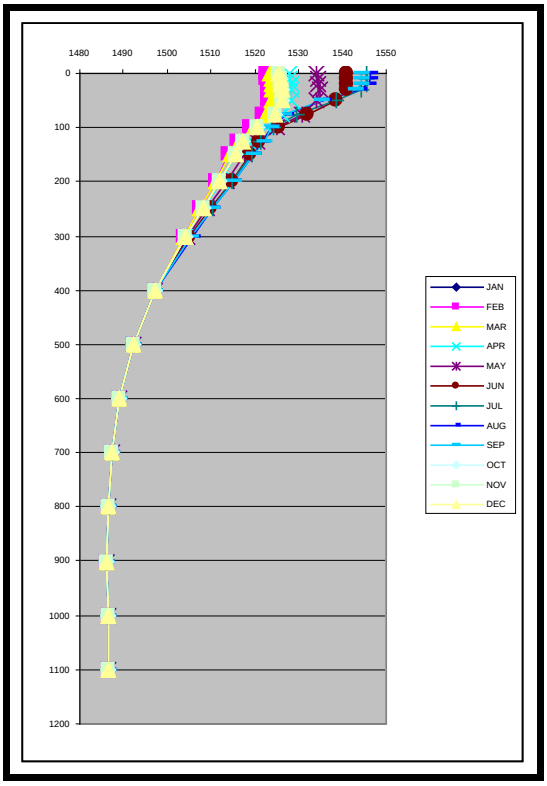

Figure A-19. Average Monthly SVPs for Province 159.

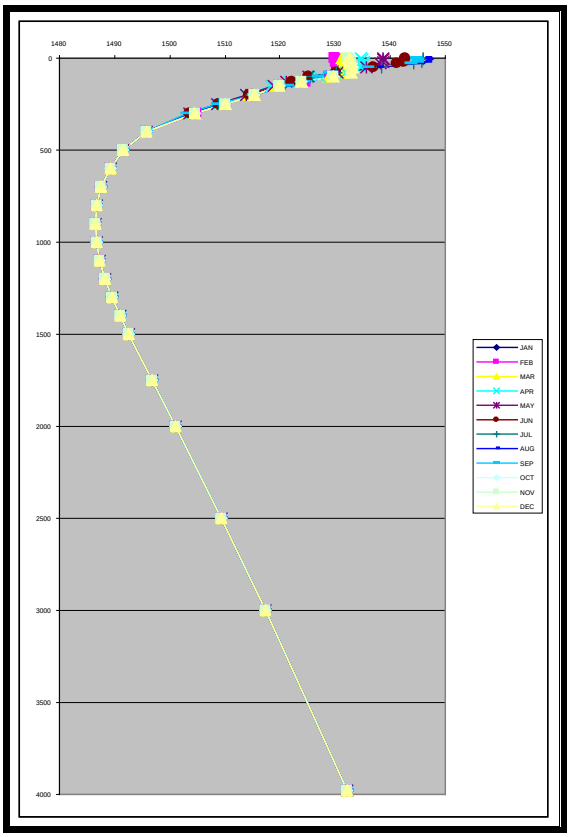

Figure A-20. Average Monthly SVPs for Province 166.

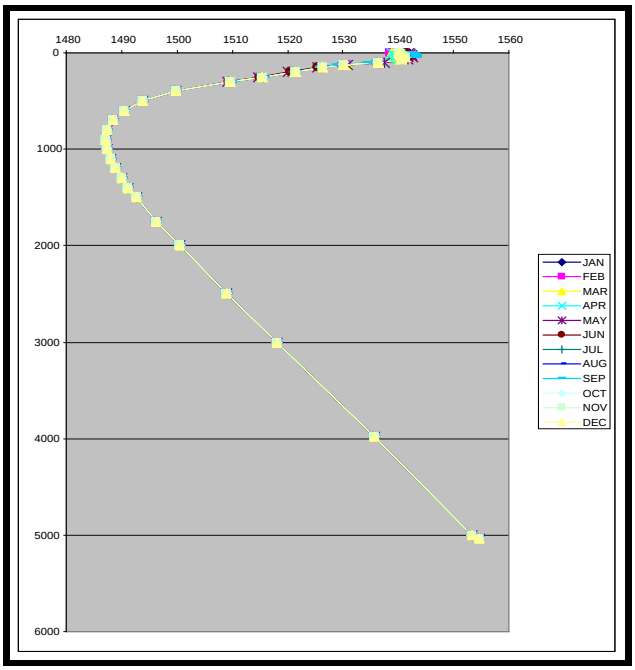

Figure A-21. Average Monthly SVPs for Province 176.

Actual airgun operations during spring, summer, and fall months would likely involve less-efficient sound propagation and therefore reduced potential environmental impact.

2.4.3.3 Bottom Topography/Bathymetry

The bathymetric database used for all modeling in this report is the U.S. Navy standard Ocean Floor Depth Digital Bathymetric Database Variable Resolution (DBDB-V), version 4.3 (level 0) (OAML, 2002). This is an unclassified version of the database that provides 0.05 arc-min data resolution in the modeled area for both latitude and longitude.

2.4.3.4 Bottom Loss

The CASS/GRAB acoustic model was used to predict transmission loss at each site. Integral to the CASS/GRAB model is the Rayleigh bottom loss model, which predicts the amount of acoustic energy loss as the eigenray is reflected off the bottom. The Rayleigh bottom loss model predicts the amount of loss as a function of incident angle of the acoustic propagation path to the bottom and the frequency being modeled. The Rayleigh bottom loss model assumes that a simple harmonic plane-wave is reflected from an interface between two fluids that have different sound speeds and densities. The characteristics of the bottom sediment determine the values of different sound speeds and densities. Bottom sediment characteristics were determined by using the NOAA National Coastal Data Development Center (NCDDC) Coastal Ecosystems Program database for the Gulf of Mexico (NOAA-NCDDC, 2009). The Gulf of Mexico sediment database depicts shelf sediment textures, hard banks, and gravel deposits on the continental shelf of the U. S. Gulf of Mexico as a map and is summarized from numerous different sources (DoN, 2007c). The sediment database was prepared from existing sources to accompany an Environmental Impact Statement, and displays general classification of bottom sediments (using the Shepard pyramid) throughout the Gulf of Mexico. It was provided by the U.S. Department of the Interior, Minerals Management Service, and Gulf of Mexico OCS Regional Office. Inputs to the Rayleigh bottom loss model sound speed differences and sediment density were inferred using the Applied Physics Laboratory-University of Washington (APL-UW) method and grain size determined from the NCDDC database.

2.4.4 Combining SVP, Bathymetry, and Bottom Sediment Data to Identify Modeling Areas

Next, the geographic distribution of the preceding three sets of data (i.e., SVP, bathymetry and bottom sediment type) were examined to identify regions of similar characteristics in order to simplify and reduce the acoustic propagation (and subsequently AIM) modeling effort, but yet adequately represent the conditions present in the Gulf of Mexico. Additionally, since marine animal distribution and density for each species also vary throughout the Gulf of Mexico, consideration of animal geographic distribution preferences were also taken into account. Section 2.5 of this appendix describes the data used to model the specific animal density for any location in the Gulf of Mexico, but in general the marine mammals can be roughly identified as shelf (i.e.,

shallow water), slope, or deep water species, for any given season. This characterization does not preclude a species presence in other water depths during that season, but it does indicate where that population may be concentrated and the range over which it is distributed.

When the SVP, bottom sediment type, bathymetry and Shelf Planning Areas were overlaid, it was determined that there was a natural and reasonable division of the Gulf of Mexico into nine regions, each of which had a nearly universal value for its various acoustic modeling parameters. For example, all three shallow (shelf) regions have the SVP profile # 159 as their predominant profile Table A-4 list the nine regions and the acoustic parameter species descriptor associated with it.

Table A-4. Regions of the Gulf of Mexico and Pertinent Parameters.

#	Acoustic Parameters			Geographic Parameters	Biological Parameters
	Water Depth	**SVP Profile**	**Sediment Type**	**Shelf Planning Area**	**Species Type**
1	shallow	159	sand (2.5)	Eastern	shelf
2	shallow	159	sand (2.5)	Central	shelf
3	shallow	159	sand (2.5)	Western	shelf
4	slope	159	sand (1.5)	Eastern	slope
5	slope	159	sand (1.5)	Central	slope
6	slope	159	sand (1.5)	Western	slope
7	deep	176	clay (9.0)	Eastern	deep
8	deep	166	clay (9.0)	Central	deep
9	deep	166	clay (9.0)	Western	deep

Note: 1) Water depth definitions: shallow 0-200 m, slope 200-1,000 m, deep >1,000 m.
2) Number in parentheses after the sediment type is the grain size.

Essentially, these nine regions can be further consolidated into four representative acoustic propagation modeling sites by:

- combining the three shallow sites into one site,
- combining the three slope sites into one site, and
- combining sites 8 and 9 into one site.

This was done and since a specific site, with azimuthally-dependent bathymetry, is necessary for the acoustic propagation modeling by the CASS/GRAB model, representative sites with specific latitude and longitude coordinates were selected for each of the four acoustically modeled sites (Table A-5, Figure A-22).

Table A-5. Acoustic Modeling Regions of the Gulf of Mexico and Representative Sites.

Model Site	**Region**	**Acoustic Parameters**			**Geographic Location**	
#	#	**Water Depth**	**SVP Profile**	**Sediment Type**	**Latitude**	**Longitude**
1	**1, 2, 3**	shallow	159	sand (2.5)	28° 15.0’ N	094° 00.0’ W
2	**4, 5, 6**	slope	159	sand (1.5)	27° 50.0’ N	092° 30.0’ W
3	**7**	deep	176	clay (9.0)	27° 15.0’ N	093° 30.0’ W
4	**8, 9**	deep	166	clay (9.0)	28° 00.0’ N	086° 30.0’ W

2.4.4.1 Wave Height or Surface Wind

With the identification of the parameters associated with the four acoustic modeling sites above and their associated environmental acoustic parameters (i.e., specific bathymetry, SVPs and bottom sediments that are associated with each site), the only environmental parameter that still need to be identified before acoustic modeling can occur is the surface wave height or the representative surface wind speeds for each site. Data from NOAA’s National Data Buoy Center (NDBC) were retrieved for buoy Number 42019, which is located off Freeport, Texas at 27° 54' 47"N, 95° 21' 36"W (NOAA-NDBC, 2008). This NDBC buoy is on the continental shelf, near the shelf edge and far enough offshore to be exposed to winds similar to those that would be observed near modeled sites # 1, 2, and 3. Thus it was used to model the wind conditions for all locations. These buoy data show a strong seasonal pattern of higher wind speeds and wave heights during the winter and reduced wind speeds and wave heights during the summer (Figures A-23 and A-24; NOAA-NDBC, 2008). During the winter average wind speed can be as high as 15 knots (kts), while in summer the average wind speed is about 8 kts. Similarly, the mean peak wind speeds approaching 20 kts in winter and dipping to near 10 kts in summer. The extremes of the wind speed distributions follow the same pattern, with the lowest values observed in July.

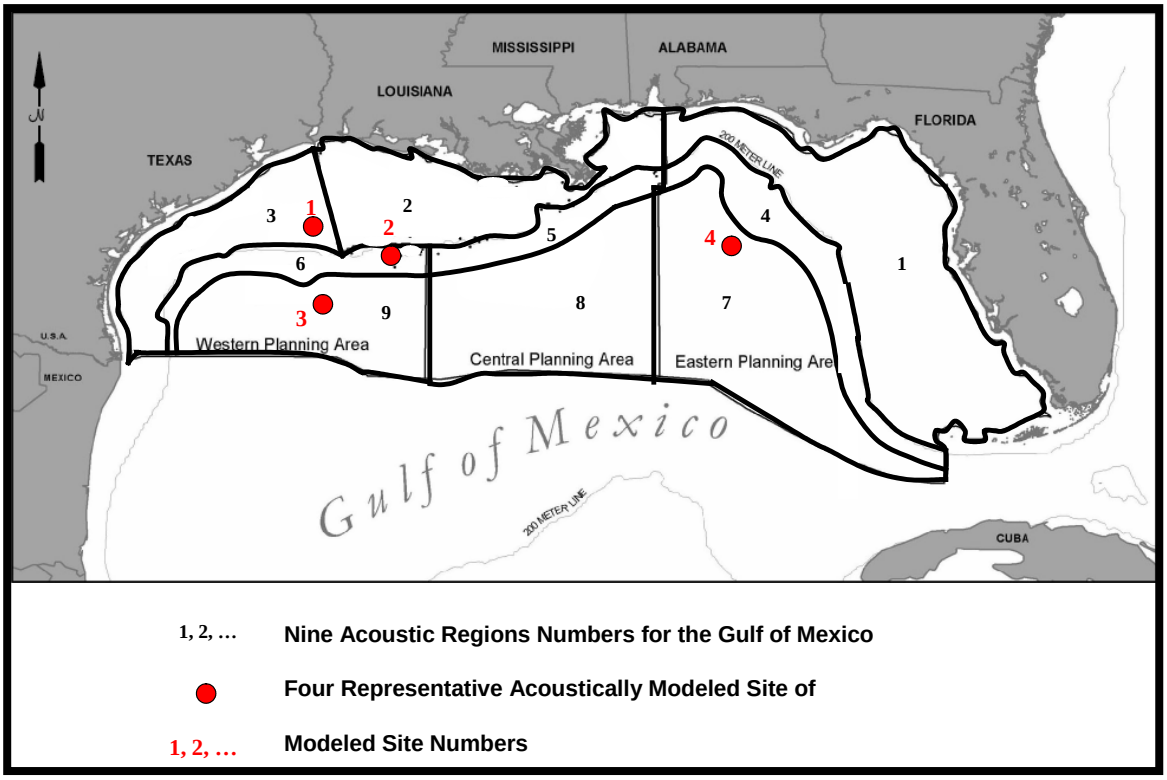

Figure A-22. Acoustic Regions and Representative Model Sites in the Gulf of Mexico.

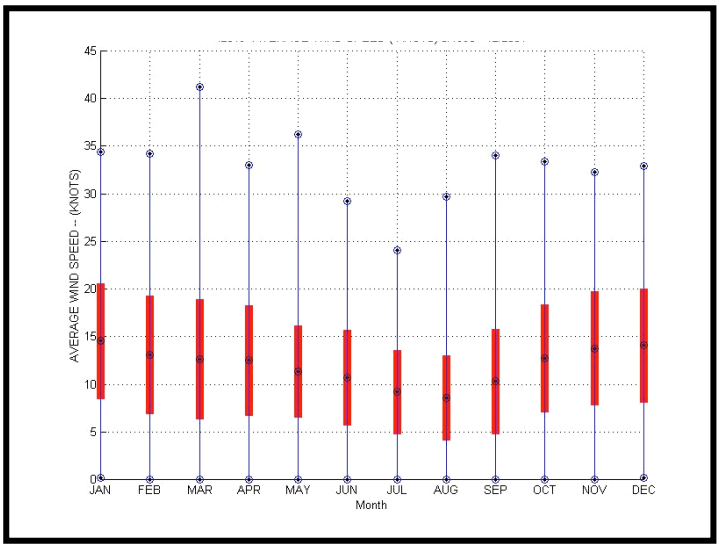

Figure A-23. Average Wind Speed Data Collected Near the Modeling Sites (NOAA-NDBC, 2008).

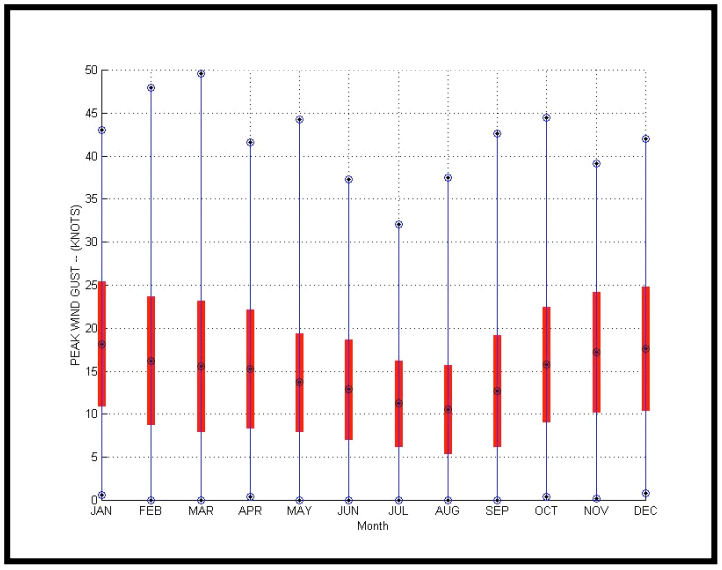

Figure A-24. Peak Wind Speed Data Collected Near the Modeling Sites (NOAA-NDBC, 2008).

Wave height data were also collected at the NDBC buoy (NOAA-NDBC, 2008). A plot of the wave height data (Figure A-25) shows the same strong seasonal pattern as the wind speed data, with mean wave heights approaching 1.5 m in winter and dipping to below 1 m in summer. These seasonal wave height data were applied conservatively (i.e., producing the least TL) for the acoustic propagation modeling.

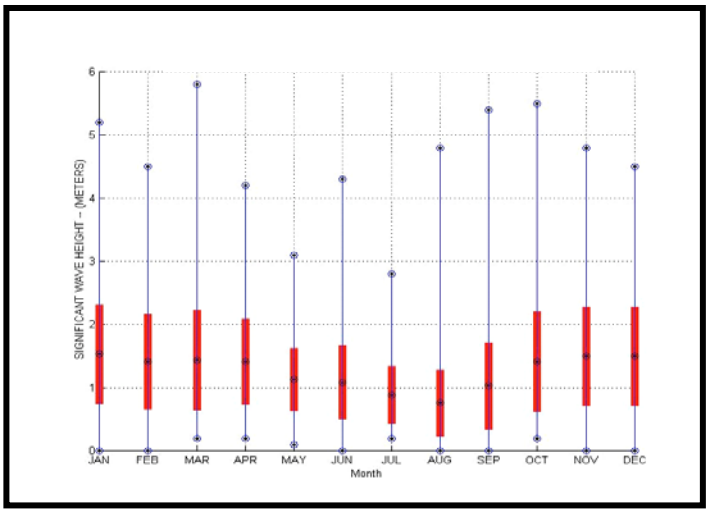

Figure A-25. Average Wave Height Data Collected Near the Modeling Sites (NOAA-NDBC, 2008).

2.4.4.2 Model Receiver Parameters

For this modeling analysis, all receivers are modeled as perfect omni-directional receivers. This is a conservative assumption, given that the marine animals that were simulated during the AIM portion of the modeling probably have some directivity for any frequency of sound that they can perceive, and better directivity as the frequency of the signal increases (§8.4 *in* Richardson et al., 1995). Additionally, the CASS/GRAB model has been programmed to coherently add all eigenrays in its pressure calculations. Therefore, during the calculation of the peak pressure and total energy arriving at the receiver, essentially, all eigenrays are added in a method that includes accounting for their phase.

2.4.5 ACOUSTIC MODELING

2.4.5.1 Model-Specified Parameters and Resolution

Prior to executing the final transmission loss acoustic modeling run, which would be used in the impact calculations, several preliminary modeling run sessions were completed to allow examination of the range of TL results and to assist in specifying the internal model parameters, such as maximum range, range and depth increments (or resolution), azimuthal resolution, etc.

It was during these preliminary model runs that the seasonal effects on the SVPs and subsequently, the TL, were examined, as described in the "Sound Velocity Profile" topic of section 2.4 above. The resulting conclusion to use the winter profiles was shown in this modeling

effort to be the most appropriate methodology as it yields nominal yet moderately conservative results (i.e., the least transmission loss, or greatest received levels occurred when the winter profiles were used) for all of the model sites and SVPs.

The second parameter examined was the azimuthal resolution of the TL runs for each site. Here, the primary variability of the model runs was highly dependent on the range-dependency of the bathymetry as the model extended outward from the source location along each bearing. This translates into different received levels (RLs) for a modeled position in the water (or a modeled animal at the position) depending on the bearing from the source. It was determined that this resolution was especially important for the shelf and slope sites, where bathymetry can vary greatly based on the azimuth chosen, but less so for the deep-water situation. A bearing resolution of 15° was found to be adequate for the shelf and slope sites, while a resolution for deep water was 90° or more. For consistency, an azimuthal bearing resolution of 15° was universally adapted for all sites.

A maximum range for the modeling of 30 km (16.2 nmi) was identified as necessary to capture all possible RL of 140 dB re 1 µPa RMS, or higher for the modeled source. This is certainly adequate for the primary acoustic threshold used in this document for Level B impacts (i.e., 160 dB re 1 µPa RMS) and it covers most of the potential range of RLs for potential future threshold approaches (e.g., use of a risk continuum). Therefore, it was adopted as the maximum range for the acoustic modeling used in this document.

Throughout the acoustic modeling, a 50 m (164 ft) range increment and a 5 m (16.4 ft) depth increment were used to resolve the sound field. This resolution extended out to the maximum range of 30 km (16.2 nmi), and the maximum depth (i.e., the ocean bottom) anywhere within 30 km of each site.

The acoustic spectrum produced by the modeled airguns includes frequencies up to 5 or 10 kHz and beyond. However, an examination of these spectra shows that for frequencies above about 1 kHz, the amplitude of these frequencies is already at least 30 dB less than the maximum 1 Hz band amplitudes in the spectrum. Also, this difference in source level is increasing at a rate of about 30 dB per octave of frequency as the frequencies increase. Therefore, the acoustic modeling used in this analysis used 1 kHz as the upper frequency of the band of frequencies modeled acoustically. Additionally, since there is some indication that many marine mammals integrate signals in one-third ($1/3^{rd}$) octave bands (Richardson et al., 1995; DoN, 1998; and DoN, 2001b), it was reasonable to use a $1/3^{rd}$ octave band analysis, or division, of the airgun's broadband signal based on the American National Standard Institute (ANSI) definitions for acoustic frequencies up to 1 kHz. (ANSI, 1984, 1986, and 2004).

2.4.5.2 Model Handling of the Broadband Seismic Signal

For each of the four sites identified in Table A-5 as representative of the acoustic propagation in the Gulf of Mexico, a set of acoustic model runs was made to be used in predicting the potential acoustic impact for each of the seismic survey types with AIM. Each of these model runs used the acoustic and model parameters identified above for all $1/3^{rd}$ octave bands below 1 kHz, and for an azimuthal resolution of 15°. Essentially, for each azimuthal resolution, the $1/3^{rd}$ octave band TL was calculated, and was then subtracted from the corresponding $1/3^{rd}$ octave band

source level to determine the 1/3rd octave band received levels for all depths and ranges along that bearing. Once all of the 1/3rd octave band RLs were calculated, they were coherently added to derive the total broadband signal for all depths and ranges along that bearing. This broadband RL for each azimuth would then be used in the AIM modeling. In this way, any frequency-dependent propagation characteristics of the environment were correctly accounted for in the modeling. For example, during the modeling effort, it was recognized that some near-surface ducting or trapping was occurring for frequencies above about 600 Hz. And, even though the source level for these frequencies was 15-20 dB less than those at 50 to 100 Hz (i.e., the highest spectrum source levels) the reduced TL for the ducted frequencies out at ranges greater than 10 km (5.4 nmi), caused those frequencies to dominate the RL at shallow depths for ranges greater than about 10 km from the sources. This modeling methodology accounted for these types of affects.

2.4.6 Discussion of the Tolstoy et al. (2004, 2009) Results and Their Applicability to Shallow Water Seismic Transmission Loss

2.4.6.1 Introduction

Recently, two papers by Tolstoy et al. (2004, 2009) have reported measured transmission loss (TL) in several specific sites in the Gulf of Mexico for seismic airgun arrays in both shallow and deep waters. With the data provided and the methods that these papers use to characterize and present the data, it appears that TL for seismic sources in shallow water has been and is being over-estimated. That is, if deep water TL methodology, like TL = 20×Log(Range) [i.e., spherical spreading], is employed and even though these assumptions appear to give reasonable and measureable results in deep water, when they are applied to shallow water, the resulting TL estimate appears to be too high. Thus, the actual distance to a particular seismic airgun sound level isopleth in shallow water is greater than that predicted from using the deep water methodology. For example, Tolstoy et al. (2004) states that TL ranges to the 160 dB isopleths for measured deep water situations are between about 1.5 and 2.5 km while, in shallow water, these ranges increase to between 7 and 12 km. Given this example, clearly something must be done to account for the lower TL in shallow water if correct estimates of potential impacts to marine mammals near these sources are to be made.

2.4.6.2 Measured TL Variability in Shallow Water

One of the principle difficulties or issues with this approach is the general characterization of the measured data by Tolstoy et al. (2004, 2009), as either "shallow" or "deep." Tolstoy et al. (2004) measurements were made in Gulf of Mexico waters approximately 30 m deep; while Tolstoy et al. (2009) data were from Gulf of Mexico waters approximately 40-60 m deep.[2] After

[2] The global oceanographic community typically considers waters less than 200 m deep as "shallow water," and analyses using the AIM model used this value. In recent environmental compliance documentation for seismic airgun operations, Lamont-Doherty Earth Observatory of Columbia University has used 100 m depth as the cutoff for "shallow water."

an examination of Figures 6 through 9 in Tolstoy et al. (2009), it is fairly obvious that the variability of TL as a function of range is greater for the measured shallow water data than the deep water data, especially when the Sound Exposure Levels (SELs) are compared. Since these data were collected by driving the source around the receivers, either in rough circles or in opening or closing spirals, much of this variability is due to the azimuthal variability of the measured TL, even when the range between the source and receivers was constant. There is always some variability in measured TL data (especially sound pressure level [SPL] data), which is caused by slight movements of sources and receivers in the water column, the direction or shape of source and receiver beams, wave motion, internal waves, and numerous other inhomogeneities of the ocean, both temporal and spatial. However, the measured deep water SEL data in Figure 7 Tolstoy et al., (2009), show considerably less azimuthal dependence (i.e., variability in TL typically of about 2-3 dB for any given range) than the shallow water data in Figure 9 of the same paper (i.e., about 6-9 dB for any given range). This higher variability of the TL in shallow water seems to be due to the variability of the bottom bathymetry and sediment, both as a function of range and azimuth, rather than the smaller variability introduced by the water column, even in deep water. This is probably at least partially due to the fact the even slight changes in bathymetry, while practically unnoticed in deep water, can cause significant changes in TL in shallow water. For example, a 20 m change of bathymetry in deep water, say, for water 2000 m deep, is not expected to change TL much, but in shallow water that is only 50 m deep, a sand bar or similar feature that can easily cause this magnitude of depth change will greatly change the TL of the signal as it passes over that feature.

2.4.6.3 Inherent Difficulties of Measuring and Estimating TL in Shallow Water

The difficulty of both measuring and estimating TL in shallow water has long been known to underwater acousticians. And this problem is further complicated in environmental compliance analyses because it is almost always necessary to estimate potential impacts to marine animals over large areas where bathymetry, bottom sediments, seasons, freshwater runoff, local currents, and weather conditions are constantly in flux. A good example of this variability is the expected difference between the shallow water location measured in Tolstoy et al. (2004) which appears to be in the sand-covered shelf (DoN, 2007c) south of the Alabama/Florida border and an area just 100 km to the west-southwest of where the outflow from the Mississippi River has deposited clays and silty-clay on the continental shelf (DoN, 2007c). The absorption of seismic acoustic energy in the clays and silts would be expected to be much higher than the sand, and the TL here would be greater. So, the question remains of how to reasonably represent the TL for a given area while also acknowledging, examining, and accounting for these numerous environmental variables, and still capturing the overall effects of the proposed action or seismic airgun operations on the environment.

The overall approach and data provided in the Tolstoy et al. (2004, 2009) papers allows one to attempt to quantify the shallow water TL for the sites measured without a complete understanding of the propagation present in those sites. For example, neither paper provides the actual sound velocity profile (SVP) for that site nor how it changes for the ranges and area covered. Hypothetically, the apparent lower TL measured in the shallow water areas could be caused by a strong surface duct that has trapped the near-surface acoustic energy, and has nothing to do with the bottom. Tolstoy et al. (2009) does mention some near-surface warming of

the SVP and a general downward refraction caused by this, but since those measurements occurred during the winter months (December, January and February), this could be just a local effect.

Based on the GDEM database (OAML, 2002) (Figure A-18), most of the historical SVP data for the shallow water in the Gulf of Mexico shows an iso-velocity profile throughout the year, with some near-surface warming in the late spring and summer months. In general, if the SVP is slightly downward-refracting, this would tend to cause the signal from near-surface sources, like seismic airgun arrays, to refract toward the ocean bottom and increase the incident angles at which they interact with the bottom. Since higher incident angles generally mean more penetration of the sound energy into the bottom and/or more scattering loss as the signal is reflected from the bottom, the overall TL for a downward-refracting environment would be expected to be greater than for the iso-velocity environment, where there is little or no refraction.

2.4.6.4 Gulf of Mexico Shallow Water Propagation Sub-categories

This discussion will now concentrate on the iso-velocity or near iso-velocity situation, since it would generally have less TL than the alternatives and it appears to be the most common historical propagation SVP in the shallow water of much of the Gulf of Mexico. In general, shallow water sound propagation has often been broken into three sub-categories (Figure A-26):

- Cross-slope (i.e., where the depth of water along the track of propagation remains about the same as the sound radiates outward from the source),
- Up-slope (i.e., where the sound moves into progressively shallower water), and
- Down-slope (i.e., where the sound moves into progressively deeper water).

Cross-slope propagation: For this situation, the ocean surface and bottom can act as a channel or duct and trap the acoustic energy between these two, roughly parallel boundaries. Also, if the ocean is calm and there is a highly reflective bottom (e.g., a sandy bottom), these azimuths from the source can act very much like a duct (i.e., there will be spherical spreading to the bottom of the duct [the ocean bottom] then cylindrical spreading [10×Log(Range)] once the water column is filled and little loss through the ocean surface and bottom boundaries).

Up-slope propagation: For this situation, each interaction or reflection from either the bottom or the ocean's surface as the signal propagates outward from the source toward shore and shallower water, causes the incident angle to the bottom to become slightly more vertical (Urick, 1985). Generally, this causes each subsequent bottom reflection to have a higher loss than the previous one and to move a shorter distance from the source on each subsequent reflection. This is based on the principle that the incident and reflected angles for a sound reflecting off a surface are equal (Figure A-27, where these equal angles are labelled as "α", "β", and "ε"). Also note in this figure that each incident angle with the bottom increases as the ray moves toward shore. Therefore, up slope propagation definitely has greater loss than cross-slope propagation.

Down-slope propagation: This situation allows the acoustic energy to spread out into a larger water column as the acoustic ray moves into deeper water than that at the source's location. This

allows the acoustic energy to spread out faster than in the duct-like cross-slope case. Thus, a down-slope situation would also be expected to have more loss than the cross-slope case. Additionally, if the SVP is slightly downward refracting, the acoustic energy will tend to stay closer to the ocean bottom, which is typically further away from those marine mammals that are shallow divers and remain near the surface for the majority of the time.

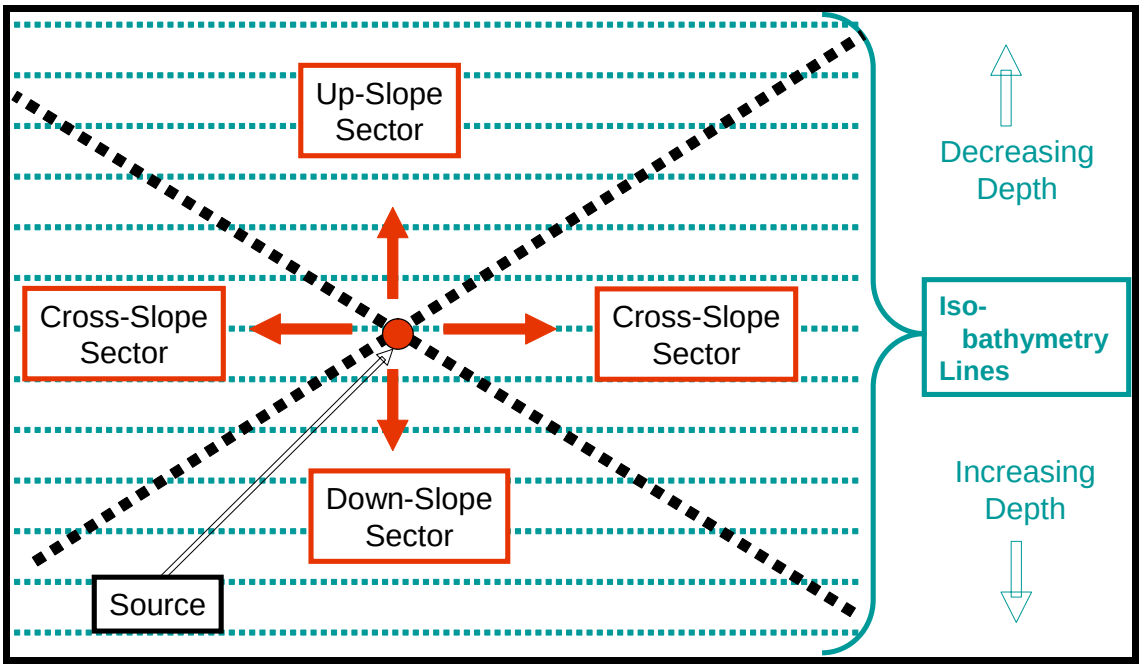

Figure A-26. Simplified geometry of shallow water propagation sub-categories.

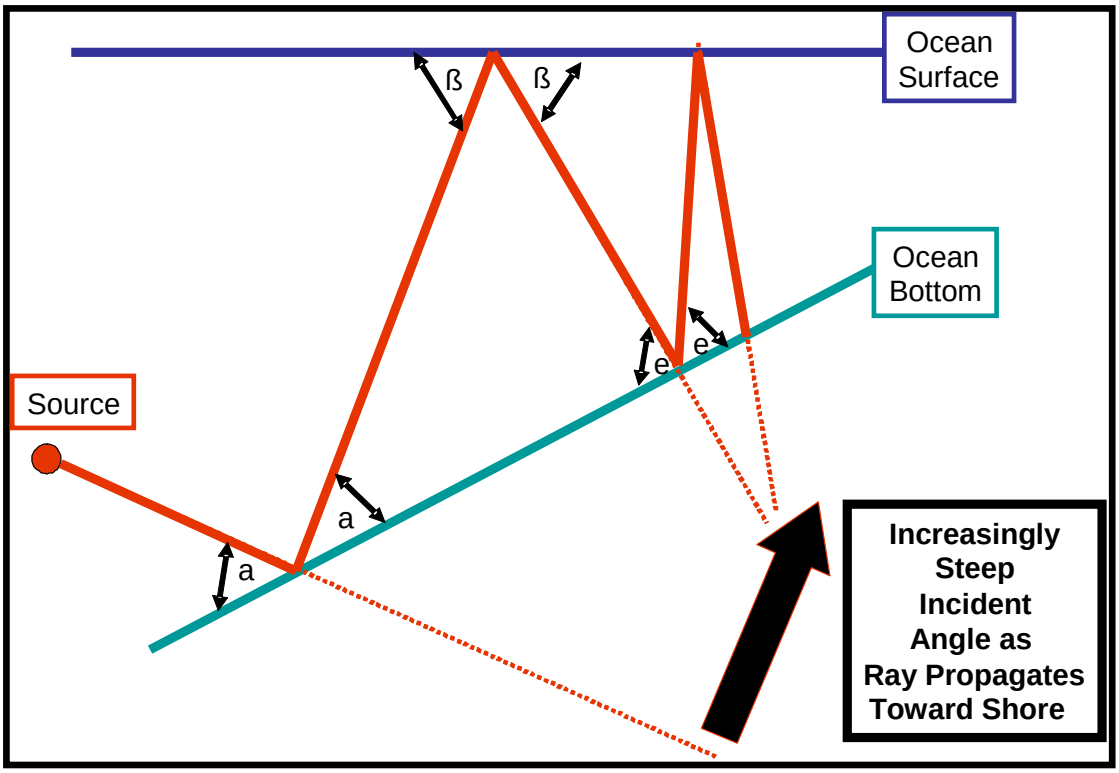

Figure A-27. Simplified geometry of the up-slope propagation sub-category.

2.4.6.5 Methods of Estimating Shallow Water TL from Seismic Airguns in the Gulf of Mexico

An examination of the shallow water Received Level (RL) plots in Tolstoy et al. (2004, 2009) show that for any given range from the source, the variance of the shallow water RL values are generally much larger than for the deep water values. Essentially, in the shallow water plots, Tolstoy et al. have combined all three sub-categories: cross-slope, down-slope and up-slope. Tolstoy et al. (2009) analyze these data and then uses a least-squares fit[3] and 95th-percentile[4] values to draw representative RL curves or equations. These equations are then used to determine ranges to the various isopleths. And in doing this, Tolstoy et al. (2009) is essentially using RL to represent TL, with assumptions about the source and the relationship "RL = SL – TL." Although this is a conservative approach, the difficulty with it is that effectively the entire TL for the shallow areas are now probably being estimated by the cross-slope subcategory. This would have the lowest TL of any of the azimuthal bearings from the source. Further, depending on the slope in the area (which will cause changes to the widths of the various sectors in Figure A-26) and the potential presence of other small bottom features (which are typically present during the measurements but may be too small to appear in bathymetry data), a case could be

[3] Least-squares fit is a mathematical procedure for finding the best-fitting curve to a given set of points by minimizing the sum of the squares of the offsets ("the residuals") of the points from the curve.

[4] 95th percentile is the value of the variable below which 95 percent of the observations fall.

made that this approach will estimate the lowest TL in that area for any given range even if it only occurs for a small number of azimuths. This occurs because most of the measurements in shallow water were conducted by driving the source on a spiral or sometimes circular track around the receivers, thus effectively sampling each range as discussed.

The approach used to predict the potential impacts used by AIM in this document does not use this methodology. By estimating TL for each 1/3rd octave frequency bin and for each 15 degrees of azimuth, the AIM approach provides a more thorough sampling and, therefore, a better representation of the variety of cases which will probably be encountered in the Gulf of Mexico, particularly in shallow water areas. It can also be argued that AIM better statistically represents the overall local underwater sound propagation, with its variances, while still capturing the situations where animals can be affected out to longer ranges.

2.4.6.6 Seismic Airgun Beampattern Issues in Shallow Water

Seismic Airgun Array Example Specifications
Ship: R/V *Marcus G. Langseth* is a 235 ft, 2,578 gross ton research vessel, owned by the National Science Foundation and operated by Lamont-Doherty Earth Observatory of Columbia University.
Airgun Array • Energy source: thirty-six 1900 psi Bolt Technology Corp. airguns of 40-360 in^3. • Four strings, each containing nine operating airguns. • Source output (downward): 0-peak is 84 bar-m (259 dB re 1 µPa at 1 m).

Another facet of the potential issues with applying the measured results from Tolstoy et al. (2004, 2009) is the issue that in shallow water, and for the lower frequencies (i.e., for frequencies between, say, 50 and 500 Hz) that the beams produced by these seismic airgun arrays (which are tuned for deep water) have not fully formed and the bottom is encountered while the beam pattern is still in the "near-field." This greatly complicates how the acoustic energy is projected from the source outward. Evidence of this effect can be seen in Figures 8 and 9 of Tolstoy et al. (2009) in the variability of the TL data for ranges less than 1 km from the array.

An examination of the deep water data in Figures 6 and 7 in Tolstoy et al. (2009) show that at about 1 km, the average SPL RMS RL is about 172 dB, while the SEL RL is about 162 dB. If a 60 dB TL in the first km (spherical spreading) is assumed from a point source, then the deep water source levels (SL) are about 132 dB re 1µPa @ 1m and 122 dB re 1 µPa^2-s @ 1 m, for the SPL RMS and SEL values, respectively. Since the beams did not completely form in the shallow water before interacting with the ocean bottom, it is anticipated that less energy is directed downward and more energy projects out horizontally into the water column. An examination of Figures 8 and 9 in Tolstoy et al. (2009) at about 1 km indicate that this effect raises the effective SL values by about 12 to 15 dB.

Furthermore, there does not appear to be very much difference between the RLs measured by inline or crossline seismic airgun shots in the variability of the data in shallow water, which further shows that the near-field inclusion of the ocean bottom disrupts the beamforming.

2.4.6.7 Significance of the Assumptions Built into the Tolstoy et al. (2004, 2009) Papers

A final significant issue with applying the results from Tolstoy et al. (2004, 2009) as a prediction of TL in shallow water is in the nature of the Tolstoy measurements. Specifically, these papers report the RLs for the R/V *Marcus G. Langseth* airgun array in two shallow water locations. The resulting RL data and curve fits, therefore, should be applicable in predicting RL values for that specific array in those locations, or possibly for other locations with similar propagation characteristics (e.g., water depth, bathymetric characteristics, SVP, bottom sediment type and depths, etc.). Additionally, these curves are limited in range covered, and actually are fitted to data between about 1 to 17 km. Thus, if any of these assumptions or implied assumptions are violated, care must be taken in any attempt to apply these curves elsewhere.

One of the embedded or hidden assumptions in the application of these curves concerns the SL of the airgun array, which is of extreme importance. The use of this term alone implies that the nominal source for this PEIS could be characterized by a point source with a SL and a beam pattern. However, as has been discussed above, in the shallow water sites, the ocean bottom is encountered before the beam is fully formed (i.e., the ocean bottom is in the "near-field" of the airgun array). Therefore, a representative point source (with accompanying beam pattern) is not easily identified, and it is highly dependent on various parameters (e.g., the water depth below the source, sediment type and slope, etc.), which were changing constantly during the Tolstoy et al. measurement efforts.

An example of the significance of this effect is the following calculation. Based on the previously identified characteristics of the *Langseth* array, the actual RMS SL can be estimated at about 249 dB re 1 µPa at 1 m (i.e., about 10 dB less than the zero-to-peak SL value). Additionally, assuming that that the *Langseth* array would have a far-field spectrum similar to that of the modeled nominal array used in this PEIS, the SEL SL for the *Langseth* array would be about 239 dB re 1 μPa^2-s at 1 m (i.e., about 10 dB less than the RMS SL value, with the correct units). Based on these estimated SLs and the intercepts at one kilometer for the Tolstoy et al. (2009) curve fits, Table A-6 shows the estimated TL that is encountered during the first kilometer from the airgun array. As an example, the RMS "least squares fit" curve experiences 68.15 dB TL in the first kilometer (e.g., TL=SL-RL or 249-180.85 = 68.15 dB). This equates to 22.7 times the log of range (i.e., TL = X×Log[R] or 68.15 = X× Log[1000] or X = 68.15/3 = 22.7). In every case, this TL is greater than one would expect from purely spherical spreading (i.e., 60 dB = 20×Log[1,000]). This is as expected because, even though the beams are not fully formed, the sound transmitted from the array is generally directed downward, interacting strongly with the bottom and probably losing energy into the bottom. Additionally, the interference with the beam formation also causes an effective lowering of the airgun array's SL. This is because not all of the components of the airgun array can contribute effectively and efficiently to the correct formation of the beam, as the airgun array was designed for. This is a classic example of an undesirable near-field phenomenon.

Table A-6 Estimated TL in the First Kilometer for Shallow Water

	RL at 1 km		TL in the first km	
	RMS RL	**SEL RL**	**RMS TL**	**SEL TL**
95th % Fit	183.62	175.84	65.38	63.16
Least-Squares Fit	180.85	172.84	68.15	66.16

Table A-7 provides the estimated TL in the first kilometer from the curve fit equations in Tolstoy et el. (2009). Additionally, the difference error between the two estimated TLs (i.e., from estimating the SLs vice using the curve fit equations to estimate TL) is provided in Table A-7. These error values show that by using the Tolstoy et al. (2009) curve fit equations alone to estimate the overall TL, the actual TL in just the first kilometer is underestimated by as much as 8.38 and 14.92 dB, depending on which metric (RMS or SEL) and which curve fit (95^{th} % fit or least-squares fit) are used. Therefore, if the airgun source used is different from that of the *Langseth*'s, this difference must be accounted for, or the ranges to the 160, 180, and 190 dB isopleths will be incorrect. Generally, if the SL for an array is less than that of the *Langseth*'s (i.e., in the case for the nominal array identified for analysis), the ranges will be overestimated, while the range for larger arrays may be underestimated.

Table A-7 Estimated TL in the First Kilometer of Shallow Water Based on Tolstoy et al. (2009) Curve Fit Equations

	TL in the first km Based on Tolstoy (2009) curve fit equations		Difference Error	
	RMS TL	**SEL TL**	**RMS**	**SEL**
95th % Fit	57.00	51.24	8.38	11.92
Least-Squares Fit	57.00	51.24	11.15	14.92

As a simple example of the effect of this issue, we will examine the RMS ranges to the 160 and 180 dB isopleths for this nominal array, using the uncorrected Tolstoy et al. (2009) equation with the "least-squares fit" equation and a corrected Tolstoy et al. (2009) equation. For the corrected approach, the nominal array's SL is: a) increased by 20 dB to account for the fact that it is assumed to be a point source (see Appendix C of the PEIS), b) decreased by 20 dB to account for the horizontal array effect (and see Appendix C of the PEIS), c) the actual SL (i.e., 230 dB_{RMS} vice the 249 dB_{RMS} Tolstoy et al. [2009] uses) , and d) experiencing 68.1 dB or 22.7×Log(R) TL in the first kilometer. Thus, the nominal array's RMS SL is about 230 dB re 1 μPa at 1 m, or about 19 dB less than the Langseth array. Table A-8 shows the ranges to the 160 and 180 dB isopleths for both approaches. By underestimating the TL in the first kilometer, and by overestimating the nominal array's SL (i.e., assuming it is 19 dB higher and equal to the Langseth array), the Tolstoy et al. (2009) equations overestimate the distance to the 160 and 180 dB isopleths for this nominal array.

Table A-8 Range to Shallow Water 160 and 180 dB Isopleth by Two Methodologies

	Range (km)		
	Using Tolstoy Least-Squares Fit Equation	**Tolstoy Corrected for: 1) SL difference and 2) TL in the first km**	**Deep Water Approximation**
180 dB Isopleth	1.4	0.13	0.3
160 dB Isopleth	12.5	1.26	3.0

Finally, it should be pointed out that the corrected values for the shallow water 160 and 180 dB isopleths for this nominal array (Table A-8) are approximately half of the value derived for deep water. These deep water values assume: 1) spherical spreading throughout the propagation process, and 2) a 20 dB loss to airgun array hypothetical SL_{RMS} for horizontal propagation of the transmitted airgun signal (MMS, 2004). Therefore, the strict and uncorrected application of the Tolstoy et al. (2009) least-squares fit equation for RMS data is still extremely conservative. That is, there is a difference of over 400% and approximately 300%, respectively, for the Level A and B isopleths, when compared to the deep water approximations. They are off by about 1,000%, when compared to the corrected Tolstoy et al. values, and therefore, should not be used.

2.4.6.8 Recommended Methodology for Estimating Shallow Water TL

Historically, there are four methods of estimating the TL for a shallow water area. They are: 1) dedicating resources (i.e., ships, planes, sources and sensors) to actually measure the in-situ TL for the site; 2) use the best available scientific databases (i.e., for bathymetry, SVPs, sediment type and structure, etc.) and models (i.e., acoustic propagation models capable of deriving a TL estimate for the depths, source frequencies, and bottom characteristic present) to predict the TL; 3) estimating the TL by intelligently extrapolating from a set of empirical data; or 4) estimating the shallow water TL without any empirical data, but considering the applicability of some basic properties of the physics of acoustics (e.g., assuming no absorption at the ocean surface and bottom, and using spherical spreading out to a range equal to water depth at the source followed by cylindrical spreading for ranges beyond that). In general, and as a first estimate, these methodologies are probably in order of decreasing accuracy. Additionally, it must be remembered that each of these approaches has its limitations. For example, even though measuring the TL may be the most accurate and reliable, it requires calibrated equipment, significant time and money expenditures, and it only captures a limited amount of data. Thus, different bearings from the source, different source water depths (to adjust for a moving source's TL), different seasons, etc., are not directly available from this method.

The issue of characterizing shallow water TL has been recognized and investigated for many years. And the advantage of using a generalized equation (i.e., as in methodology 4 above) and calibrating it with data (i.e., into equations that fall under methodology 3) has been accomplished in the Mediterranean Sea (Hastrup and Akal, 1980). In this memorandum, the authors generalize shallow water with the following equation:

$$TL = 15\times\text{Log}(R) + \{A + B\times(\text{Log}(f)) + C\times(\text{Log2}(f))\}\times R + D, \quad \text{in dB}$$

Where: A, B, C, and D are constants, based on local conditions,
f = frequency (Hz), and
R = range (m).

The authors further state that they have applied this equation to about ten different Mediterranean Sea sites for non-pulse sonars in areas where extensive TL measurements have been made. However, that quality of TL data does not exist yet for airgun arrays in the Gulf of Mexico, and the airgun source, which has a broadband signal, may significantly complicate this approach. For example, there is not just one value for the "f" term, so the question remains of which frequency(ies) should be used? Thus, further analysis with this approach is beyond the scope and time constraints of this petition.

Based on the need to complete an analysis in support of an EA or EIS, before any dedicated measurements can be completed, methodology 1 above is generally impractical for this case. Similarly, methodology 4, which typically has limited scientific data to support its assumptions, is also undesirable for EA or EIS use, unless there is no other method available. Therefore, methods 2 and 3 appear to be the best approaches. The AIM methodology and approach used to model and estimate potential impacts, as discussed here, follows methodology 2. Methodology 3 is approximated by applying calibrations for an airgun's SL and the TL in the first kilometer to the curve fit equations in Tolstoy et al. (2009) to derive a calibrated equation of TL for shallow water of depth, SVP and bottom properties similar to those observed in Tolstoy et al. (2009).

The recommended methodology to calibrate the Tolstoy et al. (2009) shallow water data is:

- Identify the SPL RMS SL in dB for the source to be used;
- Approximate the TL in the first kilometer from the source as
  TL = 22.7 × Log (r), where "r" is range in meters;
- Approximate the TL beyond the first kilometer from the source as
  TL = 68.15 + 19.0 × Log (R), where "R" is range in kilometers;
- Use the correct SPL RMS SL (i.e., the actual far-field RMS SL, which for the PEIS nominal array is 230 dB re 1 μPa @ 1 m RMS) which needs to be corrected for both the hypothetical point source correction of about +20 dB and the horizontal array correction of -20 dB; and
- Determine RL or ranges to 160 and 180 dB isopleths using the equation
  RL = SL – TL, where the appropriate TL from above is used.

Since these equations are based on the data collected in Tolstoy et al (2009) (i.e., they appear to be for an area where sand is the predominant bottom type, and sand is a highly reflective bottom), they will be conservative for most conditions, especially where the entire water column is ensonified and the actual bottom type is more absorbent (e.g., mud or silt). Care will still need to be taken if a duct is present, since these data were not collected in that type of propagation and the actual TL may not be very compatible with that measured by Tolstoy et al. (2009). Finally, if actual, reliable TL data are available for the site, it should be used to upgrade or better calibrate the Tolstoy et al. (2009) curve fit equations to that site.

2.5 MARINE MAMMAL DENSITIES

At the time of this analysis, the best available marine mammal density estimates for the Gulf of Mexico are the U. S. Navy's Navy OPAREA Density Estimates (NODE) database (DoN, 2007b). These density estimates are based on the National Marine Fisheries Services-Southeast Fisheries Science Center (NMFS-SEFSC) shipboard surveys conducted between 1994 and 2006, and were derived using a model-based approach and statistical analysis of the existing survey data using the model DISTANCE (Buckland et al. 2001). The outputs from the NODE database are four seasonal surface density plots of the Gulf of Mexico for each of the marine mammal species occurring there. Figures A-28 and A-29 are examples of these surface density plots for bottlenose dolphins in the summer and Pantropical spotted dolphins in the summer, fall and winter, respectively. The resolution or grid size in these plots is dependent on the amount of data available for each species. The density gradations are specific to each plot, but the higher value for each gradation is used in the subsequent analysis. Each of these figures has been overlaid with the boundaries of the nine acoustic model regions used in this analysis. For each of these nine regions, the average density was computed. The resulting densities are presented in Tables A-9 through A-12, for each species and season.

It should be noted that while the U.S. Navy was creating the NODE database, the NMFS was routinely consulted on the process, and provided much of the data on which the analysis is based and reviewed the resulting database. Additionally, the Gulf of Mexico data (along with similar NODE data for the east coast of the United States) were used in the Final EIS for Atlantic Fleet Active Sonar Training (DoN, 2008).

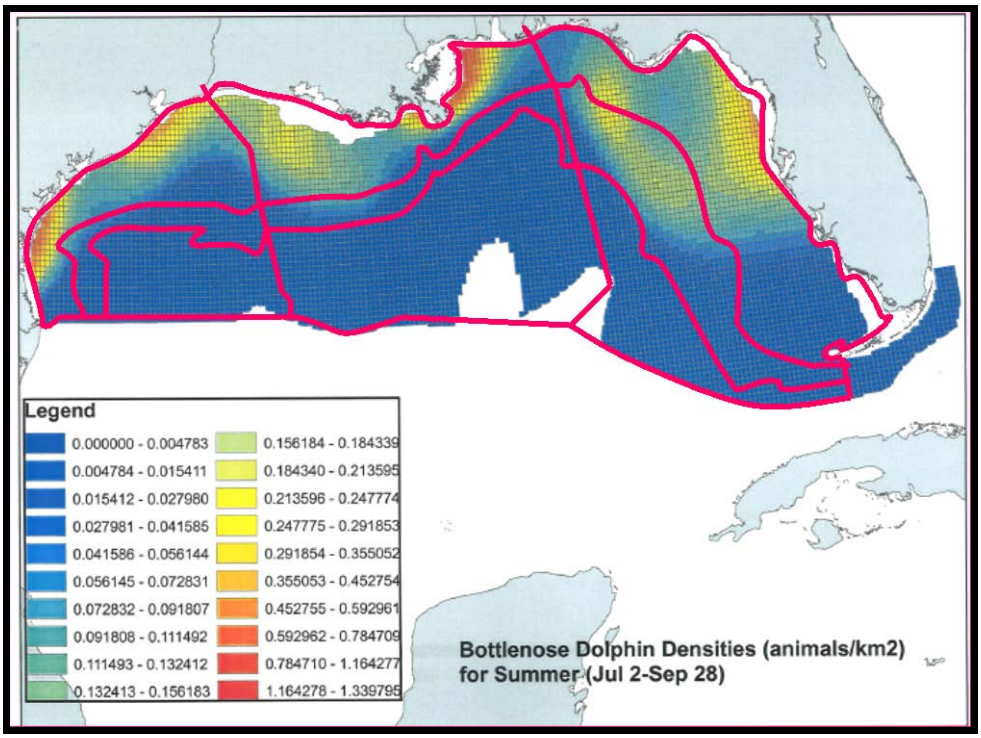

Figure A-28**. NODE Bottlenose Dolphin Density Plot for Summer (DoN, 2007b).**

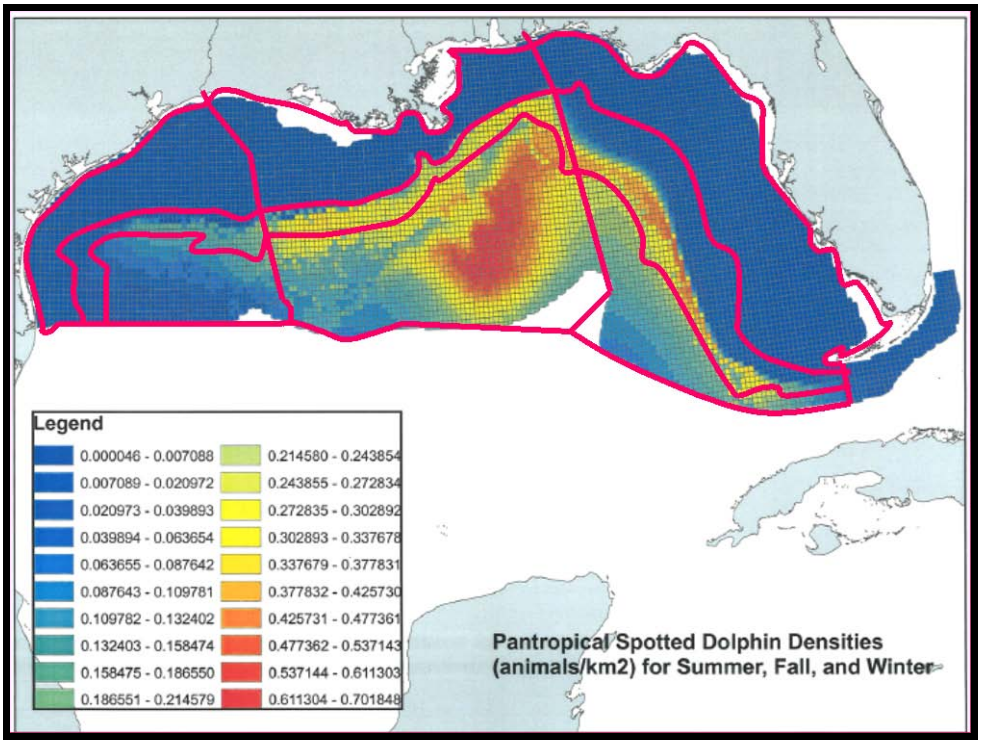

Figure A-29. NODE Pantropical Spotted Dolphin Density Plot for Summer, Fall and Winter (DoN, 2007b).

Table A-9. Gulf of Mexico Marine Mammal Densities (averaged by model site) for Spring (DoN, 2007b).

GOMEX Model Region: Depth Zone: BOEM Planning Region:	1 Shelf E	2 Shelf C	3 Shelf W	4 Slope E	5 Slope C	6 Slope W	7 Deep E	8 Deep C	9 Deep W
Marine Mammal Species									
Mysticetes									
Bryde's whale	0.0000	0.0000	0.0000	0.0001	0.0001	0.0001	0.0001	0.0001	0.0001
Odontocetes									
Atlantic spotted dolphin	0.2405	0.0367	0.0230	0.0155	0.0022	0.0155	0.0083	0.0022	0.0022
Beaked whales:	0.0002	0.0000	0.0000	0.0056	0.0047	0.0006	0.0035	0.0037	0.0015
Cuvier's									
Blainville's									
Gervais'									
Bottlenose dolphin	0.2032	0.2692	0.1452	0.2888	0.0713	0.0048	0.3887	0.0048	0.0048
Clymene dolphin	0.0023	0.0005	0.0005	0.0456	0.0456	0.0456	0.0456	0.0456	0.0456
False killer whale	0.0001	0.0000	0.0000	0.0025	0.0026	0.0026	0.0027	0.0027	0.0027
Fraser's dolphin	0.0001	0.0001	0.0001	0.0025	0.0026	0.0026	0.0019	0.0019	0.0019
Killer whale	0.0350	0.0175	0.0175	0.0003	0.0003	0.0003	0.0004	0.0004	0.0004
Kogia spp.	0.0000	0.0000	0.0000	0.0019	0.0016	0.0001	0.0037	0.0021	0.0004
Dwarf sperm whale									
Pygmy sperm whale									
Melonheaded whale	0.0009	0.0001	0.0001	0.0082	0.0086	0.0086	0.0091	0.0091	0.0091
Pantropical spotted dolphin	0.0426	0.0110	0.0110	0.2521	0.2505	0.1580	0.5317	0.5826	0.1225
Pygmy killer whale	0.0001	0.0000	0.0000	0.0010	0.0010	0.0010	0.0011	0.0011	0.0011
Risso's dolphin	0.0001	0.0001	0.0001	0.0133	0.0130	0.0042	0.0115	0.0100	0.0051
Rough-toothed dolphin	0.0040	0.0038	0.0244	0.0043	0.0045	0.0030	0.0119	0.0067	0.0017
Short-finned pilot whale	0.0003	0.0001	0.0001	0.0060	0.0060	0.0060	0.0063	0.0063	0.0063
Sperm whale	0.0001	0.0001	0.0001	0.0033	0.0060	0.0025	0.0046	0.0049	0.0020
Spinner dolphin	0.0029	0.0004	0.0002	0.1724	0.2178	0.0000	0.0062	0.0726	0.0000
Striped dolphin	0.0003	0.0002	0.0001	0.0396	0.0511	0.0126	0.0236	0.0515	0.0191

Table A-10. Gulf of Mexico Marine Mammal Densities (averaged by model site) for Summer (DoN, 2007b).

GOMEX Model Region:	1	2	3	4	5	6	7	8	9
Depth Zone:	Shelf	Shelf	Shelf	Slope	Slope	Slope	Deep	Deep	Deep
BOEM Planning Region:	E	C	W	E	C	W	E	C	W
Marine Mammal Species									
Mysticetes									
Bryde's whale	0.0000	0.0000	0.0000	0.0001	0.0001	0.0001	0.0001	0.0001	0.0001
Odontocetes									
Atlantic spotted dolphin	0.2405	0.0367	0.0230	0.0155	0.0022	0.0155	0.0083	0.0022	0.0022
Beaked whales:	0.0000	0.0000	0.0000	0.0010	0.0014	0.0010	0.0021	0.0024	0.0017
Cuvier's									
Blainville's									
Gervais'									
Bottlenose dolphin	0.1373	0.4734	0.1883	0.1034	0.0048	0.0048	0.0048	0.0048	0.0048
Clymene dolphin	0.0023	0.0005	0.0005	0.0456	0.0456	0.0456	0.0456	0.0456	0.0456
False killer whale	0.0001	0.0000	0.0000	0.0025	0.0026	0.0026	0.0027	0.0027	0.0027
Fraser's dolphin	0.0001	0.0001	0.0001	0.0025	0.0026	0.0026	0.0019	0.0019	0.0019
Killer whale	0.0350	0.0175	0.0175	0.0003	0.0003	0.0003	0.0004	0.0004	0.0004
Kogia spp.	0.0000	0.0001	0.0000	0.0002	0.0019	0.0000	0.0028	0.0061	0.0042
Dwarf sperm whale									
Pygmy sperm whale									
Melonheaded whale	0.0009	0.0001	0.0001	0.0082	0.0086	0.0086	0.0091	0.0091	0.0091
Pantropical spotted dolphin	0.0071	0.0071	0.0071	0.1986	0.2316	0.1432	0.3738	0.3285	0.2041
Pygmy killer whale	0.0001	0.0000	0.0000	0.0010	0.0010	0.0010	0.0011	0.0011	0.0011
Risso's dolphin	0.0001	0.0001	0.0001	0.0133	0.0130	0.0042	0.0115	0.0100	0.0051
Rough-toothed dolphin	0.0040	0.0038	0.0244	0.0043	0.0045	0.0030	0.0119	0.0067	0.0017
Short-finned pilot whale	0.0003	0.0001	0.0001	0.0060	0.0060	0.0060	0.0063	0.0063	0.0063
Sperm whale	0.0001	0.0001	0.0001	0.0033	0.0060	0.0025	0.0046	0.0049	0.0020
Spinner dolphin	0.0029	0.0004	0.0002	0.1724	0.2178	0.0000	0.0062	0.0726	0.0000
Striped dolphin	0.0003	0.0002	0.0001	0.0396	0.0511	0.0126	0.0236	0.0515	0.0191

Table A-11. Gulf of Mexico Marine Mammal Densities (averaged by model site) for Fall (DoN 2007b).

GOMEX Model Region: / Depth Zone: / BOEM Planning Region:	1 Shelf E	2 Shelf C	3 Shelf W	4 Slope E	5 Slope C	6 Slope W	7 Deep E	8 Deep C	9 Deep W
Marine Mammal Species									
Mysticetes									
Bryde's whale	0.0000	0.0000	0.0000	0.0001	0.0001	0.0001	0.0001	0.0001	0.0001
Odontocetes									
Atlantic spotted dolphin	0.2405	0.0367	0.0230	0.0155	0.0022	0.0155	0.0083	0.0022	0.0022
Beaked whales:	0.0000	0.0000	0.0000	0.0010	0.0014	0.0010	0.0021	0.0024	0.0017
Cuvier's									
Blainville's									
Gervais'									
Bottlenose dolphin	0.2032	0.2692	0.1452	0.2888	0.0713	0.0048	0.3887	0.0048	0.0048
Clymene dolphin	0.0023	0.0005	0.0005	0.0456	0.0456	0.0456	0.0456	0.0456	0.0456
False killer whale	0.0001	0.0000	0.0000	0.0025	0.0026	0.0026	0.0027	0.0027	0.0027
Fraser's dolphin	0.0001	0.0001	0.0001	0.0025	0.0026	0.0026	0.0019	0.0019	0.0019
Killer whale	0.0350	0.0175	0.0175	0.0003	0.0003	0.0003	0.0004	0.0004	0.0004
Kogia spp.	0.0000	0.0001	0.0000	0.0002	0.0019	0.0000	0.0028	0.0061	0.0042
Dwarf sperm whale									
Pygmy sperm whale									
Melonheaded whale	0.0009	0.0001	0.0001	0.0082	0.0086	0.0086	0.0091	0.0091	0.0091
Pantropical spotted dolphin	0.0071	0.0071	0.0071	0.1986	0.2316	0.1432	0.3738	0.3285	0.2041
Pygmy killer whale	0.0001	0.0000	0.0000	0.0010	0.0010	0.0010	0.0011	0.0011	0.0011
Risso's dolphin	0.0001	0.0001	0.0001	0.0133	0.0130	0.0042	0.0115	0.0100	0.0051
Rough-toothed dolphin	0.0040	0.0038	0.0244	0.0043	0.0045	0.0030	0.0119	0.0067	0.0017
Short-finned pilot whale	0.0003	0.0001	0.0001	0.0060	0.0060	0.0060	0.0063	0.0063	0.0063
Sperm whale	0.0001	0.0001	0.0001	0.0033	0.0060	0.0025	0.0046	0.0049	0.0020
Spinner dolphin	0.0029	0.0004	0.0002	0.1724	0.2178	0.0000	0.0062	0.0726	0.0000
Striped dolphin	0.0003	0.0002	0.0001	0.0396	0.0511	0.0126	0.0236	0.0515	0.0191

Table A-12. Gulf of Mexico Marine Mammal Densities (averaged by model site) for Winter (DoN, 2007b).

GOMEX Model Region: Depth Zone: BOEM Planning Region:	1 Shelf E	2 Shelf C	3 Shelf W	4 Slope E	5 Slope C	6 Slope W	7 Deep E	8 Deep C	9 Deep W
Marine Mammal Species									
Mysticetes									
Bryde's whale	0.0000	0.0000	0.0000	0.0001	0.0001	0.0001	0.0001	0.0001	0.0001
Odontocetes									
Atlantic spotted dolphin	0.2405	0.0367	0.0230	0.0155	0.0022	0.0155	0.0083	0.0022	0.0022
Beaked whales:	0.0000	0.0000	0.0000	0.0010	0.0014	0.0010	0.0021	0.0024	0.0017
Cuvier's									
Blainville's									
Gervais'									
Bottlenose dolphin	0.2032	0.2692	0.1452	0.2888	0.0713	0.0048	0.3887	0.0048	0.0048
Clymene dolphin	0.0023	0.0005	0.0005	0.0456	0.0456	0.0456	0.0456	0.0456	0.0456
False killer whale	0.0001	0.0000	0.0000	0.0025	0.0026	0.0026	0.0027	0.0027	0.0027
Fraser's dolphin	0.0001	0.0001	0.0001	0.0025	0.0026	0.0026	0.0019	0.0019	0.0019
Killer whale	0.0350	0.0175	0.0175	0.0003	0.0003	0.0003	0.0004	0.0004	0.0004
Kogia spp.	0.0000	0.0001	0.0000	0.0002	0.0019	0.0000	0.0028	0.0061	0.0042
Dwarf sperm whale									
Pygmy sperm whale									
Melonheaded whale	0.0009	0.0001	0.0001	0.0082	0.0086	0.0086	0.0091	0.0091	0.0091
Pantropical spotted dolphin	0.0071	0.0071	0.0071	0.1986	0.2316	0.1432	0.3738	0.3285	0.2041
Pygmy killer whale	0.0001	0.0000	0.0000	0.0010	0.0010	0.0010	0.0011	0.0011	0.0011
Risso's dolphin	0.0001	0.0001	0.0001	0.0133	0.0130	0.0042	0.0115	0.0100	0.0051
Rough-toothed dolphin	0.0040	0.0038	0.0244	0.0043	0.0045	0.0030	0.0119	0.0067	0.0017
Short-finned pilot whale	0.0003	0.0001	0.0001	0.0060	0.0060	0.0060	0.0063	0.0063	0.0063
Sperm whale	0.0001	0.0001	0.0001	0.0033	0.0060	0.0025	0.0046	0.0049	0.0020
Spinner dolphin	0.0029	0.0004	0.0002	0.1724	0.2178	0.0000	0.0062	0.0726	0.0000
Striped dolphin	0.0003	0.0002	0.0001	0.0396	0.0511	0.0126	0.0236	0.0515	0.0191

2.6 ACOUSTIC INTEGRATION MODEL© (AIM) **Modeling**

2.6.1 Introduction to AIM

To estimate how changing the acoustic source characteristics affects the acoustic exposure of animals, the Acoustic Integration Model© (AIM) was utilized (Frankel et al., 2002). AIM is a Monte Carlo-based statistical model, strongly based on two earlier models: a whale movement and tracking model developed for the census of the bowhead whale (Ellison et al., 1987), and an underwater acoustic back-scattering model for a moving sound source in an under-ice Arctic environment (Bishop et al., 1987). Because the exact positions of sound sources and animals (sound receivers for the purpose of this analysis) in any given simulation cannot be known, multiple runs of realistic predictions are used to provide statistical validity. The movement and/or behavioral patterns of sources and receivers can be modeled based on measured field data, and these patterns can be incorporated into the model. Each source and/or receiver is modeled via the "animat" concept, where each has parameters that control its speed and direction in three dimensions. In the case of the source, it is also imbued with the parameters describing its source operation over time (i.e., SL, signal duration, and spectral characteristics). It is also possible to simulate the type of diving pattern that an animal exhibits in the real world. Furthermore, the movement of the animat can be programmed to respond to environmental factors, such as water depth and sound level (this latter feature was not used in this analysis). In this way, species that normally inhabit specific environments can be constrained in the model to stay within that habitat.

Once the behavior of the animats has been programmed, the model is run. The run consists of a user-specified number of steps forward in time. For each time step, each animat is moved according to the rules describing its behavior. For each time step of the model run, the received sound levels at each receiver (i.e., each marine mammal) animat are calculated. For this analysis, AIM returns the movement patterns of the animats, and the received sound levels are calculated separately, using the acoustic propagation predictions provided by the CASS/GRAB model.

At the end of each time step, each animat "evaluates" its environment, including its 3-D location, the time, and the received sound level (if anthropogenic sound is present). If an environmental variable has exceeded the user-specified boundary value (e.g., water too shallow), then the animat will alter its course to react to the environment. These responses to the environment are entitled 'aversions'. There are a number of potential aversion variables that can be used to build an animat's behavioral pattern.

Modeling simulations for four different survey types were run at four sites in the Gulf of Mexico. The starting locations and modeling specifics for each of these sites were provided above in Table A-5.

2.6.2 AIM Simulation of the Various Seismic Survey Types

For this assessment, the creation of each modeling simulation began with the creation of a movement pattern for the seismic source vessel representing a different survey type. The survey types included Ocean Bottom Seismic survey (OBS), 2-Dimensional, 3-Dimensional and Wide Azimuth surveys (WAZ). The parameters for each survey type are provided below in Table A-13 and are illustrated in Figures A-30 – A-33.

It should be noted that the actual source level range or the maximum source level used by each survey type is known to vary somewhat from the "nominal survey" modeled by AIM. The specific maximum source level used in the modeling effort is based on the level identified in the petition and grouped as shown in Table A-20. Section 2.6.7 explains how this correction is applied to the model results.

Table A-13. Seismic Vessel Parameters for AIM Simulations.

Survey Type	Leg Length (km)	Leg Spacing (km)	Number of Modeled Legs	Total Simulation Duration (min)	Shot Interval (seconds)
OBS	4.8	0.05	96	3,528	6
2D	168	3	8	10,400	15
3D	100	0.35	14	10,400	15
WAZ (four ships)	100	0.35	14	10,400	15 (per survey) 60 (per ship)
2D Hi-Res	50	0.30	~20	~ 16,632	~ 8

2.6.2.1 Ocean Bottom Seismic survey

AIM projects were written to simulate Ocean Bottom Seismic surveys (OBS). These were small in spatial extent to represent a single 4.8 x 4.8 km block. The legs were 0.05 km apart and 4.8 km long. The vessel speed was modeled at 8 km/h, with a shot interval of 6 seconds to provide a shot every 12.5 meters. The AIM step size was set to 15 seconds to ensure an accurate representation of source movement. This was necessary in part due to the close spacing of the lines. Essentially, the AIM modeling represents the OBS survey of a single block.

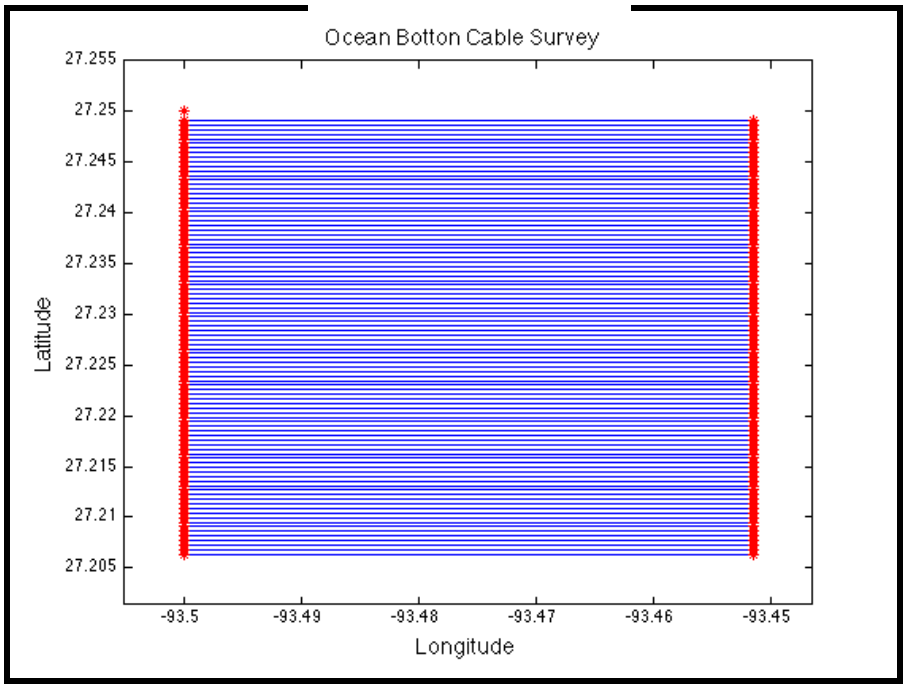

Figure A-30. Illustration of an Ocean Bottom Seismic Survey Source Pattern.

2.6.2.2 Two-Dimensional Survey

The lines for the two-dimensional survey were 166 km long, to simulate longitudinal coverage over a wide number of blocks. This is the equivalent area of about 173 blocks surveyed in the model run. The 8 lines were spaced at 3 km apart to simulate a latitudinal coverage of five blocks for the survey. The vessel speed was 8 km/h and shots were modeled every 15 seconds. The AIM model step size was 30 seconds.

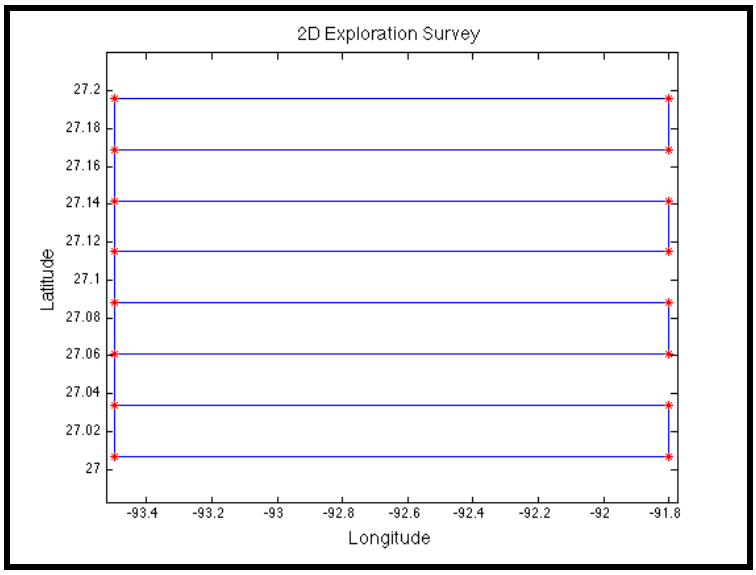

Figure A-31. Illustration of a Two-dimensional Survey Source Pattern.

2.6.2.3 Three-Dimensional Survey

A full 3-D survey might cover a width of 100 km (21 blocks) and a height of 24 km (five blocks). At a modeled speed of 8 km/h, this survey would require 52,867 minutes (~36 days). The AIM model was run for the same duration as the 2D survey (10,400 minutes). Thus, the modeled survey was 100 km wide and 4.8 km tall, for a total of about 21 blocks covered in a model run.

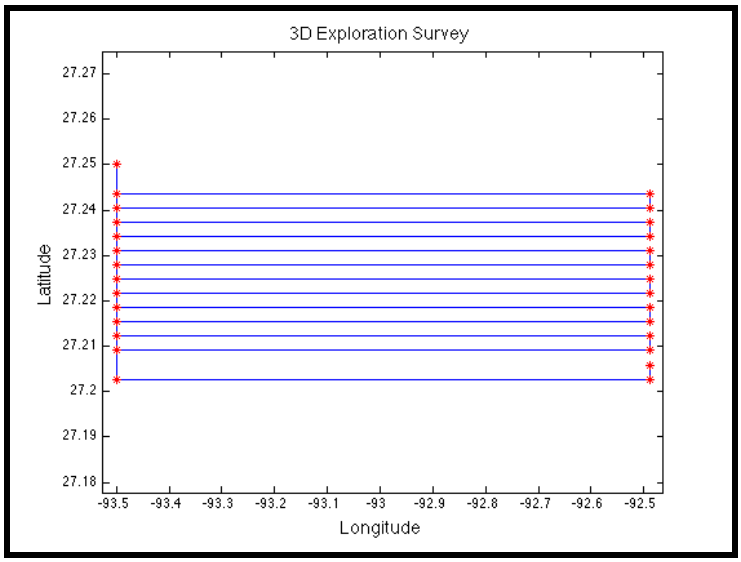

Figure A-32. Illustration of a Three-dimensional Survey Source Pattern.

2.6.2.4 Wide Azimuth Survey

Four ships were modeled for the Wide Azimuth Survey (WAZ). They formed a box 8 km long (parallel to the line) and 1 km wide (perpendicular to the line). Each ship was modeled to fire every 15 seconds. The WAZ survey was 100 km long, and had a line spacing of 0.6 km. The total duration of the simulation was 10,400 minutes, covering an area 100 km wide by 8.4 km tall, for a total of about 36.75 blocks covered in a model run.

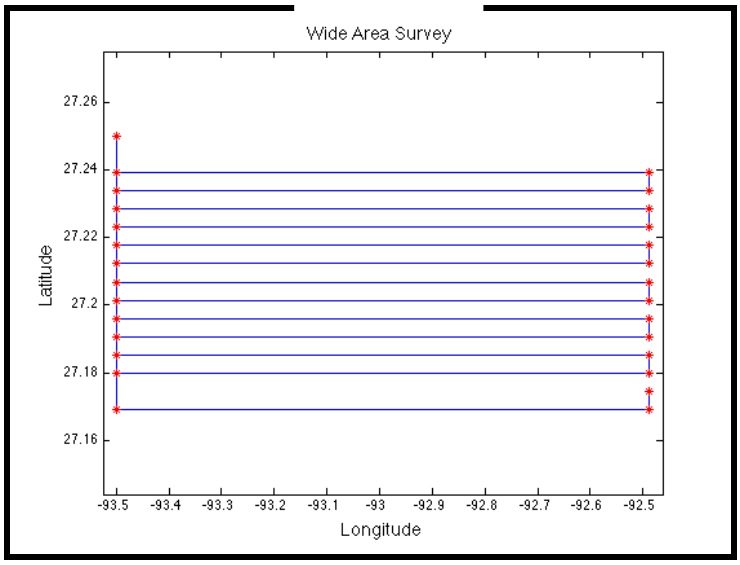

Figure A-33. Illustration of a WAZ Survey Source Pattern.

2.6.2.5 2-D High-Resolution Survey

A full 2-D High Resolution survey typically covers a block with 20 lines, with a spacing of about 300 m between lines. This equates to 96 km of survey tow per block, and takes about 2 days to complete per block. The AIM model was run for a survey of 50 km wide, legs 0.30 km apart and 4.8 km tall (equating to 16 modeled legs plus the gridded lines), for a total of about 10.4 blocks. This would take about 17.1 days of actual survey effort. Total AIM simulation duration was 16,632 min and shot interval was 8 s.

Marine mammals were simulated by creating animats that were programmed with behavioral values describing dive depth, surfacing and dive durations, swimming speed, and course change. A minimum and maximum value for each of these parameters was specified. These data were extracted from the AIM behavioral database (see sections 2.6.5 and 2.6.6 below), and were used to simulate movements and dive characteristics of individual animats for each species or species group relative to the simulated vessel source tracks at modeling locations.

After the animats were created, they were randomly distributed over each simulation area. The simulation area was delineated by four boundaries, composed of a combination of latitude and

longitude lines. These boundaries extend at least 1 degree of latitude or longitude beyond the extent of the vessel track to insure an adequate number of animats in all directions, and to ensure that the simulation areas extended beyond the area where substantial behavioral reactions might be anticipated. Each simulation had approximately 4,000 animats representing each species. In most cases, this represents a higher density of animats in the simulation (0.1 animats/km^2) than occurs in the real environment. This "over-population" allowed the calculation of smoother statistical distribution tails, and in the final analysis all results were normalized back to actual predicted population counts by species. During the AIM modeling, animats were programmed to remain within the simulation area boundaries. This behavior was incorporated to prevent the animats from diffusing out of the simulation, the result of which, if allowed, would be a systematic decrease in animat density over time. Thus, the simulations modeled the animals as a closed population with a high residency factor. This approach should be considered moderately conservative in terms of allowing for more prolonged exposures than would be expected from species with a lower residency factor.

Tables A-14 through A-18 provide the number of surveys, by blocks surveyed, for each of the nine modeled regions, both historically (i.e., for years 2004 – 2009) and by projected estimation of the anticipated level of effort (e.g., for 2010 – 2014), for each of the survey types. For OBS surveys in Table A-14, "Light" was not specifically defined, so it was assumed that 50 blocks were surveyed if "light" was specified.

Table A-14. Number of OBS Surveys in each Modeled Region, by Year and Number of Blocks (? = Information not available to BOEM or NMFS).

GOMEX Model Region: Depth Zone: BOEM Planning Region:	1 Shelf E	2 Shelf C	3 Shelf W	4 Slope E	5 Slope C	6 Slope W	7 Deep E	8 Deep C	9 Deep W
Year:									
2004	?	?	?	?	?	?	?	?	?
2005	?	?	?	?	?	?	?	?	?
2006	?	?	?	?	?	?	?	?	?
2007	?	?	?	?	?	?	?	?	?
2008	?	?	?	?	?	?	?	?	?
2009	?	?	?	?	?	?	?	?	?
2010	0	light	light	0	light	0	0	light	0
2011	0	light	light	0	light	0	0	light	0
2012	0	light	light	0	light	0	0	light	0
2013	0	light	light	0	light	0	0	light	0
2014	0	light	light	0	light	0	0	light	0

Table A-15. Number of 2-D Surveys in each Modeled Region, by Year and Number of Blocks.

GOMEX Model Region: Depth Zone: BOEM Planning Region:	1 Shelf E	2 Shelf C	3 Shelf W	4 Slope E	5 Slope C	6 Slope W	7 Deep E	8 Deep C	9 Deep W
Year:									
2004	0.0	17377.3	16155.0	0.0	16455.0	15927.2	0.0	66323.8	31854.4
2005	2778.0	9700.8	8522.9	11112.0	7639.5	7408.0	13890.0	74424.5	44448.0
2006	5556.0	1694.6	92.6	2778.0	3039.1	0.0	11871.3	32635.9	803.8
2007	0.0	0.0	0.0	4257.7	0.0	0.0	21288.7	17651.4	64.8
2008	11608.3	1503.8	0.0	4291.1	1722.4	166.7	7496.9	12945.5	1000.1
2009	0.0	138.9	0.0	0.0	0.0	0.0	0.0	0.0	0.0
2010	1852.0	926.0	0.0	1852.0	926.0	0.0	1852.0	1852.0	926.0
2011	1852.0	926.0	0.0	1852.0	926.0	0.0	2778.0	5556.0	926.0
2012	3704.0	926.0	926.0	3704.0	926.0	926.0	5556.0	9260.0	926.0
2013	3704.0	1852.0	1852.0	5556.0	1852.0	1852.0	9260.0	16668.0	3704.0
2014	3704.0	1852.0	2778.0	5556.0	1852.0	2778.0	9260.0	16668.0	5556.0

Table A-16. Number of 3-D Surveys in each Modeled Region, by Year and Number of Blocks.

GOMEX model Region: Depth Zone: BOEM Planing Region:	1 Shelf E	2 Shelf C	3 Shelf W	4 Slope E	5 Slope C	6 Slope W	7 Deep E	8 Deep C	9 Deep W
Year:									
2004	0	723	673	0	11	0	0	1490	181
2005	0	865	173	0	146	0	0	1022	73
2006	0	628	156	0	130	0	0	1836	116
2007	0	565	747	0	63	0	0	762	222
2008	0	223	113	158	0	0	158	316	0
2009	0	352	0	0	0	0	239	786	0
2010	750	400	200	800	50	20	800	400	400
2011	750	300	200	900	50	20	900	500	400
2012	900	300	100	1000	50	0	1000	500	300
2013	1000	300	50	1300	50	0	1300	600	200
2014	1000	300	50	1600	50	0	1600	800	200

Table A-17. Number of WAZ Surveys in each Modeled Region, by Year and Number of Blocks.

GOMEX Model Region: Depth Zone: BOEM Planning Region:	1 Shelf E	2 Shelf C	3 Shelf W	4 Slope E	5 Slope C	6 Slope W	7 Deep E	8 Deep C	9 Deep W
Year:									
2004	0	0	0	0	0	0	0	0	0
2005	0	0	0	0	0	0	0	0	0
2006	0	0	0	0	0	0	0	2530	0
2007	0	105	20	0	828	288	0	2382	365
2008	0	141	0	0	658	128	0	2049	160
2009	0	0	368	0	0	147	0	864	974
2010	0	200	200	0	500	400	0	778	1000
2011	0	200	200	0	450	400	0	700	1600
2012	0	200	200	0	405	400	0	630	2000
2013	0	125	200	500	365	400	0	567	1000
2014	0	100	200	500	328	400	500	510	1000

Table A-18. Number of 2-D High Resolution Surveys in each Modeled Region, by Year and Number of Blocks (? = Information not available to BOEM or NMFS).

GOMEX Model Region: / Depth Zone: / BOEM Planning Region:	1 Shelf E	2 Shelf C	3 Shelf W	4 Slope E	5 Slope C	6 Slope W	7 Deep E	8 Deep C	9 Deep W
Year:									
2004	?	?	?	?	?	?	?	?	?
2005	?	?	?	?	?	?	?	?	?
2006	?	?	?	?	?	?	?	?	?
2007	0	79.5	79.5	0	0	0	0	0	0
2008	0	65	65	0	0	0	0	0	0
2009	0	107.5	107.5	0	0	0	0	0	0
2010	0	122	122	0	0	0	0	0	0
2011	0	30	30	0	0	0	0	0	0
2012	0	35	35	0	0	0	0	0	0
2013	0	35	35	0	0	0	0	0	0
2014	0	35	35	0	0	0	0	0	0

2.6.3 Data Convolution to Create Animat Exposure Histories

The AIM simulations created a realistic animal movement track for each animat and were based on the best available animal behavioral data. It was assumed that, collectively, the ~4,000 animat tracks derived for each simulation (area/species combination) were a reasonable representation of the movements of the animals in the population under consideration. Animat positions along each of these tracks were converted to polar coordinates (range and bearing) from the source to the receivers. These data, along with the depth of the receiver, were used to extract RL estimates from the acoustic propagation modeling results provided by CASS/GRAB. For each bearing, distance, and depth from the source when it was operating at that site, the RL values were expressed as SPLs with units of dB re 1 µPa. These SPL values were computed separately for low-frequency (LF), mid-frequency (MF), and high-frequency (HF) cetaceans based on the M-weighting functions described by Southall et al. (2007) so that M-weighting could be applied if desired. M-weighting is a filter function (most akin to human C-weighting) that is applied to the acoustic signal to account for the differential hearing capabilities of different species groups. The final result was a time-history of acoustic exposures for each individual animat every 15 or 30 seconds.

Each animat's received levels were converted from SPL to intensity (Sound Exposure Level, or SEL) and summed over the duration of the exercise to generate the integrated energy level. These were expressed in terms of dB re 1µPa^2-sec or dB SEL.

2.6.4 Application of Exposure Criteria

Both the Southall et al. (2007) criteria and the traditional 160/180 dB re 1 µPa RMS criteria were applied to the results of the AIM modeling, but M-weighting is only applied to the MMPA Level A criteria proposed by Southall et al. (2007). See Table A-19 below.

2.6.5 AIM Animat Movement and Diving Pattern Details

2.6.5.1 ***Movement***

Animals move through four dimensions: three-dimensional space, plus time. Several movement parameters are used in AIM to produce a simulated movement pattern that accurately represents real animal movements. A typical dive pattern is shown below in Figure A-34. It consists of two phases; the first is a shallow respiratory sequence, which is followed by a deeper, longer dive.

These two phases are represented in the model with the values as input into the box below in Figure A-35.

The top row has the values for the shallow, respiratory dives. In this case, the animal dives from the surface to a maximum depth of five meters. The second row describes the second phase of the dive. In this phase the animal dives to a depth between 50 and 75 m. In this example, the animal spends time at both 60 and 50 m before surfacing. The pattern then repeats.

The horizontal component of the course is handled with the 'heading variance' term. It allows the animal to turn up to a certain number of degrees at each movement step. In this case, the animal can change course 20 degrees on the surface, but only 10 degrees underwater. This example is for a narrowly constrained set of variables, appropriate for a migratory animal, but larger values would be used for foraging animals or animals that are remaining in the same general area for any number of reasons.

2.6.5.2 Heading Variance

There are few published data that summarize marine mammal movement in terms of heading variance, or the amount of course change per unit time. The default setting allows the course to deviate between 0 and 30 degrees per minute.

2.6.5.3 Aversions

In addition to movement patterns, the animats can be programmed to avoid certain environmental situations. For example, this option can be used to constrain an animal to a particular depth regime. The example below (Figure A-36) constrains the animal to waters between 2,000 and 5,000 m deep. One modification was made for the AIM simulations in the animal's GOMEX habitat. Normally deep-water species were allowed to move into waters as shallow as 100 m.

Table A-19. Thresholds Applied to AIM Simulations.

Cetacean Threshold Criteria	Standard/Traditional Values	Proposed (Southall et al. 2007) Values
Level A SPL	180 dB re 1 µPa	230 dB re 1 µPa FLAT (peak)
Level A SEL	N/A	198 dB re 1 μPa^2-s (M-weighted)
Level B SPL	160 dB re 1 µPa	Use Standard/Traditional Value
Level B SEL	N/A	Use Standard/Traditional Value

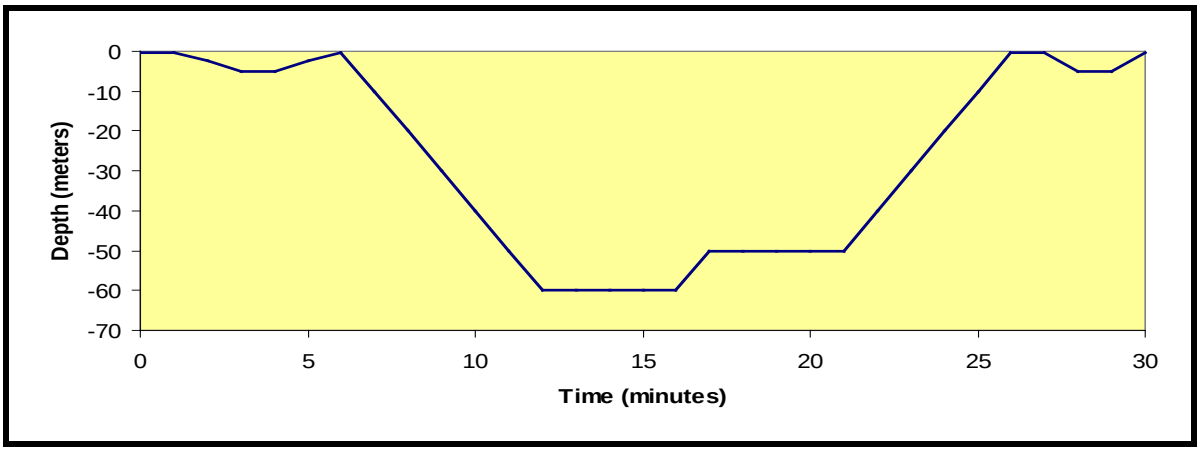

Figure A-34. Typical Animat Dive Pattern.

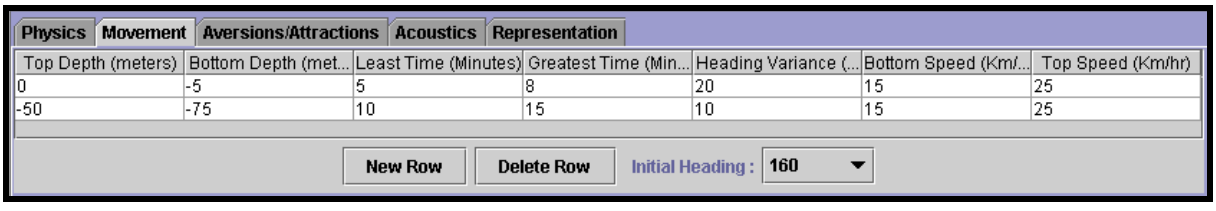

Figure A-35. Parameters Used to Specify the Dive Behavior for Figure A-34.

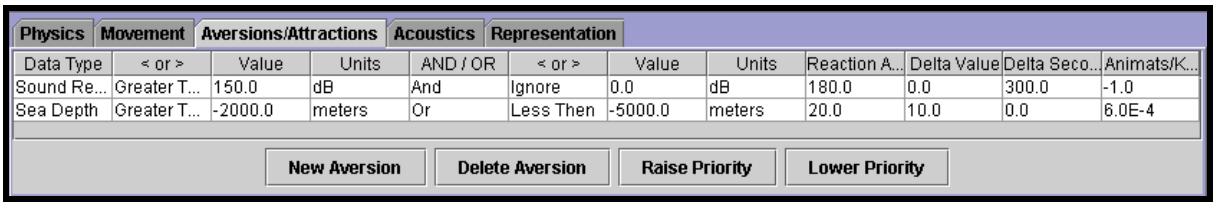

Figure A-36. Example Showing Aversions to Limit an Animat to Waters Between 2,000 and 5,000 m Deep.

2.6.6 Animal Behavior Parameters

The specific animal behavioral parameters that were used in this analysis are provided below. Where the "Surfacing/Dive Angle" column is empty, there were no meaningful data available and, as such, 75º was used as a default value. Under the "Speed Distribution" column, "Normal" indicates that the distribution of speed values between the limits was normally distributed. Under the "Depth Limit/Reaction Angle" column, the first number indicates the minimum depth limit in meters, and "reflect" indicates that if an animat moves to that shallow water limit, it will move away from the shallow water and back into deeper water.

2.6.6.1 Bryde's Whale

There is a paucity of data for this species. Since they are similar in size, data for both sei and Bryde's whales have been pooled to derive parameters. Note that Sei whales are rare in the Gulf of Mexico, but their similarities to Bryde's whales was used to determine some of their movement parameters.

Model parameters

	Min/Max Surface Time (min)	Surfacing / Dive Angle	Dive Depth (m) Min/Max (Percentage)	Min/ Max Dive Time (min)	Heading Variance (angle / time)	Min /Max Speed (km/h)	Speed Distri-bution	Depth Limit / Reaction Angle
Bryde's Whale	1/1	90/75	20/150	2/11	30	2/20	Norm.	50/ reflect

Surface Time

No direct data available, fin whale values used.

Dive Depth

No direct data available, fin whale values used.

Dive Time

Dive times ranged between 0.75 and 11 minutes, with a mean duration of 1.5 minutes (Schilling et al., 1992). Most of the dives were short in duration, presumably because they were associated with surface or near-surface foraging. The same paper reported surface times that ranged between 2 seconds and 15 minutes.

Heading Variance

Observations of foraging sei whales found that they had a very high reorientation rate, frequently resulting in minimal net movement (Schilling et al., 1992).

Speed

A tagging study found an overall speed of advance for sei whales was 4.6 km/h (Brown, 1977). The highest speed reported for a Bryde's whale was 20 km/h (Cummings, 1985). A Bryde's whale being attacked by killer whales traveled ~ 9 km in 94 minutes, with most of the travel occurring in first 50 minutes, producing an estimated speed of 10.8 km/h (Silber et al., 1990).

Habitat

Sei whales are known to feed on shallow banks, such as Stellwagen Bank (Kenney and Winn, 1986). Therefore Sei and Bryde's whales are allowed to move into shallow water.

2.6.6.2 Sperm Whale

Model parameters

	Min/Max Surface Time (min)	Surfacing / Dive Angle	Dive Depth (m) Min/Max (Percentage)	Min/ Max Dive Time (min)	Heading Variance (angle / time)	Min /Max Speed (km/h)	Speed Distri-bution	Depth Limit / Reaction Angle
Sperm Whale	8/11	90/75	600/1400 (90) 200/600 (10)	18/65	20	0.1 / 10	Norm.	200/ reflect

Surface Time

Male sperm whales in New Zealand had a mean duration on the surface of 9.1 minutes, with a range of 2-19 minutes (Jaquet et al., 2000). The distribution of surface times was non-normal, with 68% of the surface times falling between 8 and 11 minutes. These values were used for AIM modeling.

Surfacing and Dive Angles

Surfacing angles of 90° and diving angles between 60° and 90° have been reported (Miller et al., 2004).

Dive Depth

The maximum, accurately measured, sperm whale dive depth was 1,330 meters (Watkins et al., 2002). Foraging dives typically begin at depths of 300 meters (Papastavrou et al., 1989). D-tag data from the Gulf of Mexico show that most foraging dives were between the depths of 400 to 800 meters, with occasional dives between 900 and 1000 meters (Jochens et al 2008).

Sperm whale diving is not uniform. As an example, data from a paper on sperm whale diving reported different dive types (Amano and Yoshioka, 2003). AIM can now accommodate these different dive types, at different frequencies of use.

		Depth		Time	
Type of Dive	N	AIM min	AIM max	AIM min	AIM max
Dives w/ active bottom period	65	606	1082	33.17	41.63
dives w/o active bottom period	4	417	567	31.29	33.71
V shaped dives	3	213	353	12.77	20.83
Total	74				

Dive Time

Sperm whale dive times average 44.4 minutes in duration and range from 18.2-65.3 minutes (Watkins et al., 2002).

Speed

Sperm whales are typically slow or motionless on the surface. Mean surface speeds of 1.25 km/h were reported by Jaquet et al. (2000) and 3.42 km/h (Whitehead et al., 1989), while heading variance was identified in Jaquet et. al (1999). Their mean dive rate ranges from 5.22 km/h to 10.08 km/h with a mean of 7.32 km/h (Lockyer, 1997). In Norway, horizontal swimming speeds varied between 0.2 and 2.6 m/s (0.72 and 9.36 km/h) (Wahlberg, 2002). Sperm whales in the Atlantic Ocean swam at speeds between 2.6 and 3.5 km/h (Watkins et al., 1999). Based on these data, a minimum speed of 1 km/h, and a maximum speed of 10 km/h was set for sperm whales, specified with a normal distribution, so that mean speeds will be about 5 km/h.

Habitat

Sperm whales are found almost everywhere, but they are usually in water deeper than 480 meters (Davis et al., 1998). However, there have been sightings of animals in shallow water (40-100 m) (Whitehead et al., 1992; Scott and Sadove, 1997). In the Gulf of California, there was no relationship between depth or bathymetric slope and abundance, and animals were seen in water as shallow as 100 m (Jaquet and Gendron, 2002). Based on these reports, a compromise value of 200 meters will be used as the shallow water limit for sperm whales.

2.6.6.3 Beaked Whales

Data on the behavior of beaked whales are sparse. Therefore, all beaked whale species have been pooled into a single animat.

Model parameters

	Min/Max Surface Time (min)	Surfacing / Dive Angle	Dive Depth (m) Min/Max (Percentage)	Min/ Max Dive Time (min)	Heading Variance (angle / time)	Min /Max Speed (km/h)	Speed Distri-bution	Depth Limit / Reaction Angle
Beaked Whales	1/7		1000/1453 (90) 50/200 (10)	12/70	30	3/6	Norm.	253/ reflect

Surface Time

Surface times in Arnoux's beaked whales ranged from 1.2-6.8 minutes (Hobson and Martin, 1996). Sowerby's beaked whales had surface times of 1-2 minutes, during which they would blow 6-8 times (Hooker and Baird, 1999b).

Dive Depth

The minimum and maximum dive depth measured for a beaked whale was 120 and 1,453 meters, respectively (Hooker and Baird, 1999a). *Ziphius* tagged off the Canary Islands had foraging dives between 824 m and 1,267 m, while Blainsville's beaked whales dove to depths between 655 and 975 m (Johnson et al., 2004).

Dive Time

The minimum and maximum dive time measured was 16 and 70.5 minutes, respectively (Hooker and Baird, 1999a). Sowerby's beaked whales had dives between 12 and (at least) 28 minutes in the Gully in Canada (Hooker and Baird, 1999b). Arnoux's beaked whales had modal dive times between 35-65 minutes (mean = 46.4 min, SD = 13.1), with a maximum dive time of at least 70 minutes (Hobson and Martin, 1996). Tagging results with *Ziphius* had one animal diving for 50 minutes (Johnson et al., 2004). *Mesoplodon stejnegeri* were observed to dive for "10-15 minutes" in Alaska (Loughlin, 1982).

Heading Variance

Sowerby's beaked whales surfacing in the Gully were reported to have no apparent orientation, and would change orientation up to 180° between surfacings (Hooker and Baird, 1999b).

Speed

Dive rates averaged 1 m/s or 3.6 km/h (Hooker and Baird, 1999a). A mean surface speed of 5 km/h was reported by (Kastelein and Gerrits, 1991).

Habitat

The minimum sea depth in which beaked whales were found in the Gulf of Mexico was 253 meters (Davis et al., 1998). In the Gully in Canada, Sowerby's beaked whales were found in water ranging from 550 to 1,500 m in depth (Hooker and Baird, 1999b). Blainsville's beaked whales (*M. densirostris*) were found in water depths of 136 to 1,319 m in the Bahamas, and were found most often in areas with a high bathymetric slope (MacLeod and Zuur, 2005). *Mesoplodons* were found in waters from 700 m to > 1,800 m off Scotland and the Faroe Islands (Weir 2000) and between 680 and 1,933 meters in the Gulf of Mexico (Davis et al., 1998).

Group Size

Mesoplodon stejnegeri in Alaska had pod sizes between 5 and 15 animals (Loughlin, 1982).

2.6.6.4 Dwarf and Pygmy Sperm Whales (Kogia spp.)

Data on dwarf and pygmy sperm whales are rare, and these species are very similar, so data for these two species have been combined.

Model parameters

	Min/Max Surface Time (min)	Surfacing / Dive Angle	Dive Depth (m) Min/Max (Percentage)	Min/ Max Dive Time (min)	Heading Variance (angle / time)	Min /Max Speed (km/h)	Speed Distri-bution	Depth Limit / Reaction Angle
Kogia	1/2		200/1000	5/12	30	0/11	Norm.	117/ reflect

Surface Time

Observations of *Kogia* off Hawaii found that they logged at the surface for up to a "few" minutes, then dove (Baird, 2005).

Dive Depth

In the Gulf of Mexico, *Kogia* were found in waters less than 1,000 meters, along the upper continental slope (Baumgartner et al., 2001). Therefore, the dive limits of 200-1,000 meters were chosen based on similar species diving deeply to feed, and within the physical constraints of the environment. It should be noted that *Kogia* have been seen in water almost 2,000 m deep (Davis et al., 1998), but they may not be diving to the bottom.

Dive Time

Maximum dive time reported for *Kogia* is 12 minutes (Hohn et al., 1995). A rehabilitated pygmy sperm whale made long dives from 2 to 11 minutes in length at night, and shorter dives during the day (Scott et al., 2001).

Speed

Tracking of a rehabilitated pygmy sperm whale found that speeds range from 0 to 6 knots (11 km/h) with a mean value of 3 knots (5.6 km/h) (Scott et al., 2001).

Habitat

The minimum depth that *Kogia* was found in the Gulf of Mexico was 176 meters (Davis et al., 1998). Off Hawai'i, they were found in waters between 450 and 3,200 meters depth, with a mean of 1,425 meters (Baird, 2005). *Kogia* in the Philippines were found in waters from 117 to 3,744 meters in depth (Dolar and Perrin, 2003).

Group Size

Group sizes off Hawai'i ranged between 1 and 6 animals (Baird, 2005).

2.6.6.5 Blackfish: False Killer Whale, Pygmy Killer Whale, Melon-headed Whale, Pilot Whale

Studies describing the movements and diving patterns of these animals are rare and sparse. Therefore, they have been combined into a single "blackfish" category. As more data become available, these species will be split into separate animats.

Model parameters

	Min/Max Surface Time (min)	Surfacing / Dive Angle	Dive Depth (m) Min/Max (Percentage)	Min/ Max Dive Time (min)	Heading Variance (angle / time)	Min /Max Speed (km/h)	Speed Distri-bution	Depth Limit / Reaction Angle
Blackfish	1/1		5/50/ (80) 50/1000	2/12	30	2/22.4	Gamma.	200/ reflect

Surface Time

A rehabilitated long-finned pilot whale in the North Atlantic was equipped with a satellite tag and a time-depth recorder (TDR). The log survivorship plot of dive time from this animal had a curve at about 40 seconds (Mate et al., 2005). The authors did not feel that this qualified as a breakpoint to separate surface and dive behaviour. However, it does suggest that most surface intervals are less than one minute.

Dive Depth

Long-finned pilot whales in the Mediterranean were observed to display considerable diurnal variation in their dive depths (Figure A-37). During the day they never dove to more than 16 meters. However, at night, they dove to a maximum depths of 360 and 648 meters (Baird et al., 2002). Rehabilitated long-finned pilot whales dove to 312 meters on Georges Bank, which has a depth of 360 meters, so these values should not be taken as the maximum. The distribution of dive depths was also skewed toward lower values (Nawojchik et al., 2003).

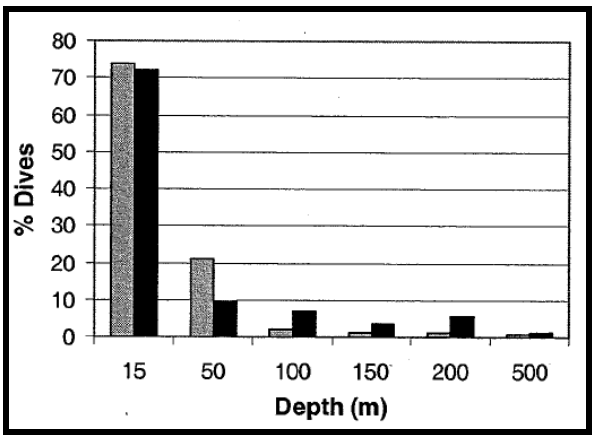

Figure A-37. Long-finned Pilot Whale Dive Depth in the Mediterranean Sea.

Dive Time

Baird et al. (2002) reported on dives of two individuals, and dive times varied between 2.14 and 12.7 minutes during the night. Animals spent all of their time in the top 16 meters during the day.

A rehabilitated long-finned pilot whale in the North Atlantic had dive times between 1 and 6 minutes (Mate et al., 2005). Other rehabilitated long-finned whales were reported to dive to at least 25 minutes, although the distribution is skewed toward shorter dives, with most lasting about two minutes (Nawojchik et al., 2003). Long-finned pilot whales off the Faroe Islands never dove longer than 18 minutes (Figure A-38) (Heide-Jørgensen et al., 2002).

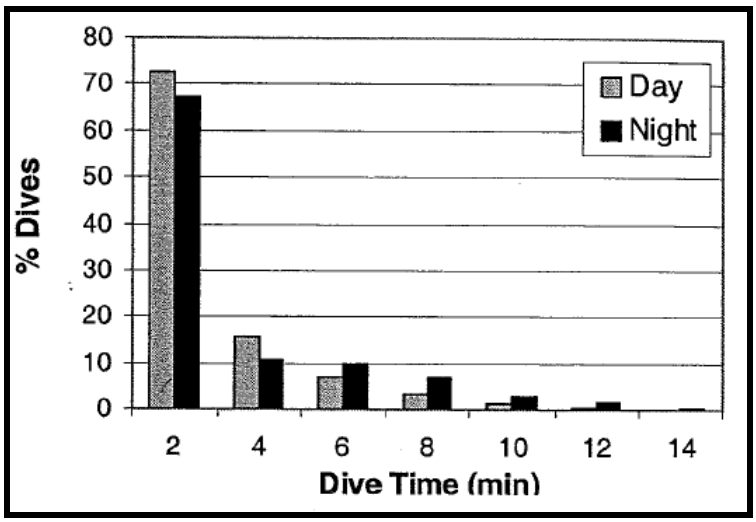

Figure A-38. Long-finned Pilot Whale Dive Times off the Faroe Islands.

Speed

Maximum speed recorded for false killer whales was 8.0 m/s (28.8 km/h) (Rohr et al., 2002), although the typical cruising speed is typically 20-24% less than the maximum speed (Fish and Rohr, 1999). This "typical" maximum of 6.24 m/s (22 km/h) was used as the maximum speed for AIM.

Shane (1995) reported a minimum speed of 2 km/h and a maximum of 12 km/h for pilot whales. It is believed that the Rohr et al. (2002) value is more accurate for maximum speed. During the day in the Mediterranean, animals slowly swam, with mean values for two animals of 0.762 and 0.885 m/s (2.85 and 3.18 km/h), while at night they swam faster, at 1.898 (6.83 km/h) and 1.523 m/s (5.48 km/h) (Baird et al., 2002). A single satellite-tracked long-finned pilot whale had a minimum speed of 1.4 km/h (Mate et al., 2005). The speeds of traveling pilot whales (*G. macrocephalus*) was estimated at 4-5 kts (7.4-9.3 km/h) (Norris and Prescott, 1961) (cited in Mate, 2005). Vertical dive speeds of three TDR tagged animals ranged from 0.79 to 3.38 m/s (2.8 to 12.2 km/h), with a mean of 1.99 m/s (7.2 km/h) (Heide-Jørgensen et al., 2002).

Habitat

The minimum water depth that pilot whales were seen in the Gulf of Mexico was 246 m (Davis et al., 1998) while off of Spain they preferred water deeper than 600 meters (Cañadas et al., 2002).

Group Size

In the Gulf of Mexico, melon-headed whales are found in groups of 35-400 (mean = 135.3, standard error (SE)=36.66, n=10) (Mullin et al., 1994).

2.6.6.6 Killer Whale

There is a remarkable paucity of quantitative data available for killer whales, considering their coastal habitat and popular appeal. Nevertheless, most data from "blackfish" were used to model *Orcinus orca*, with the exception of dive depth. The different feeding ecology of these species makes very deep dives apparently unnecessary. When additional data allow, separate animats for "resident" and "transient" killer whales will be developed.

Model parameters

	Min/Max Surface Time (min)	Surfacing / Dive Angle	Dive Depth (m) Min/Max (Percentage)	Min/ Max Dive Time (min)	Heading Variance (angle / time)	Min /Max Speed (km/h)	Speed Distri-bution	Depth Limit / Reaction Angle
Killer Whale	1/1		10/180	1/10	30	3/12	Norm.	25/ reflect

Dive Depth

Killer whales feeding on herring were observed to dive to 180 meters (Nøttestad et al., 2002). Killer whales are found in at least two "races", transients and residents. Transients feed primarily on marine mammals whereas residents feed primarily on fish. Residents were reported to dive to the bottom (173 m) (Baird, 1994). Baird (1994) also reported that while residents dive deeper than transients, the transients spent a far greater amount of time in deeper water. Individual resident killer whales in the Pacific northwest had maximum dive depths ranging between 24 and 264 meters, with a group mean maximum depth of 140.8 meters (SD=61.8, n=34) (Baird et al., 2005). The distribution of dive depths in Baird et al. (2005) was strongly skewed toward shallow values.

Dive Time

Daytime dive times for males was 2.79 minutes, significantly longer than the 2.09 minute dive times for females (Baird et al., 2005).

Speed

Uncalibrated swim speed data were presented in Baird et al. (2005). Killer whales chasing minke whales had prolonged speeds of 15-30 km/h (Ford et al., 2005), although these speeds are probably obtained only during predation. A shore-based study of southern resident killer whales in Washington State had a mean speed of 9.5 km/h, with a mean range of 4.7 to 16.1 km/h (Kriete, 2002). The mean speed of control animals was approximately 5.3 km/h, measured during a study of the response of killer whales to vessels (Williams et al., 2002). A similar study reported a mean speed of 6.64 km/h without vessels and 6.478 km/h in the presence of vessels (Bain et al,. 2005). Taken together, these three studies produced a speed range of 3 to 12 km/h for use in AIM.

Habitat

Killer whales are known to occur in very shallow water (e.g., rubbing beaches) as well as cross open ocean basins. However, they are usually coastal and most often found in temperate waters.

2.6.6.7 Risso's Dolphin

Model parameters

	Min/Max Surface Time (min)	Surfacing / Dive Angle	Dive Depth (m) Min/Max (Percentage)	Min/ Max Dive Time (min)	Heading Variance (angle / time)	Min /Max Speed (km/h)	Speed Distri-bution	Depth Limit / Reaction Angle
Risso's Dolphin	1/3		150/1000	2/12	30	2/12	Norm.	150/ reflect

Dive Depth

Dive depths of 150 -1000 meters were inferred from its squid-eating habits, and from similar species.

Dive Time

No data on dive times could be found. The values for blackfish, which have a similar ecological niche, were used.

Speed

Risso's dolphins off Santa Catalina Island were reported to have speeds that range between 2 and 12 km/h (Shane, 1995).

Habitat

Risso's dolphins were seen in water deeper than 150 meters in the Gulf of Mexico (Davis et al., 1998), but were most often observed in water depths between 300 and 750 meters. Off Chile there were seen in waters deeper than 1,000 meters (Olavarria et al., 2001). Off Spain, they were found to be deep-water species, preferring water deeper than 600 m (Cañadas et al., 2002). In all cases this association seems to be driven by the local oceanographic upwelling conditions that increase primary productivity.

Group Size

In the Pacific, group sizes were measured between 1 and 220 animals, with a geometric mean of 10.7. An estimated 76.4% of the groups contained fewer than 20 animals Leatherwood et al., 1980).

2.6.6.8 Bottlenose dolphin

Bottlenose dolphins in the Gulf of Mexico are found in separate estuarine, coastal, continental shelf and oceanic stocks (Waring et al 2009). The estuarine, coastal and continental shelf animals were modeled with the coastal animat shown below, while the oceanic stock was modeled separately.

Model parameters

	Min/Max Surface Time (min)	Surfacing / Dive Angle	Dive Depth (m) Min/Max (Percentage)	Min/ Max Dive Time (min)	Heading Variance (angle / time)	Min /Max Speed (km/h)	Speed Distri-bution	Depth Limit / Reaction Angle
Bottlenose (Coastal)	1/1		15/98	1/3	30	2/16	Norm.	10/ reflect
Bottlenose (Pelagic)	1/1		15/200	1/3	30	2/16	Norm.	101/ 1226 reflect

Surface Time

Measured surface times ranged from 38 seconds to 1.2 minutes (Lockyer and Morris ,1986; Lockyer and Morris, 1987; Mate et al., 1995).

Dive Depth

The maximum recorded dive depth for wild bottlenose dolphins is 200 meters (Kooyman and Andersen, 1969). A satellite tagged dolphin, in Tampa Bay, had a maximum dive depth of 98 meters (Mate et al., 1995). This value was used as the maximum dive depth for the coastal form of bottlenose dolphin.

Dive Time

Dive times for a juvenile bottlenose dolphin had a mean value of 55.3 seconds, although the distribution was skewed toward shorter dives (Lockyer and Morris, 1987). This is shown in their figure, reproduced here as Figure A-39.

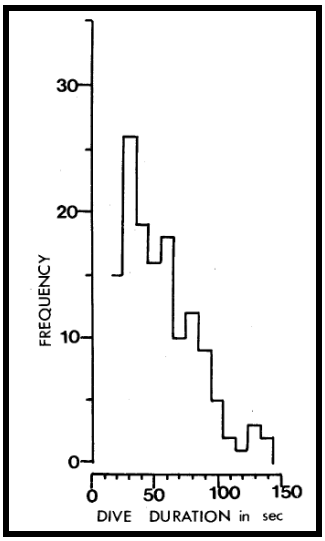

Figure A-39. Bottlenose Dolphin Dive Durations.

Speed

Bottlenose dolphins were observed to swim, for extended periods, at speeds of 4 to 20 km/h, although they could burst (for about 20 seconds) at up to 54 km/h (Lockyer and Morris, 1987). Dolphins in the Sado Estuary, Portugal had a mean speed of 1.2 m/s (4.3 km/h) and maximum speed of 3.2 m/s (11.2 km/h) (Harzen, 2002). A more recent analysis found that maximum speed of wild dolphins was 5.7 m/s (20.5 km/h), although trained animals could double this speed when preparing to leap (Rohr et al., 2002). Maximum speeds of wild dolphins in France was 4.8 m/s (17.3 km/h), with an average speed (relative to water) of 2.2 m/s (7.9 km/h) (Ridoux et al. 1997). Bottlenose dolphins off Argentina swam much faster (3.9 m/s, or 14 km/h) when in water > 10 m depth, than in shallow water (1.6 m/s, or 5.8 km/h) (Würsig and Würsig, 1979).

Habitat

In the Gulf of Mexico, bottlenose dolphins have been observed in water depths between 101 and 1,226 meters (Davis et al., 1998), However, tagged animals have been observed to swim into water 5,000 meters deep (Wells et al., 1999).

2.6.6.9 Stenella: spinner, atlantic/pantropical spotted, and striped dolphins

Most *Stenella* species have strong diurnal variation in their behavior. This was accounted for by programming two dive behaviors. The relative proportion of these dive types can be scaled by the local photoperiod with the AIM weighting parameter.

Model parameters

	Min/Max Surface Time (min)	Surfacing / Dive Angle	Dive Depth (m) Min/Max (Percentage)	Min/ Max Dive Time (min)	Heading Variance (angle / time)	Min /Max Speed (km/h)	Speed Distri-bution	Depth Limit / Reaction Angle
Stenella	1/1		Day: 5/25 (50) Night: 10/400 (10) Night: 10/100(40)	1/4	30	2/9	Norm.	10/ reflect

Dive Depth

Spinner dolphins feed during the night, and rest inshore during the daytime. At night they dive to about 400 meters to feed (Dolar et al., 2003).

Pantropical spotted dolphins off Hawai‘i also dive deeper at night than during the day. The daytime depth had a mean of 12.8 meters, with a maximum of 122 meters, whereas the nighttime mean was 57 meters, with a maximum of 213 meters (Baird et al., 2001).

Spinner dolphins off Hawaii typically track and forage upon the mesopelagic boundary layer as it migrates both vertically and horizontally at night. It appears that dolphins have to dive deeply only at the very beginning and end of the migration (Benoit-Bird and Au, 2003). Most of the time they forage at moderate depths.

Therefore, 10% of the dives will be set to be deep, 40% of the dives will be ‘typical’ foraging depths, with a maximum of 150 meters, and 50% of the dives will represent the daytime resting behaviour, ranging between 5 and 25 meters.

Dive Time

A single spotted dolphin had dive times ranging between 1 and 204 seconds (Leatherwood and Ljungblad, 1979). Pantropical spotted dolphins off Hawai‘i had a mean dive duration of 1.95 min (SD=0.92) (Baird et al., 2001). An Atlantic spotted dolphin tagged with a satellite-linked TDR had a maximum dive time of 3.5 minutes (Davis et al., 1996). A four minute dive time maximum was used for modeling purposes in AIM.

Speed

The mean speed of striped dolphins in the Mediterranean was estimated at 6.1 knots (11 km/h), and were observed to burst to 32 knots (59.3 km/h) (Archer and Perrin, 1999). A speed of 20 km/h was chosen as a typical (non-burst) maximum speed. A tagged spotted dolphin was tracked at estimated average speeds of 2.3-10.7 knots (4.3-20 km/h), with bursts exceeding 12 knots (22 km/h) (Leatherwood and Ljungblad, 1979). The estimated burst speed of spotted dolphins in the Eastern Tropical Pacific was 6 m/s (21.6 km/h) for adults and 3 m/s (10.8 km/h) for neonates (newborns). The estimated long-term top speed is 2.5 m/s (9 km/h) for adults and 1 m/s (3.6 km/h) for neonates (Edwards 2006). The Edwards (2006) paper also summarized speed estimates and duration for a number of species. Therefore, their estimate of 9 km/h will be used for long-term movements, as modeled in AIM.

Habitat

In the Gulf of Mexico, spinner dolphins were seen in water deeper than 526 meters, striped dolphins were seen in water deeper than 570 meters and spotted dolphins were seen in water deeper than 102 meters (Davis et al., 1998). Spinner dolphins in Hawaii are known to move into shallow bays during the day (Norris and Dohl, 1980).

Group Size

Group size estimates were summarized, and the majority of groups were less than 500 animals. The mean of the smaller groups was 101 animals (Archer and Perrin, 1999).

2.6.6.10 Fraser's dolphin

Model parameters

	Min/Max Surface Time (min)	Surfacing / Dive Angle	Dive Depth (m) Min/Max (Percentage)	Min/ Max Dive Time (min)	Heading Variance (angle / time)	Min /Max Speed (km/h)	Speed Distri-bution	Depth Limit / Reaction Angle
Fraser's Dolphin	1/1		10/700	1/6	30	2/9	Norm.	100/ reflect

Dive Depth

Fraser's dolphins dive to about 600-700 meters to feed, much deeper than spinner dolphins (Dolar et al., 2003). Numerous records indicated that the primary prey of Fraser's dolphins is found at great depth (Caldwell et al., 1976; Miyazaki and Wada, 1978; Robison and Craddock, 1983), although there has been at least one report of near-surface feeding (Watkins et al., 1994). All other behavioral parameters are taken from *Stenella* species, since there are no direct data for Fraser's dolphin.

Dive Time

Dive time has been increased to six minutes, to account for the deeper dives.

2.6.6.11 Rough-toothed dolphin

Model parameters

	Min/Max Surface Time (min)	Surface / Dive Angle	Dive Depth (m) Min/max (Percentage)	Min/ Max Dive Time (min)	Heading Variance (angle / time)	Min /Max Speed (km/h)	Speed distri-bution	Depth limit / reaction angle
Rough-toothed dolphin	1/3		50/600	3/5	30	5/16	Norm.	194/ reflect

Dive Depth

No dive depth data are available; depths are based upon other species. Since rough-toothed dolphins primarily forage on squid, a deep dive depth is chosen.

Dive Time

The maximum dive time reported for rough-toothed dolphins was 15 minutes (Miyazaki and Perrin, 1994). A more typical range was 0.5 to 3.5 minutes (Ritter 2002).

Speed

Bow-riding rough-toothed dolphins were observed at 16 km/h (Watkins et al., 1987). Porpoising rough-toothed dolphins off the Canary Islands were tracked at >3 knots (5.6 km/h) (Ritter, 2002).

Habitat

Rough-toothed dolphins were seen in water deeper than 194 meters (Davis et al., 1998). Rough-toothed dolphins off the Canary Islands were most often seen in water 100-1,000 m deep, with occasional shallow water sightings, and one group was seen in water 2,500 m deep (Ritter, 2002). Off French Polynesia, animals

were found between 1.8 and 5.5 km offshore, in water between 1,000 and 2,000 meters deep (Gannier and West, 2005).

Group Size

Rough-toothed dolphins off French Polynesia had a mean group size of 10.8 individuals, with a range of 1-35 animals (Gannier and West, 2005).

2.6.7 AIM Results and Adjustments

The output results from AIM found in Tables A-20 and A-21 below provide the number of Level A and Level B harassment takes for each species, by season, modeled region and survey type that exceeded the specific threshold considered. Following the AIM runs, the resulting "ping-histories" or the individual received level values for each of the modeled animats are corrected to account for the correct survey type source level (per Table A-22). This is required because the initial AIM modeling set up assumed the "nominal source" was used. Also, the source level is corrected by the M-weighting correction for that species type. Finally, these results were then corrected to adjust for two parameters in the modeling: 1) the density of animats/animals in the modeled area; and 2) the actual number of blocks that will be surveyed in each modeled region. As discussed previously, the animal densities used in the AIM modeling were deliberately kept high to ensure that a statistically valid result was obtained. Typically, these "modeled" densities are at least an order of magnitude greater than the actual marine mammal density present in the region. Therefore, the modeling result is corrected or scaled by the ratio of the actual density divided by the modeled density. Similarly, the number of potential impacts also is scaled to derive a "per block survey" level of potential impacts. The predicted potential impacts can then be calculated by multiplying this value by the number of surveys of that type to be performed in that year, and summing the potential impacts to that species from all survey types combined.

Table A-20. Estimates of Potential Level A and Level B Harassment Impacts Using AIM and Historic Thresholds.

	Level A (180 dB)						Level B (160 dB)					
Marine Mammal Species	**2012**	**2013**	**2014**	**2015**	**2016**	**2017**	**2012**	**2013**	**2014**	**2015**	**2016**	**2017**
Mysticetes												
Bryde's whale	2.1	1.9	2.0	2.1	0.03	0.03	60.4	42.0	12.8	21.7	118.1	100.1
Odontocetes												
Atlantic spotted dolphin	6647.8	1984.1	282.9	1007.0	9841.7	8034.4	126106.7	35502.2	4394.8	17996.7	182775.1	149084.9
Beaked whales:	77.5	66.7	16.3	29.8	159.1	132.1	1870.5	1434.4	443.0	751.2	3745.4	3184.4
Cuvier's												
Blainesville's												
Gervias'												
Bottlenose dolphin	27925.6	11629.0	1787.0	6229.0	58691.6	47999.2	265774.6	118531.9	26384.7	63431.7	460514.0	379802.9
Clymene dolphin	3109.1	2541.3	771.7	1273.6	6190.4	5257.8	24927.4	17229.8	4301.4	8025.3	49496.3	41423.1
False Killer whale	215.3	176.1	46.5	82.4	442.6	372.3	2635.2	2043.2	676.6	1084.1	5117.4	4383.0
Fraser's dolphin	162.7	130.3	40.4	65.4	323.1	274.5	1460.3	1019.0	308.4	524.7	2831.6	2401.1
Killer whale	820.3	322.1	78.4	167.5	1119.8	928.2	21418.8	7891.6	1628.0	3944.1	29273.6	24126.7
Kogia spp.	266.0	271.6	77.1	124.7	532.3	453.8	1336.3	1280.3	502.9	728.0	2399.1	2119.6
Dwarf sperm whale												
Pygmy sperm whale												
Melonheaded whale	754.8	614.1	158.1	283.4	1555.4	1306.1	8849.5	6811.8	2252.7	3613.8	17122.8	14659.7
Pantropical spotted dolphin	25073.7	18969.7	5523.1	9816.7	51802.1	43606.2	215647.6	148395.2	39765.9	76291.2	441142.2	367083.6
Pygmy killer whale	85.5	72.7	19.7	34.0	176.9	148.9	990.7	762.4	250.7	400.7	1922.9	1649.1
Risso's dolphin	1280.0	828.0	190.8	404.8	2716.9	2246.6	9687.2	6199.2	1853.9	3432.2	19862.9	16684.0
Rough-toothed dolphin	987.8	655.6	129.1	290.1	2030.8	1681.9	9840.8	7226.6	1970.8	3431.7	18032.3	15251.0
Short-finned pilot whale	442.7	372.3	101.3	173.7	900.9	760.0	6115.1	4689.3	1530.4	2469.7	11921.1	10201.7
Sperm whale	217.1	167.7	52.0	90.3	442.6	372.3	2377.2	1833.5	605.6	979.6	4684.7	4015.7
Spinner dolphin	4643.3	3273.3	1202.6	1975.6	8762.5	7466.9	68655.0	34767.6	8648.8	19246.0	139045.2	115052.4
Striped dolphin	5458.3	1924.1	683.2	1100.1	4122.8	3550.9	19240.6	12572.3	3592.8	6600.5	38143.7	31999.1

Table A-21. Estimates of Potential Level A and Level B Harassment Impacts Using AIM and Historic Thresholds with Southall et al. (2007) Applied.

	Level A (SPL-230, SEL-215 dB)						Level B (160 dB)					
Marine Mammal Species	**2012**	**2013**	**2014**	**2015**	**2016**	**2017**	**2012**	**2013**	**2014**	**2015**	**2016**	**2017**
Mysticetes												
Bryde's whale	0.02	0.03	0.03	0.03	0.03	0.03	60.4	42.0	12.8	21.7	118.1	100.1
Odontocetes												
Atlantic spotted dolphin	69.6	49.3	19.1	23.2	123.4	100.9	126106.7	35502.2	4394.8	17996.7	182775.1	149084.9
Beaked whales:	0.1	0.1	0.1	0.1	0.1	0.1	1870.5	1434.4	443.0	751.2	3745.4	3184.4
Cuvier's												
Blainesville's												
Gervias'												
Bottlenose dolphin	1010.2	426.2	65.9	234.8	2182.5	1785.8	265774.6	118531.9	26384.7	63431.7	460514.0	379802.9
Clymene dolphin	278.1	224.6	67.3	109.0	539.2	460.8	24927.4	17229.8	4301.4	8025.3	49496.3	41423.1
False Killer whale	3.2	2.6	3.0	3.0	2.5	3.4	2635.2	2043.2	676.6	1084.1	5117.4	4383.0
Fraser's dolphin	2.9	2.7	2.9	3.1	2.8	3.6	1460.3	1019.0	308.4	524.7	2831.6	2401.1
Killer whale	32.0	11.5	1.0	4.6	45.7	37.4	21418.8	7891.6	1628.0	3944.1	29273.6	24126.7
Kogia spp.	0.8	0.5	0.7	0.6	0.4	0.7	1336.3	1280.3	502.9	728.0	2399.1	2119.6
Dwarf sperm whale												
Pygmy sperm whale												
Melonheaded whale	12.6	17.2	12.3	12.8	10.8	13.1	8849.5	6811.8	2252.7	3613.8	17122.8	14659.7
Pantropical spotted dolphin	1045.9	864.7	365.0	520.2	1835.1	1609.2	215647.6	148395.2	39765.9	76291.2	441142.2	367083.6
Pygmy killer whale	1.0	0.7	0.9	0.8	0.6	0.9	990.7	762.4	250.7	400.7	1922.9	1649.1
Risso's dolphin	1.7	1.6	1.7	1.5	1.4	1.6	9687.2	6199.2	1853.9	3432.2	19862.9	16684.0
Rough-toothed dolphin	1.9	2.0	1.5	1.7	1.6	1.4	9840.8	7226.6	1970.8	3431.7	18032.3	15251.0
Short-finned pilot whale	7.6	9.3	7.4	7.4	6.1	8.3	6115.1	4689.3	1530.4	2469.7	11921.1	10201.7
Sperm whale	19.1	13.9	3.6	6.8	40.7	33.8	2377.2	1833.5	605.6	979.6	4684.7	4015.7
Spinner dolphin	394.1	256.1	69.7	132.8	782.0	650.5	68655.0	34767.6	8648.8	19246.0	139045.2	115052.4
Striped dolphin	189.4	162.4	53.0	83.6	356.6	305.8	19240.6	12572.3	3592.8	6600.5	38143.7	31999.1

3.0 SUMMARY

This appendix provides the detailed information that went into the analysis of the potential impacts to marine mammals in the Gulf of Mexico from prospective G&G operations during the 2010-2014 timeframe. These results are presented in Chapter 4. The DPEIS of which this appendix will be a part will also support the NMFS G&G rulemaking process; specifically, the DPEIS will serve as the NEPA analysis for G&G operations in the GOMEX.

4.0 LITERATURE CITED

Amano M, and M. Yoshioka. 2003. Sperm whale diving behavior monitored using a suction-cup-attached TDR tag. Marine Ecology Progress Series 258:291-295.

ANSI (American National Standard Institute). 2004. American National Standard Institute (ANSI)—American national standard acoustic terminology. S1.1.Acoustical Society of America. New York, New York.

ANSI (American National Standard Institute). 1984. American National Standard Institute (ANSI)—American national standard preferred frequencies, frequency levels and band numbers for acoustic measurements. S1.6. Acoustical Society of America, New York, New York.

ANSI (American National Standard Institute). 1986. American National Standard Institute (ANSI)—American National Standard Method for Measurement of Impulsive Noise. S12.7. Acoustical Society of America. New York, New York.

Archer, F.I., II, and W.F. Perrin. 1999. Stenella coeruleoalba. Mammalian Species 603:1-9.

Bain D, E., Smith JC, Williams R, Lusseau D. 2005. Effects of Vessels on behavior of southern resident killer whales (*Orcinus* spp.). In: 15th Biennial Conference on the Biology of Marine Mammals.

Baird, R.W. 1994. Foraging behavior and ecology of transient killer whales (*Orcinus orca*). In. Simon Fraser University, pp 159.

Baird, R.W. 2005. Sightings of dwarf (*Kogia sima*) and pygmy (*K. breviceps*) sperm whales from the main Hawaiian Islands. Pacific Science 59:461-466.

Baird, R.W, Borsani, J.F., Hanson, M.B., Tyack, P.L. 2002. Diving and night-time behavior of long-finned pilot whales in the Ligurian Sea. Marine Ecology Progress Series 237:301-305.

Baird, R.W., Hanson, M.B., Dill, L.M. 2005. Factors influencing the diving behaviour of fish-eating killer whales: sex differences and diel and interannual variation in diving rates. Can. J. Zool. 83:257-267.

Baird, R.W., Ligon, A.D., Hooker, S.K., Gorgone, A.M. 2001. Subsurface and nighttime behaviour of pantropical spotted dolphins in Hawai'i. Can. J. Zool. 79:988-996.

Baumgartner, M.F., Mullin, K.D., May, L.N., Leming, T.D. 2001. Cetacean habitats in the northern Gulf of Mexico. Fishery Bulletin Seattle 99:219-239.

Benoit-Bird, K.J., Au, W.W.L. 2003. Prey dynamics affect foraging by a pelagic predator (*Stenella longirostris*) over a range of spatial and temporal scales. Behavioral Ecology and Sociobiology 53:364-373.

Bishop, G.C., Ellison, W.T., Mellberg, L.E. 1987. A simulation model for high-frequency under-ice reverberation. J. Acoust. Soc. Am. 82:275-285.

Brown, S.G. 1977. Some results of sei whale marking in the southern hemisphere. Report of the International Whaling Commission Si1:39-43.

Buckland, S.T., D.R. Anderson, K.P. Burnham, J.L. Laake, D.L. Borchers, and L. Thomas. (2001). Introduction to Distance Sampling: Estimating abundances of biological populations. New York, NY, Oxford University Press.

Caldwell, D.K., Caldwell, M.C., Walker, R.V. 1976. First records for Fraser's dolphin (*Lagenodelphis hosei*) in the Atlantic and the melon-headed whale (*Peponocephala electra*) in the western Atlantic. Cetology 25:4.

Cañadas, A., Sagarminaga, R., Garcia, T.S. 2002. Cetacean distribution related with depth and slope in the Mediterranean waters off southern Spain. Deep Sea Research Part I Oceanographic Research Papers 49:2053-2073.

Cummings, W.C. 1985. Bryde's whale *Balaenoptera edeni* Anderson, 1878. In: Ridgway SH, Harrison R (eds) Handbook of marine mammals, Vol. 3: The sirenians and baleen whales. Academic Press, London, pp 137-154.

Davis, R.W., Fargion G.S., May, N., Leming, T.D., Baumgartner, M., Evans, W.E., Hansen, L.J., Mullin, K. 1998. Physical habitat of cetaceans along the continental slope in the north-central and western Gulf of Mexico. Marine Mammal Science 14:490-507.

Davis RW, Worthy GAJ, Würsig B, Lynn SK, Townsend FI. 1996. Diving behavior and at-sea movements of an Atlantic spotted dolphin in the Gulf of Mexico. Mar. Mamm. Sci. 12:569-581.

Dolar L, Perrin W. 2003. Dwarf sperm whale (Kogia sima) habitats in the Philippines. In: 15th Biennial conference on the biology of marine mammals, Greensboro, NC, pp 44.

Dolar MLL, Walker WA, Kooyman GL, Perrin WF. 2003. Comparative feeding ecology of spinner dolphins (*Stenella longirostris*) and Fraser's dolphins (*Lagenodelphis hosei*) in the Sulu Sea. Marine Mammal Science 19:1-19.

DoN (Department of the Navy). 2008. Final Atlantic Fleet Active Sonar Training Environmental Impact Statement/ Overseas Environmental Impact Statement. Department of the Navy, 12 December 2008.

DoN (Department of the Navy). 2007a. Final Supplemental Environmental Impact Statement for Surveillance Towed Array Sensor System Low Frequency Active (SURTASS/LFA) Sonar. Department of the Navy, April 2007.

DoN (Department of the Navy). 2007b. Navy OPAREA Density Estimates (NODE) for the GOMEX OPAREA. Department of the Navy, Naval Facilities Engineering Command, Atlantic: Norfolk, VA. Contract N62470-02-D-9997, Task Order 0046. Prepared by GeoMarine Inc. August 2007.

DoN, 2007c. Marine Resource Assessment for the Gulf of Mexico, Department of the Navy, U.S. Fleet Forces Command, Norfolk, VA, Contract # 62470-02-D-9997, CTO-0030, Prepared by Geo-Marine Inc., Hampton, VA, 2007.

DoN (Department of the Navy). 2001a. Final Overseas Environmental Impact Statement and Environmental Impact Statement for SURTASS/LFA. Department of the Navy, January 2001.

DoN (Department of the Navy). 2001b. Final Environmental Impact Statement Shock Testing the USS Churchill. Department of the Navy, February 2001.

DoN (Department of the Navy). 1998. Final Environmental Impact Statement Shock Testing the Seawolf Submarine. Department of the Navy, May 1998.

Dozier, L.B., and R.C. Cavanagh. 1993. Overview of selected underwater acoustic propagation models. AEAS Report 93-101. Contract N00014-90-D-0250 (D.O. 0005). Office of Naval Research, Advanced Environmental Acoustic Support Program, Arlington, Viriginia.

Edwards EF. 2006. Duration of unassisted swimming activity for spotted dolphin (*Stenella attenuata*) calves: implications for mother-calf separation during tuna purse-seine sets. Fishery Bulletin 104:125-135.

Ellison WT, Clark CW, Bishop GC. 1987. Potential use of surface reverberation by bowhead whales, *Balaena mysticetus*, in under-ice navigation: preliminary considerations. In: IWC, pp 329-332.

Finneran, J.J., Carolyn E. Schlundt, and Sam Ridgway. 2005. Temporary Shift in bottlenose dolphins *(Tursiops truncates*) exposed to mid-frequency tones. JASA Vol. 118 No. 4, pp 2696-2705.

Finneran JJ, Schlundt CE, Dear R, Carder DA, Ridgway SH. 2002. Temporary shift in masked hearing thresholds in odontocetes after exposure to single underwater impulses from a seismic watergun. Journal of the Acoustical Society of America 111:2929-2940.

Fish, F.E., Rohr, J.J. 1999. Review of Dolphin Hydrodynamics and Swimming Performance. In. Spawar, pp 196.

Ford JKB, Ellis GA, Matkin DR, Balcomb KC, Briggs D, Morton AB. 2005. Killer whale attacks on minke whales: Prey capture and antipredator tactics. Marine Mammal Science 21:603-618.

Frankel AS, Ellison WT, Buchanan J. 2002. Application of the Acoustic Integration Model (AIM) to predict and minimize environmental impacts. IEEE Oceans 2002:1438-1443.

Gannier A, West KL. 2005. Distribution of the Rough-Toothed Dolphin (*Steno bredanensis*) around the Windward Islands (French Polynesia). Pacific Science 59:17-24.

Greene, C.R., Jr. (1997). Physical Acoustic Measurements. In W. J. Richardson (Ed.), *Northstar marine mammal monitoring program, 1996* (LGL Report 2121-2, Section 3). LGL Ltd. reportfor BP Exploration (alaska) Inc., Anchorage , AK, and National Marine Fisheries Service, Silver Spring, MD. 245 pp.

Harzen SE. 2002. Use of an electronic theodolite in the study of movements of the bottlenose dolphin (*Tursiops truncatus*) in the Sado Estuary, Portugal. Aquatic Mammals 28:251-260.

Hastrup, Ole F. and Tuncay AKAL, 1980. "A simple Formula to Calculate Shallow-Water Transmission Loss by Means of a Least Squares Surface Fit Technique" SACLANTCEN Memorandum SM-139, SACLANT ASW Research Centre, La Spezia, Italy.

Hatton L. 2008. Technical Report to Marine Acoustics, Inc. on The GUNDALF Modelling Results for a Specified Airgun Array.

Heide-Jørgensen MP, Bloch D, Stefansson E, Mikkelsen B, Ofstad LH, Dietz R. 2002. Diving behaviour of long-finned pilot whales *Globicephala melas* around the Faroe Islands. Wildlife Biology 8:307-313.

Hobson RP, Martin AR. 1996. Behaviour and dive times of Arnoux's beaked whales, *Berardius arnuxii*, at narrow leads in fast ice. Canadian Journal of Zoology 74:388-393.

Hohn A, Scott M, Westgate A, Nicolas J, Whitaker B. 1995. Radiotracking of a rehabilitated pygmy sperm whale. In: Eleventh biennial conference on the biology of marine mammals, Orlando, FL, pp 55.

Hooker, SK, Baird, RW. 1999a. Deep-diving behaviour of the northern bottlenose whale, *Hyperoodon ampullatus* (Cetacea: Ziphiidae). Proceedings of the Royal Society of Biological Sciences: Series B. 266:671-676.

Hooker SK, Baird RW. 1999b. Observations of Sowerby's beaked whales, *Mesoplodon bidens*, in the Gully, Nova Scotia. Canadian Field-Naturalist 113:273-277.

Jaquet N, Dawson S, Slooten E. 2000. Seasonal distribution and diving behaviour of male sperm whales off Kaikoura: Foraging implications. Canadian Journal of Zoology 78:407-419.

Jaquet N, Gendron D. 2002. Distribution and relative abundance of sperm whales in relation to key environmental features, squid landings and the distribution of other cetacean species in the Gulf of California, Mexico. Marine Biology 141:591-601.

Jaquet N, Whitehead H. 1999. Movements, distribution and feeding success of sperm whales in the Pacific Ocean, over scales of days and tens of kilometers. Aquatic Mammals 25:1-13.

Jochens, A., D. Biggs, K. Benoit-Bird, D. Engelhaupt, J. Gordon, C. Hu, N. Jaquet, M. Johnson, R. Leben, B. Mate, P. Miller, J. Ortega-Ortiz, A. Thode, P. Tyack & B. Würsig. 2008. Sperm whale seismic study in the Gulf of Mexico, Summary Report, 2002-2004. 341.

Johnson M, Madsen PT, Zimmer WMX, Aguilar de Soto N, Tyack PL. 2004. Beaked whales echolocate on prey. Proceedings of the Royal Society of London Series B-Biological Sciences 271:S383-S386.

Kastak, D., B. L. Southall, R. J. Schusterman and C. R. Kastak. 2005. Underwater temporary threshold shift in pinnipeds: Effects of noise level and duration. Journal of the Acoustical Society of America 118(5)**:** 3154-3163.

Kastak, D., R. J. Schusterman, B. L. Southall and C. J. Reichmuth. 1999. Underwater temporary threshold shift induced by octave-band noise in three species of pinniped. Journal of the Acoustical Society of America 106(2)**:** 1142-1148.

Kastelein RA, Gerrits NM. 1991. Swimming, diving, and respiration patterns of a Northern bottlenose whale (*Hyperoodon ampullatus*, Forster, 1770). Aquatic Mammals 17:20-30.

Kenney RD, Winn HE. 1986. Cetacean high-use habitats of the northeast United States continental shelf. Fish. Bull. 84:345- 357.

Kooyman GL, Andersen HT. 1969. Deep diving. In: Andersen HT (ed) Biology of marine mammals. Academic Press, pp 65-94.

Kriete B. 2002. Bioenergetic changes from 1986 to 2001 in the southern resident killer whale population, *Orcinus orca*. In, pp 26.

Leatherwood S, Ljungblad DK. 1979. Nighttime swimming and diving behavior of a radio tagged spotted dolphin *Stenella attenuata*. Cetology 34:1-6.

Leatherwood S, Perrin WF, Kirby VL, Hubbs CL, Dahlheim M. 1980. Distribution and Movements of Risso's Dolphin *Grampus griseus* in the Eastern North Pacific. Fishery Bulletin Washington D C 77:951-964.

Lockyer C. 1997. Diving behaviour of the sperm whale in relation to feeding. Bulletin de l'Institut Royal des Sciences Naturelles de Belgique Biologie 67:47-52.

Lockyer C, Morris R. 1987. Observations on diving behavior and swimming speeds in a wild juvenile *Tursiops truncatus*. Aquatic Mammals 13:31-35.

Lockyer C, Morris RJ. 1986. The history and behavior of a wild, sociable bottlenose dolphin (*Tursiops truncatus*) off the north coast of Cornwall (England, UK). Aquatic Mammals 12:3-16.

Loughlin TR. 1982. Observations of *Mesoplodon stejnegeri* in the central Aleutian Islands, Alaska. Journal of Mammalogy 63:697-700.

MacLeod CD, Zuur AF. 2005. Habitat utilization by Blainville's beaked whales off Great Abaco, northern Bahamas, in relation to seabed topography. Marine Biology 147:1-11.

Madsen P. T. (2005). Marine mammals and noise: Problems with root-mean-squared sound pressure level for transients. Journal of the Acoustical Society of America, 117, 3952-3957.

Mate BR, Lagerquist BA, Winsor M, Geraci J, Prescott JH. 2005. Movements and dive habits of a satellite-monitored longfinned pilot whale (*Globicephala melas*) in the northwest Atlantic. Marine Mammal Science 21:136-144.

Mate BR, Rossbach KA, Nieukirk SL, Wells RS, Irvine AB, Scott MD, Read AJ. 1995. Satellite-monitored movements and dive behaviour of a bottlenose dolphin (*Tursiops truncatus*) in Tampa Bay, Florida. Mar. Mamm. Sci. 11:452-463.

McCauley, R.D., M.-N. Jenner, C. Jenner, K.A. McCabe, and J. Murdoch. 1998. The response of humpback whales (*Megaptera novaengliae*) to offshore seismic survey noise: preliminary results of observations about a working seismic vessel and experimental exposures. APPEA J. 38:692-707.

Miller PJO, Johnson MP, Tyack PL, Terray EA. 2004. Swimming gaits, passive drag and buoyancy of diving sperm whales *Physeter macrocephalus*. Journal of Experimental Biology 207:1953-1967.

Miyazaki N, Perrin WF. 1994. Rough-toothed dolphin *Steno bredanensis* (Lesson, 1828). In: Ridgway SH, Harrison R (eds) Handbook of marine mammals, Volume 5: The first book of dolphins. Academic Press, London, pp 1-21.

Miyazaki N, Wada S. 1978. Frasers Dolphin *Lagenodelphis hosei* in the Western North Pacific. Scientific Reports of the Whales Research Institute Tokyo:231-244.

Mullin KD, Jefferson TA, Hansen LJ, Hoggard W. 1994. First sightings of melon-headed whales (*Peponocephala electra*) in the Gulf of Mexico. Marine Mammal Science 10:342-348.

Nawojchik R, St Aubin DJ, Johnson A. 2003. Movements and dive behavior of two stranded, rehabilitated long-finned pilot whales (*Globicephala melas*) in the northwest Atlantic. Marine Mammal Science 19:232-239.

NMFS. (2005). Endangered Fish and Wildlife; Notice of Intent to Prepare an Environmental Impact Statement. **Fed. Register** 70(7):1871-1875.

NOAA-NCDDC (National Oceanic and Atmospheric Administration-National Coastal Data Development Center). 2009. Gulf of Mexico coastal habitat mapping application. http://www.ncddc.noaa.gov/website/CHP/viewer.htm. Accessed November 2008.

NOAA-NDBC (National Oceanic and Atmospheric Administration-National Data Buoy Center). 2008. National Data Buoy Center—Station 42019. http://www.ndbc.noaa.gov/station_page.php?station=42019. Accessed November 2008.

Norris KS, Dohl TP. 1980. Behavior of the Hawaiian Spinner Dolphin, *Stenella longirostris*. Fish. Bull. 77:821-849.

Norris KS, Prescott JH. 1961. Observations on Pacific cetaceans of Californian and Mexican waters. University of California Publications in Zoology 63:291-402.

Nøttestad L, Ferno A, Axelsen BE. 2002. Digging in the deep: Killer whales' advanced hunting tactic. Polar Biology 25:939-941.

NRC (National Research Council). 2003. Ocean noise and marine mammals. Washington, D.C.: National Academies Press.

Olavarria C, Aguayo LA, Bernal R. 2001. Distribution of Risso's dolphin (*Grampus griseus*, Cuvier 1812) in Chilean waters. Revista de Biologia Marina y Oceanografia 36:111-116.

Oceanographic and Atmospheric Master Library (OAML). 2002. Oceanographic and Atmospheric Master Library. Commander, Navy Meteorologic and Atmospheric Command, Stennis Space Center, Mississippi.

Papastavrou V, Smith SC, Whitehead H. 1989. Diving behavior of the sperm whale *Physeter macrocephalus* off the Galapagos Islands, Ecuador. Can J Zool 67:839-846.

Richardson, W.J., C.R. Greene Jr., C.I. Malme, and D.H. Thomson. 1995. Marine Mammals and Noise. Academic Press, San Diego, CA.

Ridoux V, Guinet C, Liret C, Creton P, Steenstrup R, Beauplet G. 1997. A video sonar as a new tool to study marine mammals in the wild: measurements of dolphin swimming speed. Mar. Mamm. Sci. 13:196-206.

Ritter F. 2002. Behavioural observations of rough-toothed dolphins (*Steno bredanensis*) off La Gomera, Canary Islands (1995-2000), with special reference to their interactions with humans. Aquatic Mammals 28:46-59.

Robison BH, Craddock JE. 1983. Meso Pelagic Fishes Eaten by Frasers Dolphin *Lagenodelphis hosei*. Fishery Bulletin Washington D C 81:283-290.

Rohr JJ, Fish FE, Gilpatrick JW. 2002. Maximum swim speeds of captive and free-ranging delphinids: Critical analysis of extraordinary performance. Marine Mammal Science 18:1-19.

Schilling MR, Seipt I, Weinrich MT, Kuhlberg AE, Clapham PJ. 1992. Behavior of individually-identified sei whales *Balaenoptera borealis* during an episodic influx into the southern gulf of maine in 1986. U S Natl Mar Fish Serv Fish Bull 90:749-755.

Scott MD, Hohn AA, Westgate AJ, Nicolas JR, Whitaker BR, Campbell WB. 2001. A note on the release and tracking of a rehabilitated pygmy sperm whale (*Kogia breviceps*). Journal of Cetacean Research and Management 3:87-94.

Scott TM, Sadove SS. 1997. Sperm Whale, *Physeter macrocephalus*, sightings in the shallow shelf waters off Long Island, New York. Mar. Mamm. Sci. 13:317-320.

Shane SH. 1995. Behavior patterns of pilot whales and Risso's dolphins off Santa Catalina Island, California. Aquatic Mammals 21:195-197.

Silber GK, Newcomer MW, Pérez-Cortés HM. 1990. Killer Whales (*Ornicus orca*) attack and kill a Bryde's whale (*Balaenoptera edeni*). Can. J. Zool. 68:1603-1606.

Southall BL, Bowles AE, Ellison WT, Finneran JJ, Gentry RL, Greene CR, Jr., Kastak D, Ketten DR, Miller JH, Nachtigall PE, Richardson WJ, Thomas JA, Tyack PL. 2007. Marine mammal noise exposure criteria: Initial scientific recommendations Aquatic Mammals 33:411-521.

Tolstoy, M., J. Diebold, L. Doermann, S. Nooner, S. C. Webb, D. R. Bohnenstiehl, T. J. Crone, and R. C. Holmes (2009), Broadband calibration of the R/V *Marcus G. Langseth* four-string seismic sources, *Geochem. Geophys. Geosyst.*, 10, Q08011, doi:10.1029/2009GC002451

Tolstoy M, Diebold JD, Webb SC, Bohnenstiehl DR, Chapp E, Holmes RC, and Rawson M. 2004. Broadband calibration of R/V *Ewing* seismic sources. Geophysical Research Letters, Vol 31, L14310.

Urick, R.J. 1983. Principles of Underwater Sound 3rd ed. McGraw-Hill, New York

Wahlberg M. 2002. The acoustic behaviour of diving sperm whales observed with a hydrophone array. Journal of Experimental Marine Biology and Ecology 281:53-62.

Waring, G. T., E. Josephson, K. Maze-Foley & P. E. Rosel. 2009. U.S. Atlantic and Gulf of Mexico Marine Mammal Stock Assessments - 2009. 340. Woods Hole, MA: Northeast Fisheries Science Center, NMFS, NOAA, U.S. Dept. of Commerce.

Watkins WA, Daher MA, DiMarzio NA, Samuels A, Wartzok D, Fristrup KM, Gannon DP, Howey PW, Maiefski RR, Spradlin TR. 1999. Sperm whale surface activity from tracking by radio and satellite tags. Marine Mammal Science 15:1158-1180.

Watkins WA, Daher MA, DiMarzio NA, Samuels A, Wartzok D, Fristrup KM, Howey PW, Maiefski RR. 2002. Sperm whale dives tracked by radio tag telemetry. Marine Mammal Science 18:55-68.

Watkins WA, Daher MA, Fristrup K, Sciara GN. 1994. Fishing and Acoustic Behavior of Fraser's Dolphin (*Lagenodelphis hosei*) near Dominica, Southeast Caribbean. Caribbean Journal of Science 30:76-82.

Watkins WA, Tyack P, Moore KE, di Sciara GN. 1987. *Steno bredaneisis* in the Mediterranean Sea. Marine Mammal Science 3:78-82.

Weinberg, H., D.L. Deavenport, E.H. McCarthy, and C.M. Anderson. (2001). "Comprehensive Acoustic System Simulation (CASS) Reference Guide." NUWC-NPT, TM 01-016, Naval Undersea Warfare Center, Division, Newport, RI , March 2001.

Weir CR. 2000. Sightings of beaked whales species (Cetacea: Ziphiidae) in the waters to the north and west of Scotland and the Faroe Islands. Eur. Res. Cet. 14:239-243.

Wells RS, Rhinehart HL, Cunningham P, Whaley J, Baran M, Koberna C, P. CD. 1999. Long distance offshore movements of bottlenose dolphins. Mar. Mamm. Sci. 15:1098-1114.

Whitehead H, Brennan S, Grover D. 1992. Distribution and behaviour of male sperm whales on the Scotian shelf Canada. Can J Zool 70:912-918.

Whitehead H, Smith SC, Papastavrou V. 1989. Diving behavior of the sperm whales, (*Physeter macrocephalus*), off the Galapagos Islands. Can. J. Zool. 67:839-846.

Williams R, Bain DE, Ford JKB, Trites AW. 2002. Behavioural responses of male killer whales to a 'leapfrogging' vessel. Journal of Cetacean Research and Management 4:305-310.

Würsig B, Würsig M. 1979. Behavior and Ecology of the bottlenose dolphin, (*Tursiops truncatus*) in the South Atlantic. Fish. Bull. 77:399-412.